Setting Transmission Line Out-of-Step Relays in Complex Power Systems

By

Anand Gole

A thesis submitted to the Faculty of Graduate Studies of

The University of Manitoba

in partial fulfilment of the requirements of the degree of

Master of Science

Department of Electrical and Computer Engineering

University of Manitoba

Winnipeg, Canada

Abstract

Large disturbance in power systems such as network faults, line switching, generator disconnections and rejection of large loads may result in a transient mismatch between the power generation and consumption that could lead to oscillations in the synchronous machine rotor angles. These oscillations, (referred to as power swings) can be damaging if they result in out-of-step (OOS) conditions. Power swings can result in unwanted relay operations that may further aggravate the disturbance leading to blackouts as the August 10, 1996, Western North America blackout. OOS protection can be employed to detect such power swings and strategically block certain protection elements to avoid undesired operations or trip and disconnect the network at specific points to minimize outages.

Typically, OOS protection examines the measured impedance at the relay location to detect power swings and determine whether they result in OOS conditions. The settings for OOS relays are specific to the power system and relay location. The current practice of determining OOS relay settings is not an exact science and requires engineering judgement. There may be scenarios where a relay cannot perfectly protect against all out-of-step events without compromising the security.

In this thesis, a general methodology which can be used to identify OOS relay settings is presented. It exploits the OOS relay models available in dynamic simulation programs to measure swing speeds and determine preliminary relay settings which are further refined to fit specific conditions. A test system developed in PSSE is used to test the proposed methodology with simulations performed in PSSE software. The settings found from the proposed methodology are further tested by applying to a detailed electromagnetic transient simulation performed in PSCAD software.

Acknowledgments

I would like to thank Professor Rajapakse, the support, guidance, and patience provided are greatly appreciated and this research could not be completed without his help.

I would also like to thank Dr. Bathiya Jayasekara who provided guidance and further inputs to help push me in the right directions to complete my research. I also extend my thanks the Dr. Dharshana Muthumuni and Manitoba Hydro Internal as they provided me the flexibility to complete the research while continuing my work at MHI.

Finally, I would like University of Manitoba for providing me the opportunity and support to conduct my research.

Dedication

This report is dedicated to my family and friends who have always supported me with love and encouragement.

Contents

List of Tables

List of Figures

List of Abbreviations

AC	Alternating Current
CMLD	Composite Load Model
EMT	Electro Magnetic Transient
kV	Kilovolt
kA	Kilo-Amps
LTC	Load Tap Changer
MVAR	Mega-Var
MVWG	Modeling and Validation Working Group
MW	Mega-Watts
OOS	Out-of-step
OSB	Out-of-Step Blocking
OST	Out-of-Step Tripping
pu	per unit
SVC	Static Var Compensator
TOWI	Trip-on-Way-In
TOWO	Trip-on-Way-Out
WECC	Western Electricity Coordination Council
ZIP	Zero Impedance Load

Chapter 1 – Introduction

1.1. Background

Certain network events such as network faults, line switching or generator disconnection may result in a sudden change in the electrical power output of synchronous generators, however the mechanical power input to these generators will not suddenly change. This can result in a power mismatch that may lead to oscillations in the synchronous machine rotor angels leading to power swings [1]. These power swings may be stable and result in a new network equilibrium. Alternatively, power swings may be unstable, such unstable power swings are referred to as out-of-step (OOS) conditions.

Power swings can result in unwanted relay operations that may further aggravate the network stresses. Such cascading events can result in large blackouts similar to the August 10, 1996 disturbance in Western North American network [2][3], where a fault caused by a line flashing and grounding to a tree resulted in tripping a generating unit at McNary Day, Washington, USA. These events resulted in mild negatively damped oscillations as generation increased to compensate for the lost McNary Generation. These oscillations resulted in tripping of the ties between California and neighboring systems, the connections between Arizona, New Mexico and Nevada, the connection between Utah and Colorado

OOS conditions are rare and will typically occur only for heavily loaded conditions that the networks should ideally avoid operating under. As systems expand, new load and generation are connected, and the power transfer through certain corridors will increase. As power transfers near their limit, network upgrades may be implemented. New transmission lines or other system components (SVC, capacitor banks, etc.) may be added to the network. Sometimes, additional transmission lines may not be desirable, in such situations, network operators may allow the lines to operate at highly loaded levels, increasing the probability of OOS conditions.

During OOS conditions, power flows in the network fluctuate. If the fluctuations continue, large oscillations in power can damage equipment (generators, transformers, etc.). Once an OOS condition occurs, a solution to avoid equipment damage is to break the system at strategic locations to form two or more stable power islands[4]. Additionally, during OOS and large power swings, distance relays can see the measured impedance entering operating zones and inadvertently trip (like a fault). This could further aggravate the situation.

Therefore, out-of-step protection is employed to detect power swings and OOS conditions. OOS protection relays strategically block the distance protection relays from tripping and/or disconnect the network at specific points to separate the power system into islands and reduce damage to the network [3][4].

1.2. Out-of-Step Protection

Conventional out-of-step protection schemes examine the impedance at a specified location to identify power swings. The scheme must distinguish between stable and unstable power swings in order the determine whether the OOS protection should trip an interface (unstable power swing) or temporarily block other protection elements, like distance protection (stable power swing). To accomplish this, appropriate blinder setting must be identified, and timer settings should be selected so that the relay would distinguish between power swings and faults. These settings are highly dependent on the network conditions and are determined through a series of dynamic simulations for may different operating conditions. The out-of-step protection theory is further discussed in Chapter 2.

1.3. Motivation

Out-of-step protection can be an essential component of the overall transmission network protection system. The settings for OOS relays are specific to the relay location and are highly sensitive to network configuration and operating conditions. Therefore it is not possible to have a general set of parameters applicable to any OOS relay and the task of determining the specific relay parameters can be a difficult one. Setting OOS relays is not an exact science and requires some engineering judgement. There may be situations where perfect settings cannot be determined and there may be false alarms or false dismissals under certain operating conditions.

However, it is desirable to have a general methodology to identify appropriate relay parameters for a given OOS relay in a particular power transmission network. In this research, a procedure to determine preliminary relay settings that should operate for most of the expected network conditions is presented.

1.4. Objectives

The main objective of this research is to develop and validate a general method to identify preliminary OOS relay parameters appropriate for OOS protection in a complex network. These initial relay settings would provide a good starting point for designing the OOS protection schemes but may require additional modifications based on the network.

To develop a general procedure for determining acceptable OOS relay parameters, an understanding of OOS protection theory must be established. The method inevitably involves dynamic simulations and therefore, the process involves the use of a suitable simulation software. Finally, the developed procedure must be validated. To achieve the main objective, the following tasks must be completed.

1. Review literature on OOS protection and approaches used for determining settings.
2. Develop a test network model appropriate for OOS studies.
3. Develop a step-by-step procedure to select the OOS protection settings.
4. Apply relay settings procedure to the test network model and examine whether the relay operates correctly under all studied operating conditions with the setting determined.

1.5. Thesis Outline

This thesis is comprised of six chapters, described below:

Chapter 1: Provides background, motivation, and objective of this research project.

Chapter 2: Reviews relevant literature concerning out-of-step phenomenon, out-of-step protection relays, and information on detailed load models. This section provides detailed explanation of how out-of-step occurs and investigates the current protection methods and challenges. This section also presents information regarding the specific models used in the test network model.

Chapter 3: Discusses in detail the study model created to perform the out-of-step studies. This chapter presents the studied network conditions and description of preliminary model parameter selection. A study model is created in both PSSE and PSCAD EMT simulation software; a discussion is provided detailing required adjustments to match the two models. A validation demonstrates that the models are adequately similar for the required OOS studies.

Chapter 4: Presents the general approach to identify the out-of-step relay settings. A discussion concerning the limiting factors when determining relay settings is presented. This chapter considers alternative methods for determining requisite network and impedance characteristics.

Chapter 5: Demonstrates the methodology developed. Relay settings are identified for a test network by employing the methodology presented in Chapter 4. Additional network studies are performed to validate relay settings.

Chapter 6: Presents a summary of research and the conclusions with suggestions for future work.

Chapter 2 – Background and Literature Review

The objective of this chapter is to provide a detailed description of the theory behind out-of-step events and out of step protection. The typical challenges faced when performing out-of-step analysis and relay setting are also presented in this chapter.

2.1. Out-of-Step Phenomenon

2.1.1 - Two-Machine System

A two-machine system is a simple way to examine the cause and effect of out-of-step and is discussed in [5]. A simple representation of the two-machine system is presented in Figure 1.

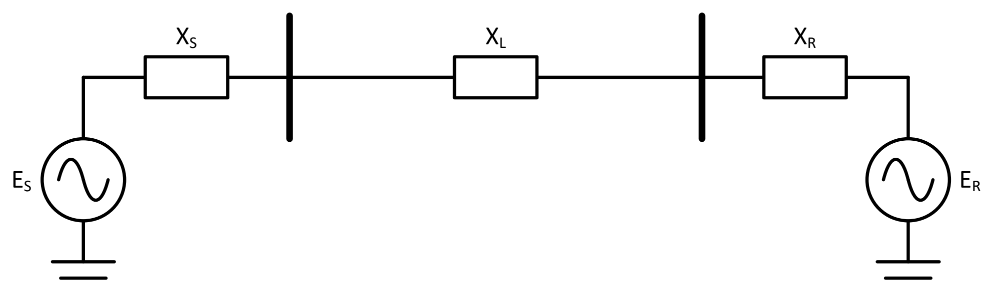

Figure 1: Two-Source System [5]

The power transfer of this system can be described using eq. 2.1:

$$P = \frac{E_S \cdot E_R}{X} \sin(\delta) \qquad (2.1)$$

Where:

E_S – internal voltage magnitude of the sending end machine

E_R – internal voltage magnitude of the receiving end machine

δ – angle difference between the sending and receiving end internal voltages

X – The total reactance between sending and receiving end voltages.

The active power of the two-machine system assuming constant internal voltages (E_S and E_R) and constant impedance (X) is plotted in Figure 2.

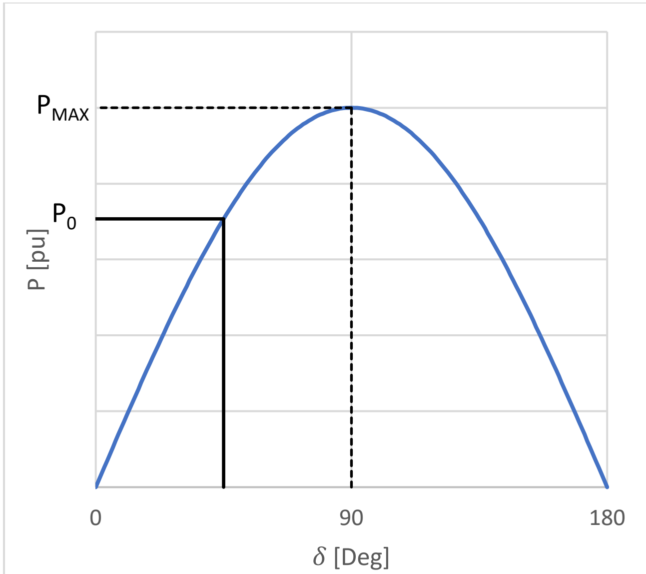

Figure 2: Active power transfer in a two-machine system [5]

Figure 2 clearly shows that the power transfer greatly depends on the angle between the two machines, with the peak power transfer occurring when the angle δ is equal to 90 degrees.

If we consider a fault on the transmission line, located m per unit distance from the sending end, the effective transmission reactance between the sending and receiving end will increase depending on the type of fault which occurs. A graphical representation of the fault is presented in Figure 3.

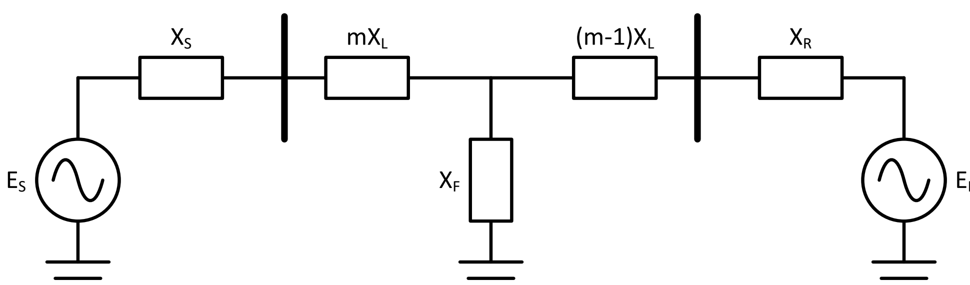

Figure 3: Two-Source System, fault applied on transmission line [5]

A fault on the system will result in a different power-angle characteristic compared to the system intact conditions. A P-δ plot demonstrating the approximate difference in power flow between the sending and receiving for different types of faults on the transmission line is presented in Figure 4.

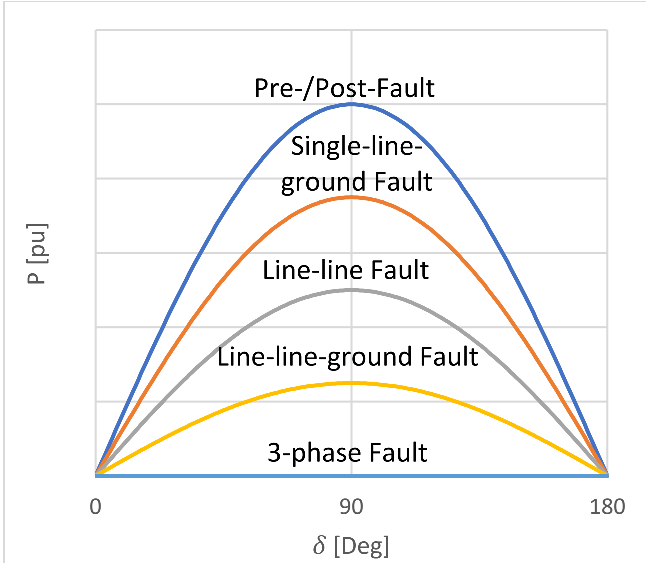

Figure 4: Active power transfer in a two-machine system [5]

As shown in Figure 4, a single-line-ground fault will have the least impact on the power transfer between the sending and receiving end, while a three-phase fault will have the largest effect, reducing the power transfer between ends to zero.

2.1.2 - Dynamic Stability and Equal Area Criterion

During normal operation, a generator will generator an electrical torque equal to the mechanical torque on the rotor shaft. At steady state, the generator will run at a constant speed, at a point where the electrical and mechanical torque match. When a fault occurs, there will be a decrease in the power transfer resulting in a decrease of the electrical torque. The mismatch in the electrical and mechanical torque will result in the generator rotor accelerating, this phenomenon may lead to unstable network conditions.

The equal area criterion [5][6][7] is a method of determining the transient stability of a two-machine system. This method considers the plot of power-transfer and power angle and determines whether the system has dynamic stability.

Consider the two-source power system presented above, when operating in steady state the system operates at a point δ_0 and transfers power P_0. When a fault is applied, the power will be reduced to P_F. As described earlier, this will result in a decrease in the electrical torque and as a result the generator rotor will begin to accelerate and the angle δ will increase, this is illustrated by the red line in Figure 5 below.

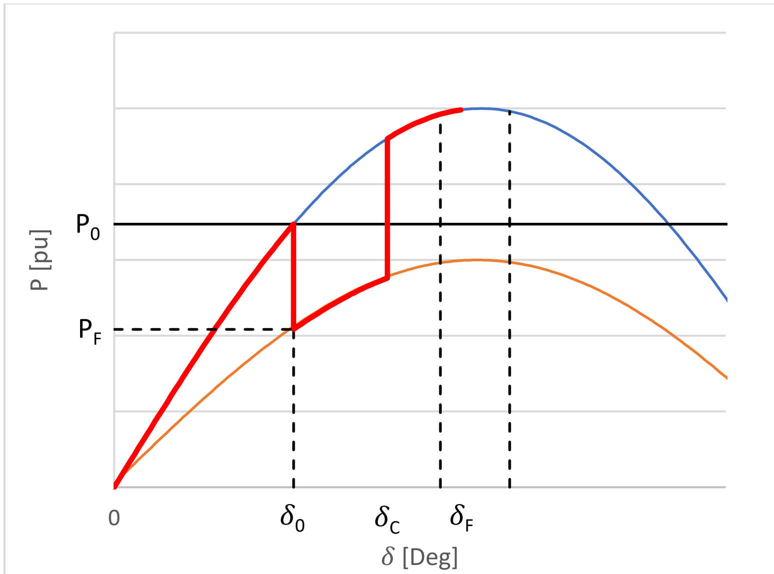

Figure 5: Two-Machine system, power-angle trajectory during fault

After some time, the fault will be cleared, at this point the angle will be at a point δ_C. There is a decelerating torque acting on the rotor because the electric power P_C at angle δ_C is larger than the mechanical power input P_0. Due to the inertia of the system, the angle cannot immediately begin returning to the δ_0 point. Due to the rotor system inertia, when the fault is cleared, the angle will continue to increase to a point δ_F, as depicted in Figure 6. The point δ_F should correspond to the point where the energy lost during the deceleration (area 2) is equal to the energy gained during acceleration (area 1).

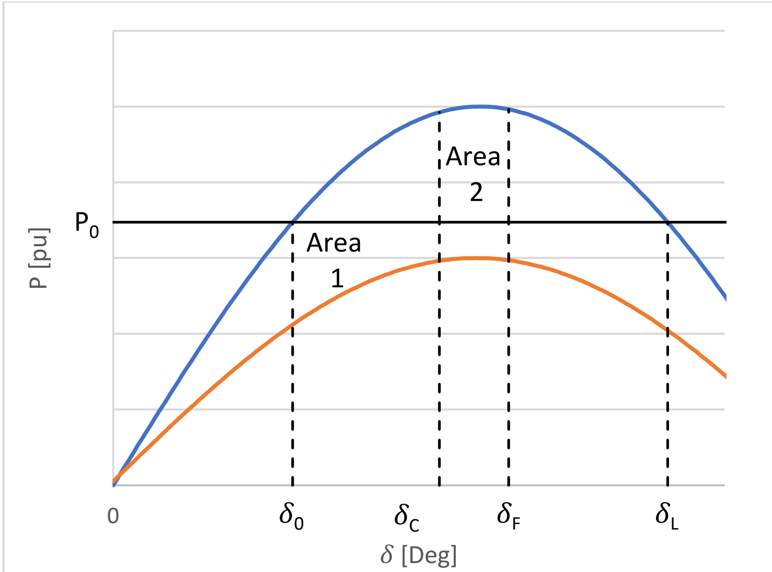

Figure 6: Two-Machine system, Equal Area Criteria – transiently stable [3]

If δ_F is smaller than δ_L (as shown in Figure 6), then the system is transiently stable (stable power swing), and if the system is sufficiently damped the angle difference should return to the original balance point δ_0. If area 2 is smaller than area 1 by the time δ has reached δ_L, as shown in Figure 7, then further increases of δ will result in the electrical power output being less then the mechanical power. This will cause the rotor to again accelerate and angle δ will further increase beyond recovery.

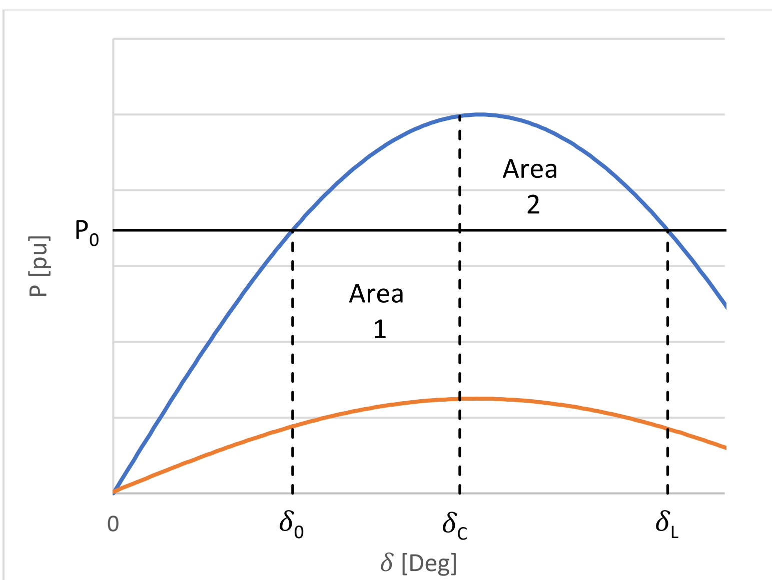

Figure 7: Two-Machine system, Equal Area Criteria – transiently unstable [5]

The scenario depicted in Figure 7 is a transiently unstable scenario or an unstable power swing. When unstable conditions exist, one of the generators rotates at a speed different from the other generator. Poles slipping will occur while the two machines are operating at different speeds. This loss of synchronism between the generators is referred to as an out-of-step condition.

2.2. Out-of-Step Relays

When a system becomes out-of-step (OOS), it could affect the power delivered to customers and could seriously damage equipment. When out-of-step conditions are identified, it is desirable to separate the system so that the areas where the OOS is occurring will not impact the rest of the networks. Out-of-step relays[5][8][9][10] can be used to detect OOS conditions and separate the system at strategic locations to mitigate and reduce the impact of the OOS conditions.

2.2.1 - Example of OOS Relay Calculations

The basics of power swing stability and power swing phenomena is described in [9]. It also provides details of how the out-of-step relay measurements may be calculated. Consider the two-machine system introduced in Section 2.1, with a protective relay connected at the sending end bus (Bus S) as shown in Figure 8.

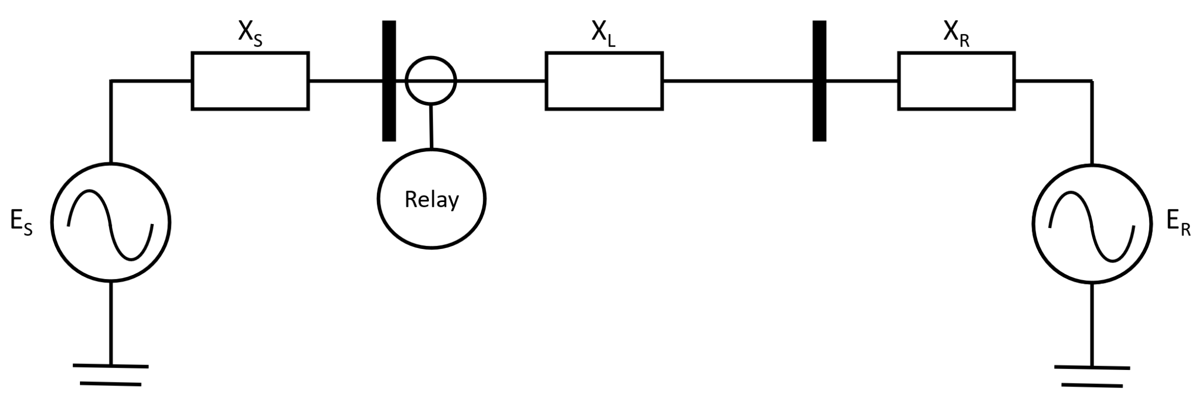

Figure 8: Two-Source System with protective relay [9]

The current and voltage seen by the relay are calculated using eq.2.2 and 2.3:

$$I = \frac{E_S - E_R}{Z_S + Z_L + Z_R} \tag{2.2}$$

$$V_S = E_S - I * Z_S \tag{2.3}$$

The impedance seen by the protection relay at Bus S (sending end) is calculated from the voltage and current as shown in eq. 2.4.

$$Z_{Relay} = \frac{V_S}{I} \tag{2.4}$$

Where:

V_S – Voltage at Bus S

I – Current flowing from Bus S to Bus R

During the steady state operation, the machines operate at the same frequency ($f_S = f_R$). During a power swing the two-machines will no longer operate at the same frequencies. The instantaneous voltage and current are calculated considering the rotor phase angle of both machines. The rotor angle for each machine is calculated according to the eq. 2.5 and 2.6.

$$\varphi_{ES}(t) = \theta_{ES} + 2\pi f_S t \tag{2.5}$$

$$\varphi_{ER}(t) = \theta_{ER} + 2\pi f_R t \tag{2.6}$$

Where:

θ_{ES} – initial rotor angle of sending end machine

θ_{ER} – initial rotor angle of receiving end machine

f_S – frequency at sending end machine

f_R – frequency of receiving end machine

the instantaneous values for current and the sending/receiving end voltages can be calculated using eq 2.7, 2.8 and 2.9 respectively.

$$|I|e^{j\varphi_I(t)} = \frac{(|E_S|e^{j\varphi_{ES}(t)} - |E_R|e^{j\varphi_{ER}(t)})}{|Z_T|e^{j\theta_{ZT}(t)}} \tag{2.7}$$

$$|V_S|e^{j\varphi_{VS}(t)} = |E_S|e^{j\varphi_{ES}(t)} - |I|e^{j\varphi_I(t)} * |Z_S|e^{j\theta_{ZS}} \tag{2.8}$$

$$|V_R|e^{j\varphi_{VR}(t)} = |E_R|e^{j\varphi_{ER}(t)} + |I|e^{j\varphi_I(t)} * |Z_R|e^{j\theta_{ZR}} \tag{2.9}$$

A power swing is a three-phase phenomena, the above equations represent the phase A quantities, phase B and phase C are shifted by 120˚ and 240˚ respectively.

The impedance as seen by the relay can be calculated with eq 2.10:

$$Z_S(t) = \frac{|V_S|}{|I|} e^{j(\varphi_{VS}(t) - \varphi_I(t))} \tag{2.10}$$

The trajectory of the impedance locus is plotted in Figure 9. The impedance trajectory depends on the ratio between the sending and receiving end internal voltage magnitudes (E_S/E_R) and the electrical center of the network (midpoint of the total system impedance $Z_T= Z_S + Z_L + Z_R$).

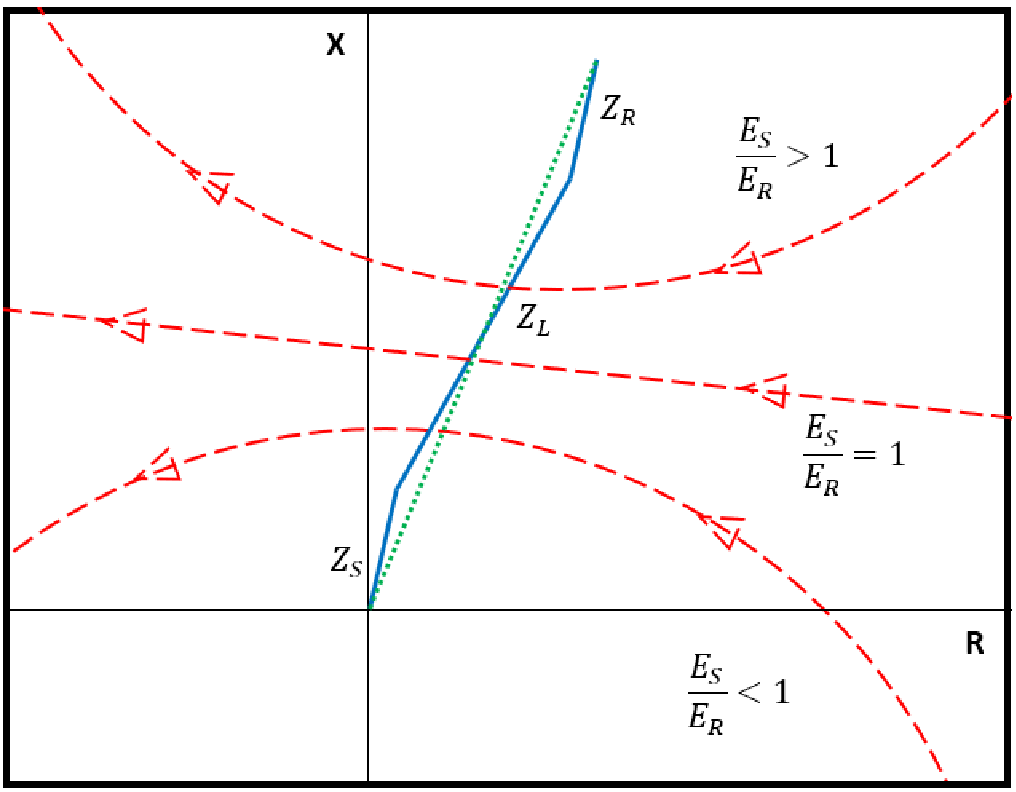

Figure 9: Impedance swing trajectories seen by protection relay[9]

When both voltage magnitudes (E_S and E_R) are equal, the swing locus is a straight line, perpendicular to the total impedance Z_T and passing through the electrical center at $\delta = 180^\circ$. If E_R is larger than E_S, the impedance trajectory will be a circle which passes just above the electrical center. Conversely if E_S is smaller than E_R, the trajectory will be a circle passing just below the electrical center. The direction of the impedance trajectory depends on the frequencies of each machine. If f_S is larger than f_R the impedance trajectory is from right to left, if f_S is smaller than f_R the impedance trajectory is from left to right.

When considering a real power system, the machine frequencies are not constant, and the voltage magnitudes are influenced by many factors in power system network. An illustration of the power swing trajectory in a typical power system is presented in Figure 10. Included in the figure are two example impedance zones for distance protection relay.

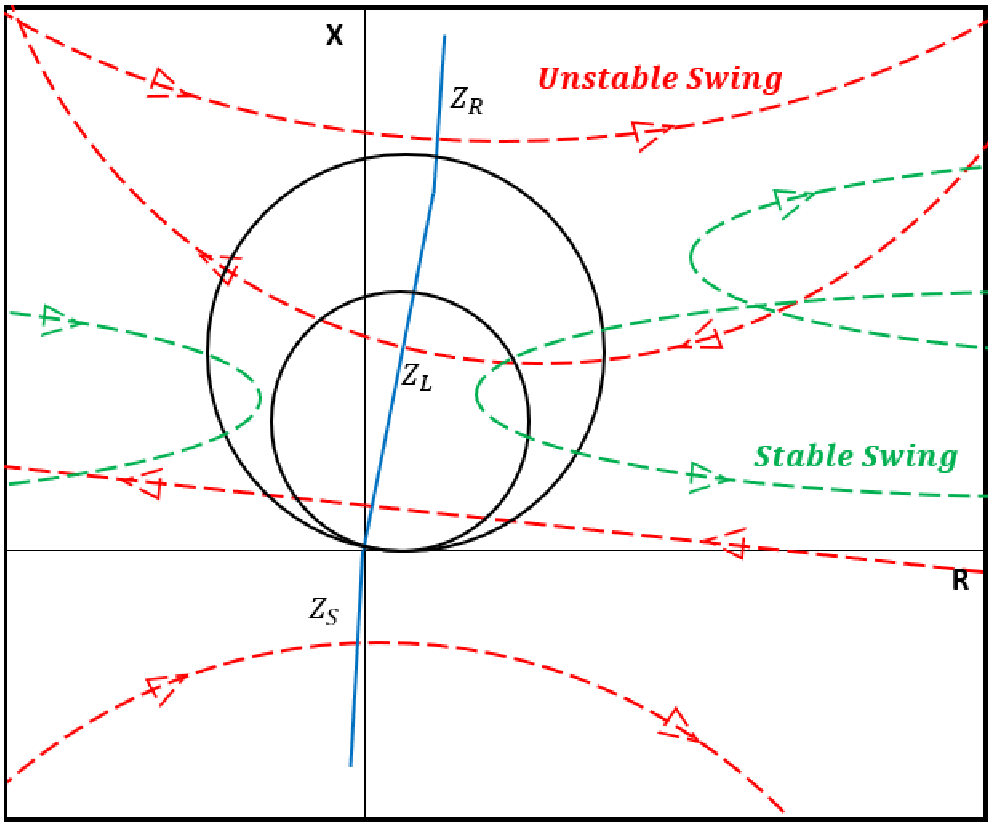

Figure 10: Impedance swing trajectories seen by protection relay in a "Real" power system.[9]

After a disturbance, there will be oscillations and power swings in the network, these may be stable swings or unstable swings as depicted in Figure 10. As demonstrated in Figure 10, it is possible for the impedance to enter a protection zone even during a stable power swing, this could cause the distance relays to activate and cause undesired tripping. Using out of step relays, it is possible to develop logic to trip during an unstable power swing (OOS condition) and block distance protection elements from tripping for stable power swings.

2.2.2 - Out-of-Step Relay Background

Details of out-of-step relays are presented in [9] along with a discussion of blocking and tripping relays. An out-of-step relay will typically measure the impedance at a specific location and determine whether any observed impedance swings are stable or unstable. During a power swing, the impedance profile changes slowly, during a fault the impedance will change very quickly (nearly instantaneously). The out-of-step relay will use the speed of the impedance swing to differentiate between swing events and faults. Depending on the relay settings/capabilities, the relay can issue blocking signals, or tripping signals.

The OOS relay uses impedance characteristics and timers to determine the speed of the impedance swing. Typically, a timer will be initiated once the impedance swing locus enters the impedance characteristic, if the swing locus can travel the distance of the impedance characteristic before the timer expires the event will be classified as a fault, if the timer expires and then the impedance travels the distance the event is classified as an OOS event.

2.2.3 - Power Swing Detection Schemes

There are numerous ways in which a power swing can be detected by a relay[9][11], several of these different methods will be discussed below.

A) Traditional Methods

The traditional methods typically employ the use of blinders or impedance characteristics to measure the positive impedance as seen by the relay to determine the rate-of-change of the impedance and identify power swings. There are three typical schemes:

- Single-blinder schemes
- Two-blinder schemes
- Concentric characteristic schemes

These schemes are described below.

a. Single-Blinder Schemes

The single-blinder scheme consists of one blinder pair, consisting of a left and right-side blinder. The blinder pair can be used to detect unstable power swing and out-of-step conditions. When the impedance swing enters one side of the blinder a timer will commence, if after a specified amount of time the impedance swing exits the other side of the blinder, an unstable power swing is detected. A simple diagram of a single-blinder scheme is presented in Figure 11.

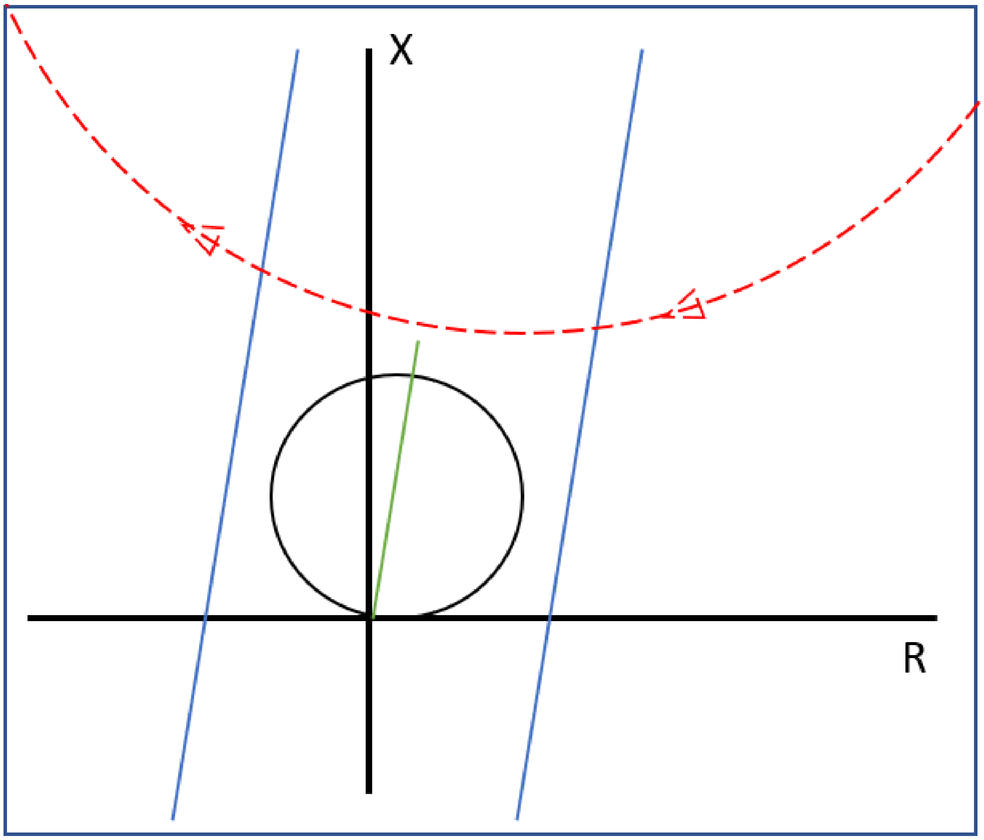

Figure 11: Single-blinder scheme (including MHO – zone operating characteristic)[9]

The single blinder swing cannot be used for out-of-step blocking (OSB) during stable power swings because with only one blinder, the impedance will have crossed the total impedance line before a block signal could be issued. The single blinder can implement out-of-step tripping (OST), and the tripping function will be like trip-on-way-out (TOWO): when the tripping signal is issued, the impedance will have already crossed the line and the angle will be moving further away from 180˚.

b. <u>Two-Blinder (double-blinder) scheme</u>

The two-blinder scheme uses two pairs of blinders, the inner and outer blinders, as the name implies. The inner blinders are set so that both the left and right blinders are inside the left and right blinders of the outer blinders. The inner and outer blinders are separated by an impedance ΔZ. An example of the two-blinder scheme is presented in Figure 12.

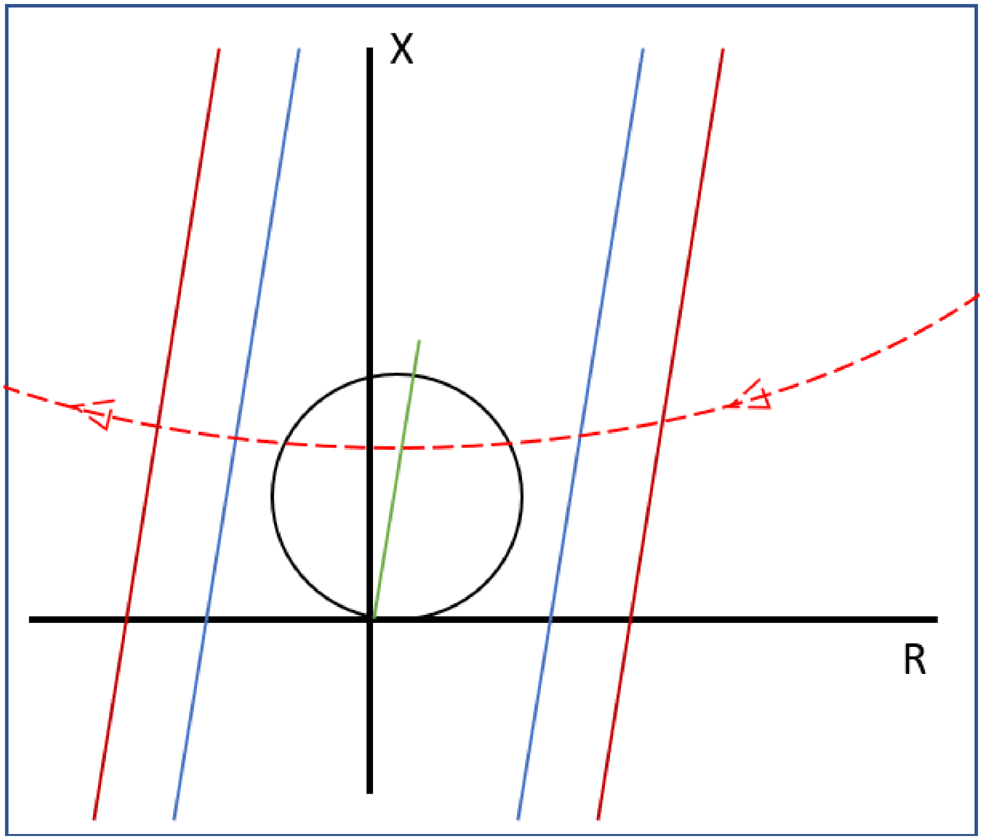

Figure 12: Double-blinder scheme (including MHO distance element)[9]

The two-blinder scheme can be used for either OSB and OST functions and in some situation both. As stated previously, disturbances may result in stable power swings, where no element tripping is required, or unstable power swings, where network separation should be used to protect the system. With the use of two timers, a two-blinder scheme can distinguish between stable power swings, unstable power swings and faults. The first timer Tost is used to determine if an event is a fault or an impedance swing, the second timer Tosb is used to determine whether the impedance swing is stable or unstable. The timer Tosb must be larger than Tost. Both timers are set to begin when the impedance loci cross the outer blinder.

During a fault, the impedance will cross from the outer to inner blinder nearly instantaneously. During a power swing, the impedance will travel at a slower speed. If the impedance loci can cross from outer to inner blinder before the timer Tost expires, a fault is determined, if Tost expires and then the impedance loci cross the inner blinder, a swing is determined, the swing may be stable or unstable. If the impedance loci stays between the outer and inner blinder for a period longer than Tosb, the swing is moving slowly and is likely a stable power swing.

In the event of a fault, neither OST nor OSB functions should operate, the distance protection should take action to mitigate the fault. In the event of an unstable power swing, the OST function should activate and separate the network. During a stable power swing the OSB function should block the distance protection from operation as no element tripping is required. These points are summarized in Table 1.

Table 1: Double-blinder OSB/OST actions

Time (t) to travers ΔZ	Action
t < Tost	No action, distance protection will activate
Tost < t < Tosb	OST relays should separate network
Tosb < t	OSB should block distance protection from activation

c. Concentric Characteristic Schemes

The operation of the concentric characteristic scheme is very similar to the two-blinder scheme, with the primary difference being that instead of an inner and outer blinder, the concentric characteristic scheme uses two concentric impedance characteristics. A few examples of concentric characteristics are presented in Figure 13.

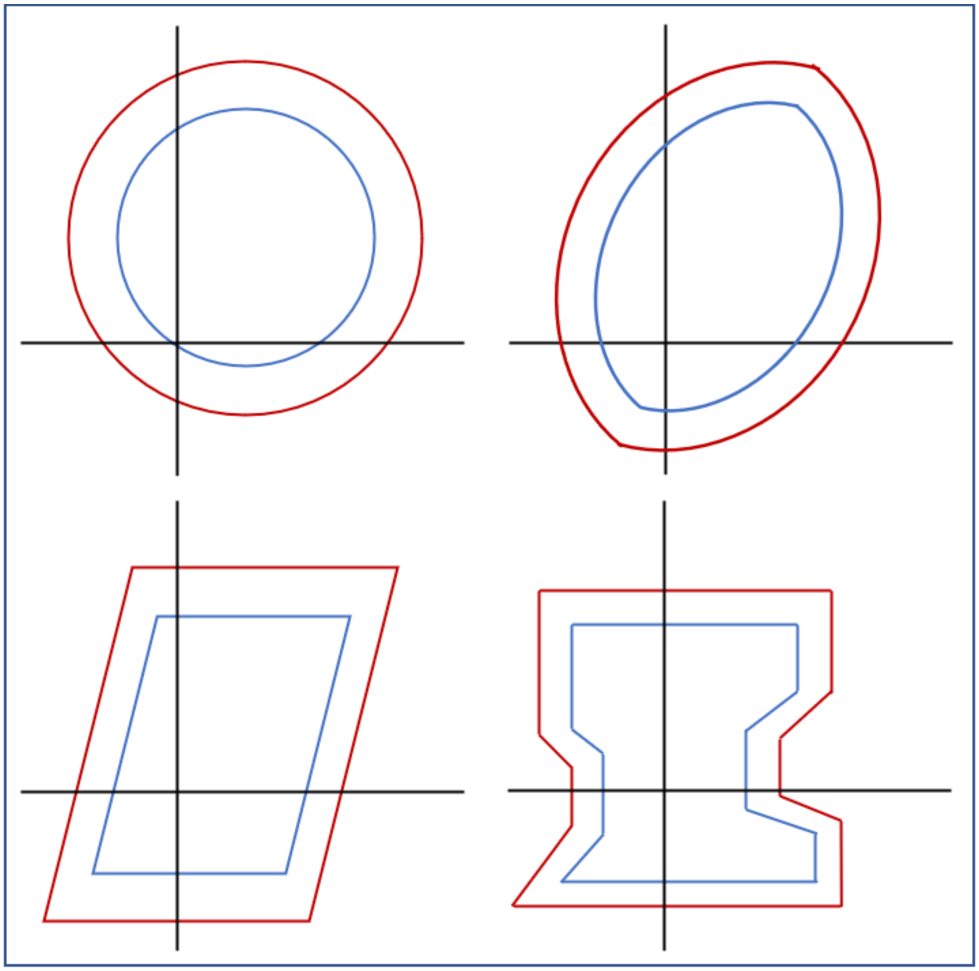

Figure 13: Concentric characteristic schemes[9]

Like the two-blinder method, the concentric characteristic schemes can be used for both OSB and OST functions. The inner characteristic may be an existing distance protection zone or a specific impedance characteristic for detecting power swings, the outer characteristic is usually an impedance characteristic specifically for power swing detection.

When applying the OST function, sometimes a modified concentric characteristic is used which has three characteristics (outer, middle, and inner). When using the three characteristics for OST functions two timers are required. The first timer begins when the impedance loci enters the outer characteristics, the second time will begin when the impedance loci enters the middle characteristic. If both times have elapsed and then the impedance enters the inner characteristic, an unstable power swing is declared and the OST. A three-impedance characteristic scheme is presented in Figure 14.

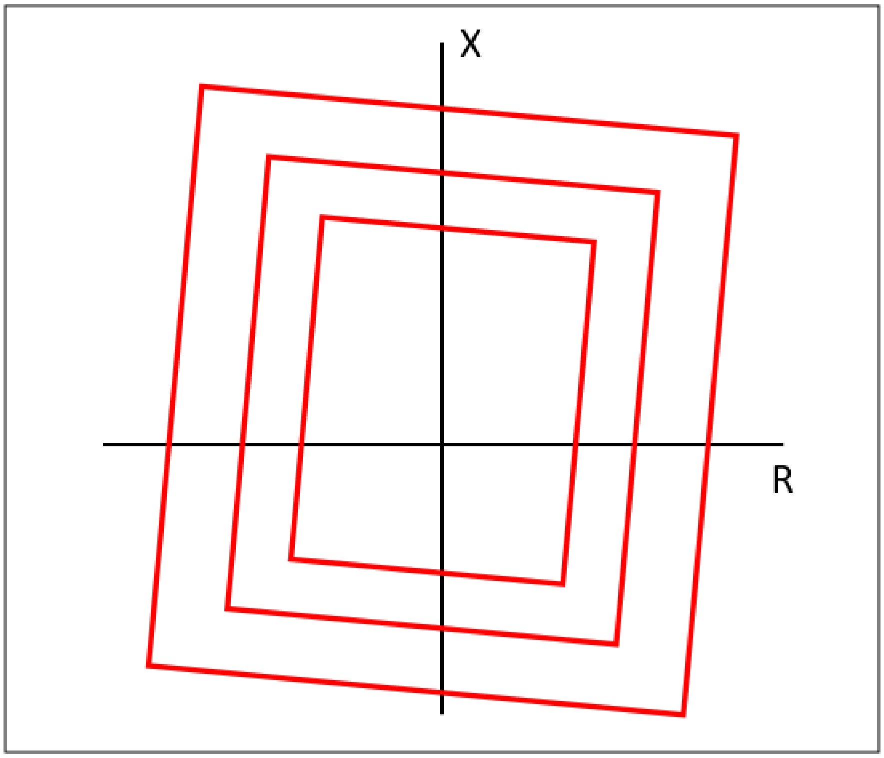

Figure 14: Three-characteristic OST scheme[9]

B) Non-Traditional Methods

In addition to the traditional power swing methods presented above, there are non-traditional methods as well, these include:

- Continuous superimposed ΔI
- Continuous Impedance ΔZ calculation
- Swing-Center voltage (V cosφ) and Its Rate-of-Change

These methods are briefly described below.

a. <u>Continuous superimposed ΔI</u>

The continuous superimposed current method is primarily used for OSB functions. The method works by taking continuous current (I) measurement and comparing the present measurement with a value recoded 2 cycles previously, which is stored in a buffer. If difference is greater than 5% of the nominal current, then a delta current (ΔI) is detected. If for 3 cycles there is a continuous ΔI measurement, then a power swing is determined and OSB functions should assert.

This method can detect very fast power swings that are usually more difficult to detect using conventional methods. However, if the slip rate is very slow (below 0.1Hz) it may be difficult to detect if the current difference between the present and 2 cycle measurement are less than 5% the nominal current. An illustration of the continuous superimposed current method is shown in Figure 15.

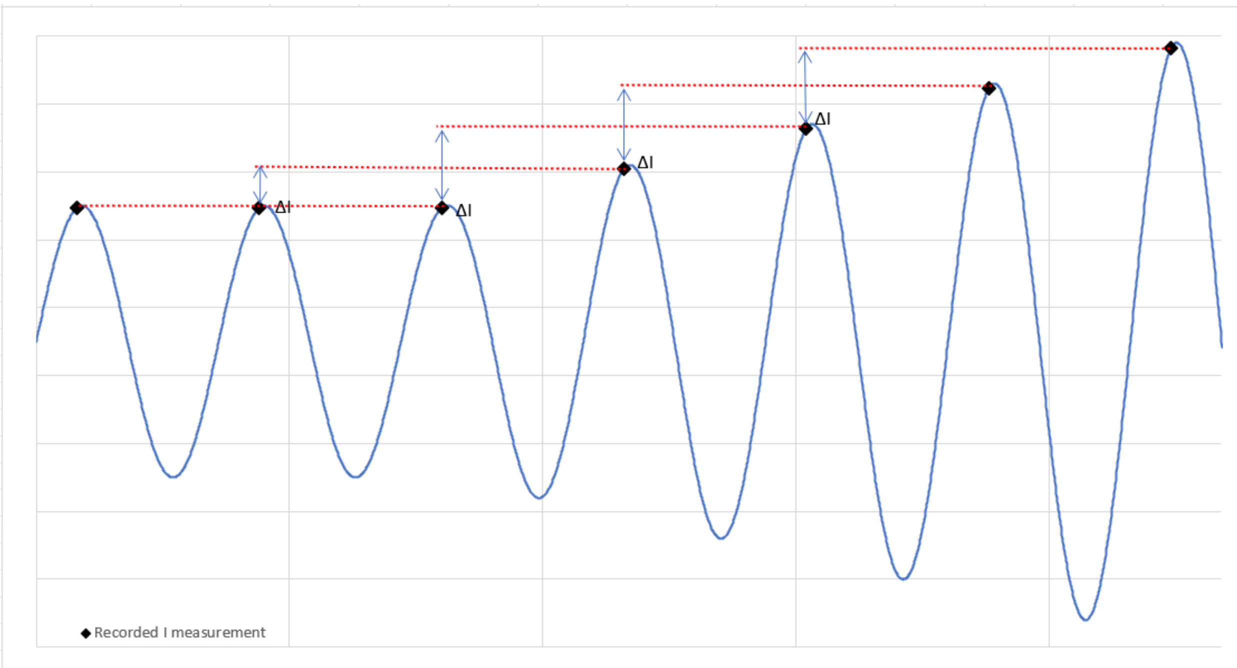

Figure 15: Continuous Superimposed Current Method[9]

b. <u>Continuous Impedance ΔZ calculation</u>

The continuous impedance ΔZ calculation method works by calculating the R and X values of the impedance and comparing the values with previous calculating based on criteria of monotony, continuity, and smoothness to detect power swings. This method is also used for OSB functions.

The R and X values of the impedance are calculated for each quarter (1/4) cycle and the previous values are stored in memory. Criteria thresholds are calculated automatically based on previous values stored in memory. There are three criteria that are briefly discussed below.

Monotony – used to ensure the direction of the impedance movement has not changed, this is done using the derivatives of R and X.

Continuity – used to ensure the impedance trajectory is not stationary, this is done by evaluating whether the distance between concurrent R and X values exceed a threshold.

Smoothness – used to ensure no abrupt changes in the impedance movement, this is done by comparing the ratios of successive differences in R and X and ensuring they are below a threshold.

The thresholds used in the above criteria are not static, they are automatically calculated and updated based on the previous values. If the above criteria are fulfilled for successive calculations (typically 6), then a power swing is declared. The declaration of a power swing will not be removed until there are successive calculations where the above criteria are not met. When performing the OSB, the blocking signal will not be issued until the swing enters a starting polygon characteristic which is automatically calculated to encompass the blocked zones. Additional details of the continuous impedance calculation method can be found in [9].

c. Swing-Center voltage (V cosφ) and Its Rate-of-Change

As discussed in section 2.1.1, when considering a two-machine system, the electrical center of the system is the midpoint of the total impedance of the line and sources. The voltage at the electrical center is referred to as the swing-center voltage. During a power swing, the voltage at the electrical center will go to zero when the angle between the two machines is 180˚. A phasor diagram of a two-machine system with SCV is presented in Figure 16

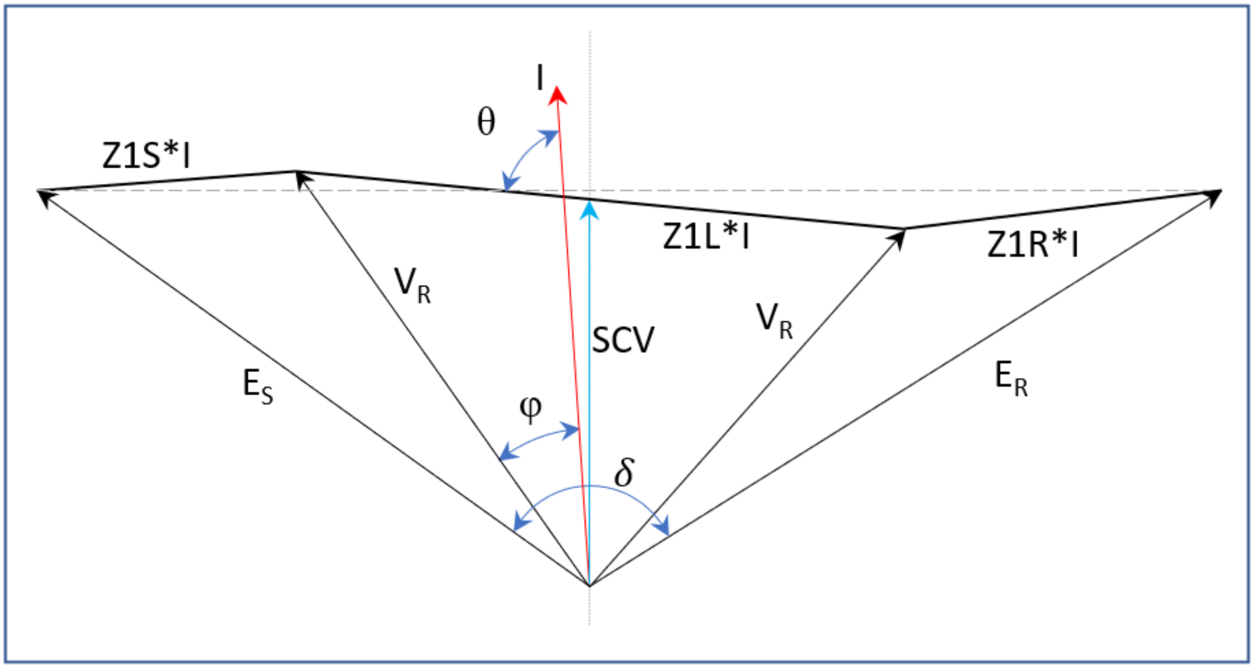

Figure 16: Swing Center Voltage – voltage phasor diagram, Two-machine system[9]

In a homogenous high-voltage power system the impedance angle θ is close to 90˚. Figure 17 presents an update phasor diagram considering this homogenous system.

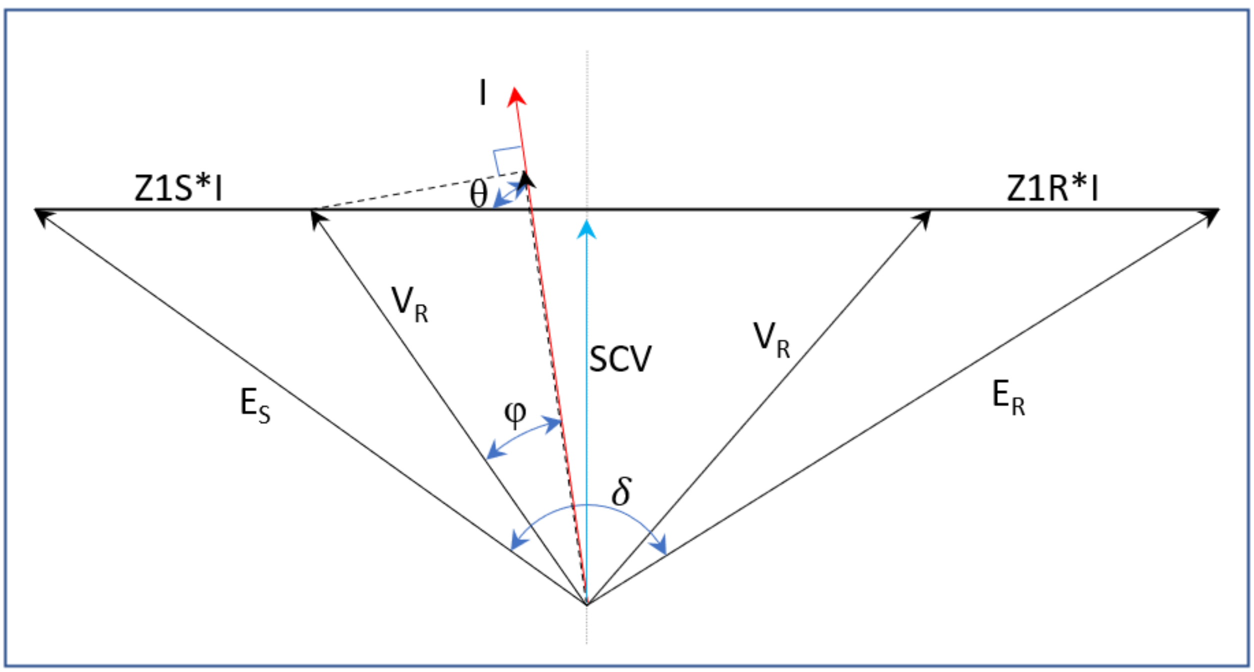

Figure 17: Swing Center Voltage – voltage phasor diagram, Two-machine system (alternate)

At the relay, the swing center voltage can be approximated as shown in eq. 2.11.

$$SCV \approx |V_S|cos\varphi \tag{2.11}$$

Where:

V_S = amplitude of the locally measured volage (at relay)

φ = angle between VS and local current (at relay)

When detecting the power swing, it is the rate of change of the SCV that is most important, and the small approximation presented in eq. 2.11 should not impact the effectiveness of detecting power swings.

If we assume that the source voltages ES and ER are equal to the positive-sequence voltage E1, then the positive-sequence swing-center voltage (SCV1) can be simplified as eq. 2.12.

$$SCV1 = E1\cos\left(\frac{\delta}{2}\right)\frac{d\delta}{dt} \tag{2.12}$$

From eq. 2.12, the swing-center voltage will be zero when the angle (δ) is 180˚ and will be at maximum when the angle is 0˚. By taking the time derivative of SCV1, the rate-of-change can be determined, this is shown in eq. 2.13.

$$\frac{d(SCV1)}{dt} = -\frac{E1}{2}\sin\left(\frac{\delta}{2}\right)\frac{d\delta}{dt} \tag{2.13}$$

Equation 2.13 demonstrates the relationship between the rate-of-change of SCV and the two-machine slip frequency, dδ/dt.

The SCV and its rate-of-change method have the following advantages:

- The SCV is independent of the system source and line impedance,
- The SVC is bounded with strict limits of 0 and 1 pu.
- Method capable of detecting slow swings and very fast swings.

2.2.4 - Out-of-Step Blocking and Out-of-Step Tripping

In this section, the out-of-step blocking and tripping function are discussed in detail.

Out-of-step Blocking (OSB)

The purpose of out-of-step blocking is to block relay elements that are prone to tripping during power swings. Even while blocked, the relay elements should maintain the functionality to trip if a fault is detected. OSB is usually done for Zone 1 and Zone 2 protection but not for Zone 3.

Out-of-step tripping relays will generally require two impedance characteristics, this could be in the form of two blinders or concentric impedance characteristics. An example of an OOS blocking characteristic is shown in Figure 18.

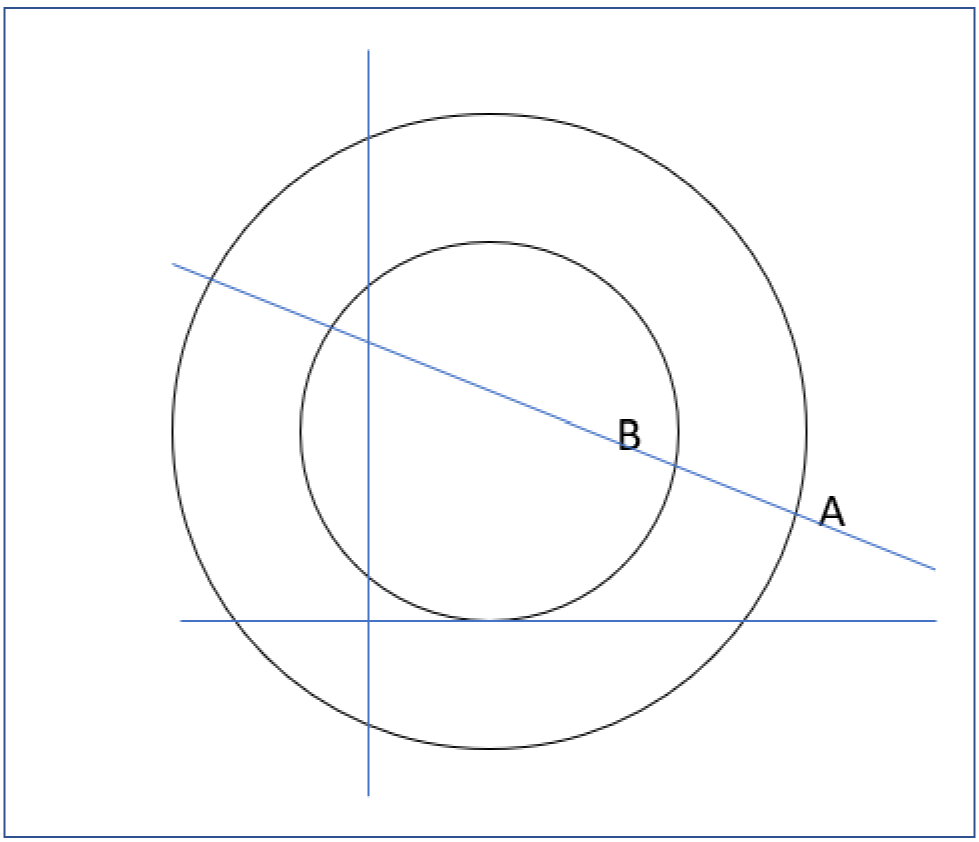

Figure 18: Example Out-of-step Blocking (OSB) characteristic [8]

As can be seen in Figure 18, during an impedance swing, the impedance locus will pass through the impedance characteristic. An out-of-step blocking timer (OBT) will begin the instance that the impedance enters the outer characteristic (point A in the above diagram). If the impedance locus travels the length between the outer to inner characteristics (from point A to point B) after a specified amount of time, then the swing will be considered an out-of-step event and the blocking unit will operate. If the impedance locus crosses from A to B before the specified blocking time, the event will be considered as a fault no blocking operations occur.

When setting OSB, care should be taken to ensure that the OSB characteristics do not encroach on the load characteristic (point) of the system and should be outside of the outermost overreaching zone of the phase distance element that will be blocked.

Out-of-step Tripping (OST)

The purpose of out-of-step tripping is to discriminate between stable and unstable power swings and separate the power system if a loss of synchronism is detected. When an unstable power swing is detected the Out-of-step relay can issue a tripping command to the local breaker or to a remote breaker.

There are a few schemes that can be used for out-of-step tripping (OST) operation. Many of the impedance characteristics used for OSB can also be used for OST. There are however additional schemes that can only provide OST functionality and not OSB functionality, such as the single blinder scheme.

The typical OST scheme consists of two impedance characteristics that are parallel to the characteristic system impedance, one on either side of the characteristic impedance. Figure 19 shows an example of an OST characteristic.

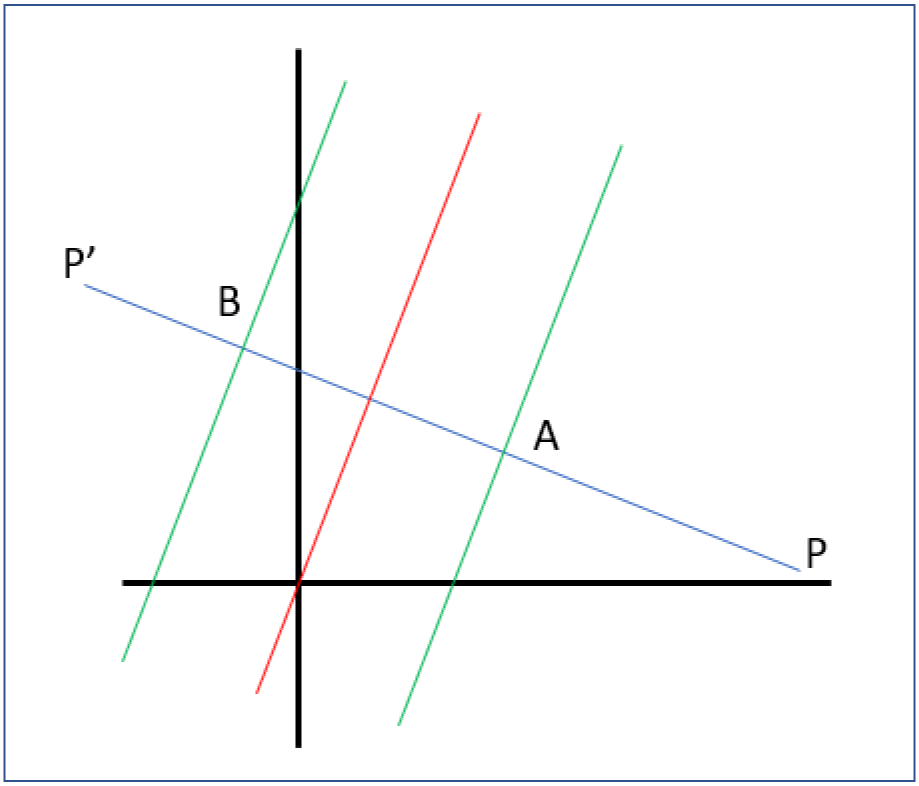

Figure 19: Example Out-of-step Tripping (OST) characteristic [8]

Figure 19 shows an unstable power swing which travels from point P to P’, the power swing crosses the characteristic impedance, this indicates that there is a loss of synchronism.

There are certain conditions that should be met when tripping issuing the OST signal:

- When separating the system there should be a balance of load and generation in the isolated system, if not load should be shed or generation curtailed.
- The “angle” should not be too close to 180˚. As the angle nears 180, there is a much larger chance of a restrike of breaker.
- Due to the changing system conditions, the electrical center of the system may change and the selection of optimal area for separation may shift. As such, it is important for system operators to supervise the system conditions to ensure best operation.

System with OSB and OST

A system that includes both OSB and OST will typically have two concentric impedance characteristics, an inner impedance enclosed by an outer impedance. When the impedance loci (swing) enters the outer characteristics, two times will start, one tripping timer (OSTD) and one blocking timer (OSBD). The OSTD timer should be set as the minimum time that must elapse before the event is declared as an OOS. The OSBD timer will be set longer so that stable power swings may be detected, and the blocking functions can be enabled.

2.2.5 - Trip-On-Way-In (TOWI) Vs. Trip-On-Way-Out (TOWO)

Once the relay logic has decided that a tripping operation is necessary, there are two options for the timing of the relay trip, Trip-on-way-in (TOWI) or Trip-on-way-out (TOWO), a description of these tripping methods is provided in [12]. As discussed in previously, the relay schemes typically consist of two blinders or impedance characteristics and timers. Figure 20 provides an example.

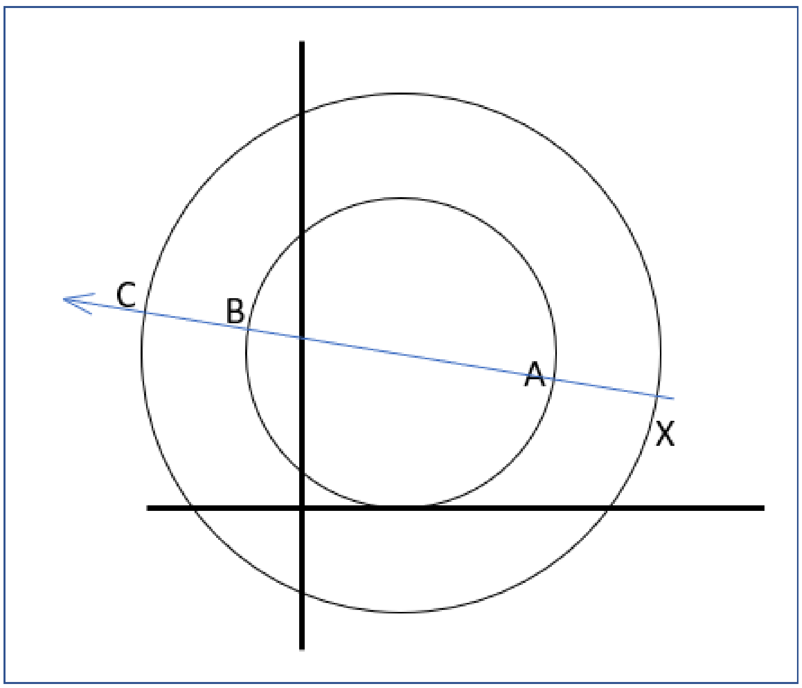

Figure 20: TOWI vs. TOWO Tripping characteristics.

When the impedance loci enters the outer blinder (Point X) of characteristic a timer will begin, if the timer expires and the impedance swing enters the inner characteristic then the swing is identified, and a trip will occur. If the trip occurs when the impedance enters the inner characteristic (Point A) this is referred to as Trip-on-way-in (TOWI), if the trip occurs when the impedance exits the characteristic (Point B) it is referred to as Trip-on-way-out (TOWO). In some schemes, when using TOWO, the relay may trip when the impedance exits the outer circle (such as point C).

There are two factors to consider when deciding between TOWI and TOWO, the voltage phase angle difference and the speed of the operation. As the impedance swing moves toward the electrical center the angle will approach 180°, tripping the relay when the angle is near or equal to 180° will stress the breaker and may result in a restrike. When using a TOWI scheme, the angle is approaching the electrical center. On the other hand, if a TOWO scheme is selected, the angle will be moving away from the 180° point and is less likely to cause a restrike.

If the speed of operation is an important factor, a TOWI scheme will have faster operation as there is a very small time delay between when the swing is detected and when the tripping operation is executed. There may be situations where the time delay which is added for a TOWO scheme may result is the system becoming unstable.

2.3. Typical Out-of-Step Relay Model (SLNOS)

In the PSSE simulation program, the SLNOS1 model is used to simulate OOS relay. The PSSE Documentation [13][14] provides a description of the SLNOS1 model. The SLNOS1 is a generalized straight-line blinder out-of-step relay. The relay can be used for both blocking and tripping functions and can trip either the local line or up to three remote lines.

The relay is designed to determine an out-of-step condition by measuring the time it takes for the apparent impedance locus to pass through a defined zone, which depends on the type of blinder specified. The SLNOS1 relay can implement both double blinder and single blinder schemes, as shown in Figure 21.

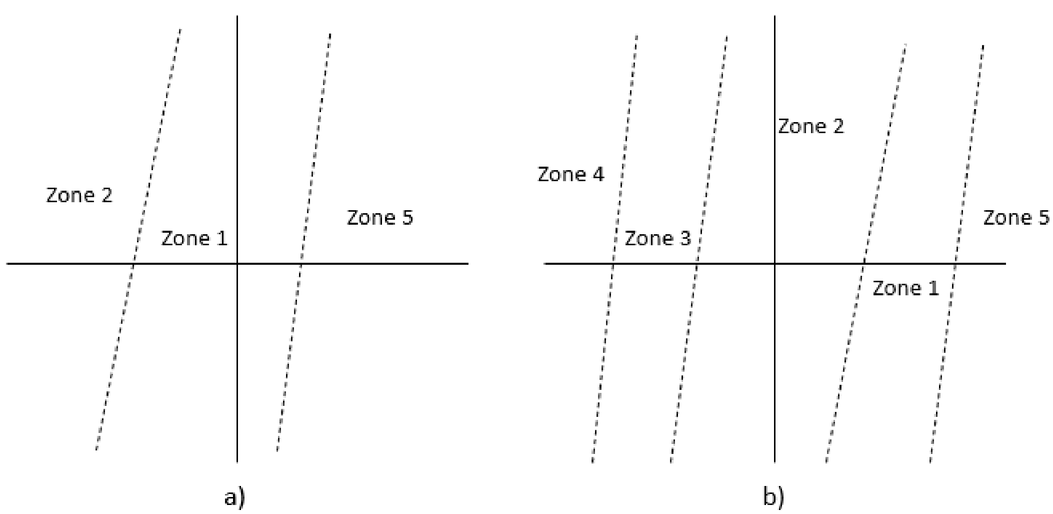

Figure 21: Blinder Zones (a) Single Blinder Scheme, (b) Double Blinder Scheme

The SLNOS1 relay model uses the same logic for detecting out-of-step conditions as explained in 2.2 . For a single blinder scheme, the OOS signal is issued if the apparent impedance crosses from Zone 2 to Zone 5 or vice-versa. For a double-blinder scheme the OOS signal is issued if the apparent impedance crosses from and outer zone (Zone 4 or 5) through the intermediate zone (Zone 1 and 3) into the inner zone (Zone 2) after a predetermined time has elapsed. Additional blinders are also available to limit the upper and lower limits of the blinders.

The SLNOS1 relay can be used to supervise another relay. The SLNOS1 can control the permissive flag of a supervised relay, disabling the tripping capability if an OOS is deterred by the SLNOS1.

Table 2 and Table 3 present the dynamic model parameters (referred to as ICONs and CONs) required when setting the SLNOS1. General parameters are used initially, and actual values will be determined after initial studies are performed.

Table 2: SLNOS1 relay: Required ICON information.

ICONs	Description	
M	1 – Single blinder tripping -1 – Single blinder blocking 2 – Double blinder tripping -2 – Double blinder blocking	
M+1	Operation mode: 0 – Monitor 1 – Monitor and operate	
M+2	From bus number	Transfer trip 1
M+3	To bus number	
M+4	Circuit ID	
M+5	From bus number	Transfer trip 2
M+6	To bus number	
M+7	Circuit ID	
M+8	From bus number	Transfer trip 3
M+9	To bus number	
M+10	Circuit ID	
M+11	Supervisory ICON number (if supervising another relay)	

Table 3: SLNOS1 relay: Required CON information.

CONs	Description
J	Interzone travel time (cycles)
J+1	Angle of first pair of impedance units (α)
J+2	Intercept of first line
J+3	Intercept of second line
J+4	Angle of second pair of impedance units (β)
J+5	Intercept of third line
J+6	Intercept of fourth line
J+7	Threshold current (pu)
J+8	Self trip breaker time (cycles)
J+9	Transfer trip breaker and delay time (cycles)
J+10	First blinder type (+1 or +2)
J+11	First blinder intercept (pu)
J+12	First blinder rotation (degrees)
J+13	Second blinder type (+1 or +2)
J+14	Second blinder intercept (pu)
J+15	Second blinder rotation (degrees)

2.4. Detailed Load Models (CMLD)

Accurate modeling of loads in time-domain stability simulations is a very challenging task when developing accurate system models for planning and operational studies. Unlike other components (generators, lines, etc.), loads usually represent an aggregate of smaller devices in the system. The aggregate is also constantly changing due to customer use and has seasonal variations such as the increase in the use of air conditioners in summer or heaters in the winter, the load profile would also be different depending on whether residential loads of industrial/commercial loads dominate. To more accurately model these details the composite load model (CMLD) was developed.

The composite load model was originally developed by the Western Electricity Coordinating Council's (WECC) Modeling and Validation Working Group (MVWG) and a version of the model is available in many simulation software tools (such as PSS/e).

The PSSE documentation [13][14] provides details of the composite load model (CMLD). The CMLD is a simulation model designed to simulate the dynamic behavior of a load using an aggregate of three-phase models (Motor A, B and C), a single-phase air conditioner motor (Motor

D), electronic loads and static loads, all connected to a low-voltage bus. The general network diagram of the CMLD model is presented in Figure 22.

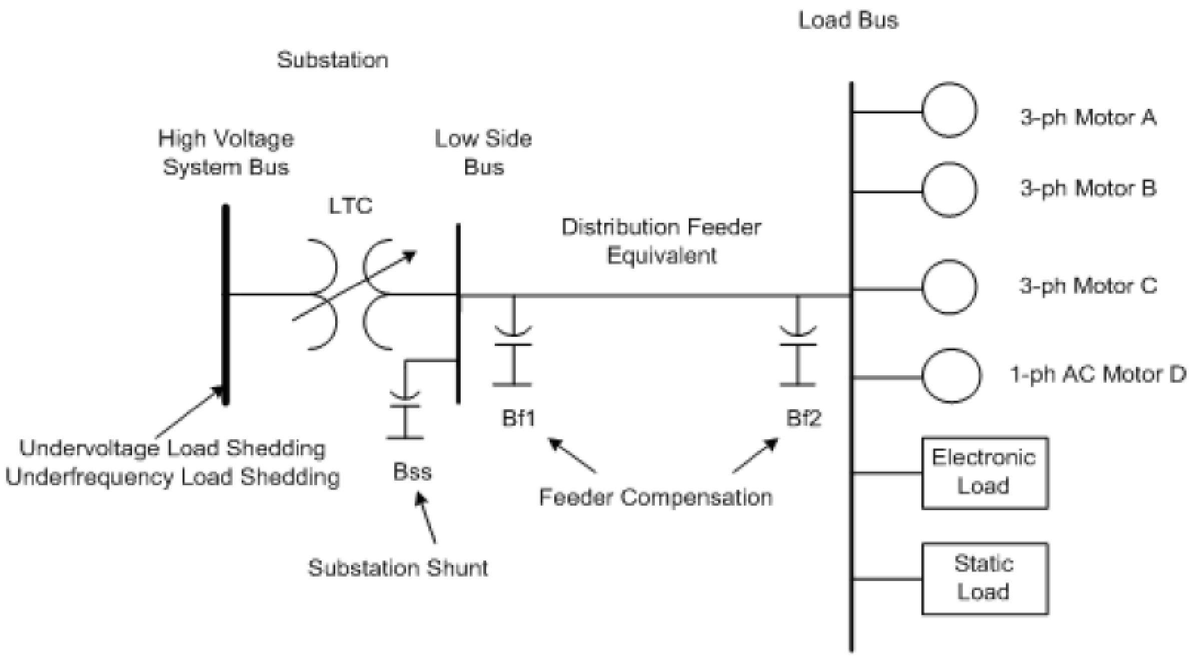

Figure 22: Composite Load Model (CMLD) general model[13]

The CMLD is usually applied to loads connected at the high voltage level, the CMLD model is comprised of the following components:

- Substation transformer with load tap changer (LTC) control
- Substation shunt
- Distribution feeder equivalent
- Feeder Compensation
- Motor Loads (Motors A, B, C, D)
  - Motors A, B and C represent three-phase induction motors
  - Motor D represents a single-phase air conditioner motor with built in protection
- Electrical loads
- Static Load
- Load Shedding

The full set of input parameters for the PSSE CMLD model is presented in the appendix. Here we will briefly highlight some of the details and features of the model.

When specifying the distribution of the load into the different components of the CMLD model, the load will be split based on specified percentages for each Motor (A-D) and the Electronic load, the remaining load not assigned to either a motor or the Electronic load will be assigned to the static load portion.

In the PSSE model of the CMLD the Motor models A, B and C are represented by the induction motor model CIM6BL from the standard model library. The Motor D model (representing an air conditioner) using the user-defined model ACMTBL.

The electronic load portion of the model varies as a function of the voltage. There are two specified voltage thresholds for the electronic load portion, Vd1 and Vd2. The load P and Q are constant if the volage is at a minimum value of Vd1. The P and Q will reduce linearly relative to the voltage level if it is between Vd1 and Vd2 when the voltage is Vd2 or below the load will be zero. Additionally, the CMLD model includes two steps undervoltage load shedding with user settable parameters for all Motors A-D.

When creating the CMLD model, it is possible to specify whether the model applies to a single load or to a group of loads, the groups may be specified based on owner, zone, or area.

2.5. Similar Work that is Done in this Field

The main challenge when developing the protection schemes is the computational effort and time required to identify the study conditions to test and perform all required network studies to identify the required parameters to set the relay settings.

There are similar works being done to address some of the challenges involved with OOS protection including investigating methods to improve the process of developing and setting relay protection schemes. In this section, similar work in the field will be presented.

2.5.1 - Zero-Setting Out-of-Step Blocking Protection

Zero-setting power-swing blocking protection is a protection scheme that can be implemented without the requirement for extensive network studies to identify relay settings. This method considers the swing center voltage (SCV) as discussed in 2.2. The zero-setting power-swing blocking protection is discussed in detail in [15] and is summarized here.

Zero-setting power-swing detection for OSB

Traditional methods use rate of change of impedance, zero-setting power-swing blocking considers the SVC which has already been discussed. The logic for the zero-setting power-swing blocking function is presented in Figure 23.

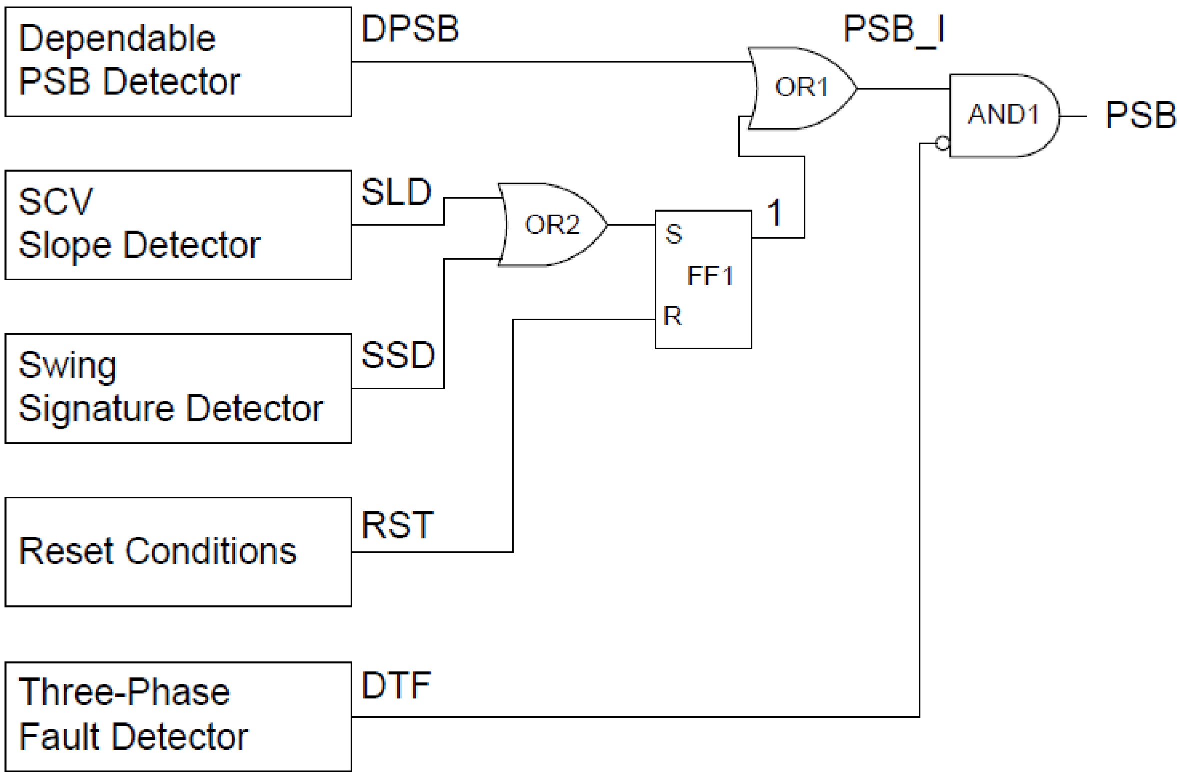

Figure 23: Zero-setting power-swing blocking logic function[15]

The function contains the following components:

- SCV slope detector

This monitors absolute value of positive-sequency swing-center voltage (SCV1) rate of change, magnitude, and output of a discontinuity detector. This generates a OSB signal if the rate of change (|d(SVC1)/dt|) is significant, as in a power swing. The generator the OSB signal the rate of change must be above a specified minimum and the magnitude of the SVC1 must be within a set of maximum and minimum limits, additionally the pos-seq impedance must be within a starter zone.

The starter zone is a zone selected to reduce the sensitivity of the power-swing detector by limiting to only pos-seq impedance trajectories that have a chance to enter mho element characteristics during power swing. The actual area covered by the starter zone is not critical and will be set to encompass all mho characteristics that must be blocked by OOS protection.

The output of the slope detector is blocked if rate of change exceeds a set limit of if the discontinuity detector is above a certain threshold. The slope detector will detect most power-swings, but in difficult situations may not operate. The slope detector is supplemented with two additional detectors to aid in detecting the power swing under difficult situations, the swing signature detector and dependable OSB detector.

- Swing Signature Detector

This detector complements the slope detector and supplements the dependable OSB under certain situations. This detector operates on the fact that if a fault detector picks up during a power swing, no discontinuity will be present on the SCV1 signal prior to detection because the fault detection is not the result of an actual fault. This is done by storing the first-order derivative, dSCV1, continuously in a buffer memory over an interval of a few cycles. The maximum value in the buffer is determined and referred as $dSVC1_{MAX}$, for a real fault $dSVC1_{MAX}$ will be very high (because of the discontinuity caused by the fault). Older samples are compared to $dSVC1_{MAX}$, if the fault is real, the samples should be below $dSCV1_{MAX}$, if the fault is the result of a power-swing then the values should be above $dSVC1_{MAX}$. The swing signature detector will assert if the fault is determined to be caused by a power-swing.

- Dependable OSB Detector

This detector asserts the OSB signal where neither the slope detector nor the swing signature detector can detect a power swing fast enough (such as after a lasting external fault has been cleared). This detector issues a temporary OSB signal that provides the slope detector to identify whether a power swing occurred, this is to compensate for the pickup delay of the slope detector. There are general rules as to when the dependable OSB detector will assert, these are summarized in Table 4.

Table 4: General rules for asserting dependable OSB signal.

External Forward Faults	Reverse faults
- Fault detector signal lasted for several cycles - No power swing detected - No trip issued by relay - At least one Zone 1 phase-mho has picked up	- No power swing detected - Fault detector signal lasted for several cycles has been cleared - No trip issues by relay - A Zone 2 mho-phase has picked up within time delay

- <u>Three-phase fault detector</u>

Monitors the SVC1 signal to detect if a three-phase fault occurs on a transmission line during a power swing, if a fault occurs a discontinuity will be present in the SCV1 waveform. The discontinuity can be monitored when the second derivative of the SCV1 signal takes a higher value than usual, also the SVC1 should have a low value and very small rate of change.

- <u>Reset Condition</u>

Monitors conditions to determine that the power swing has receded and issues a reset signal to the main flip-flop as depicted in Figure 23.

<u>Use of zero-setting power-swing detection for OST</u>

The requirement for excessive studies to determine OST settings could be eliminated if the OST functions could use the output of a robust OSB function that makes certain that the network is experiencing a power swing and not a fault. The zero-setting power-swing detection method described in this section could be used by an OST scheme to guarantee that events are power swings and not faults.

The OST function could simply monitor the trajectory of the measured impedance to identify when the impedance crosses the complex plane from either left-to-right or right-to-left and issue a TOWO at a desired phase-angle.

The paper [15] presents an OST function designed to take advantage of the reliable OSB that will not require any stability studies if one wants to apply TOWO. The OST function offers the following options.

- TOWO during first slip cycle

- TOTO after a set number of slip cycles has occurred
- TOWI before completion of the first slip cycle

The OST scheme monitors the positive-sequence impedance in the complex plane. The scheme still requires two sets of reactive and two sets of resistive blinders like the traditional OST schemes, but here, the blinder settings can be easily calculated.

2.5.2 - Method for Setting OOS Blocking and Tripping Using Dynamic Simulations

The paper [16], proposes a method for setting OOS relay setting for blocking and tripping. An example is provided based on a real-life event that occurred in Peru.

Description of Event

The paper presents a simulation of a real out-of-step event that occurred in the Peruvian system. The North-Center area (SICN) and South area (SISUR) of the Peruvian network are connected by a set of two parallel lines as shown in Figure 24. This link is approximately 600 km between Mantaro and Socabaya, with Cotaruse located somewhere between. On January 10, 2010, a phase-to-phase fault occurred on line L-2053, a simultaneous single phase-to-ground fault occurred on line L-2054 as show in Figure 24

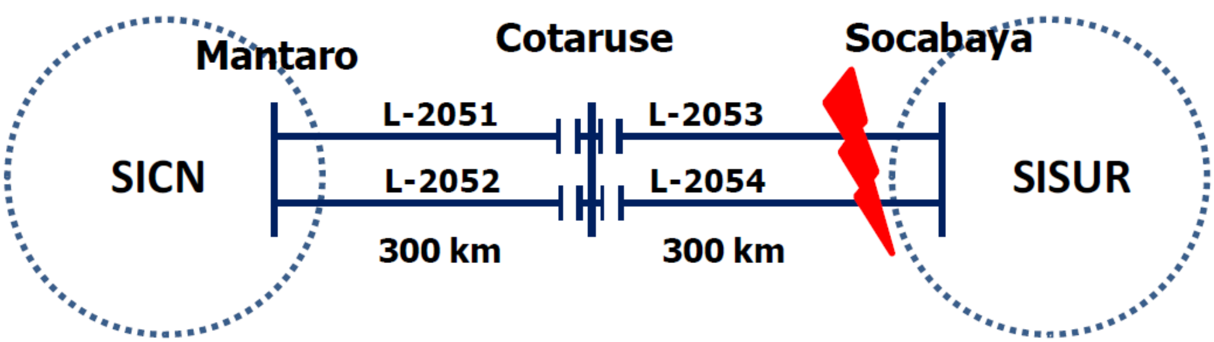

Figure 24: Peruvian network example diagram (taken from [16])

Both circuits L-2053 and L-2054 were tripped by line differential relays, L-2053 tripped three-phase, while L-2054 tripped a single phase. These disconnects resulted in a weakened connection (2 of 6 phases still connected) between the North-center and South areas and a power swing resulted. Power swings are usually considered three-phase events, but in situations such as this with a single-phase tripping and reclosing, a power swing can occur during the dead time (when reclose is in progress).

Some measurements demonstrating the power-swing as observed on line L-2054 is presented in Figure 25. The impedance measures during the OOS event are shown in Figure 26.

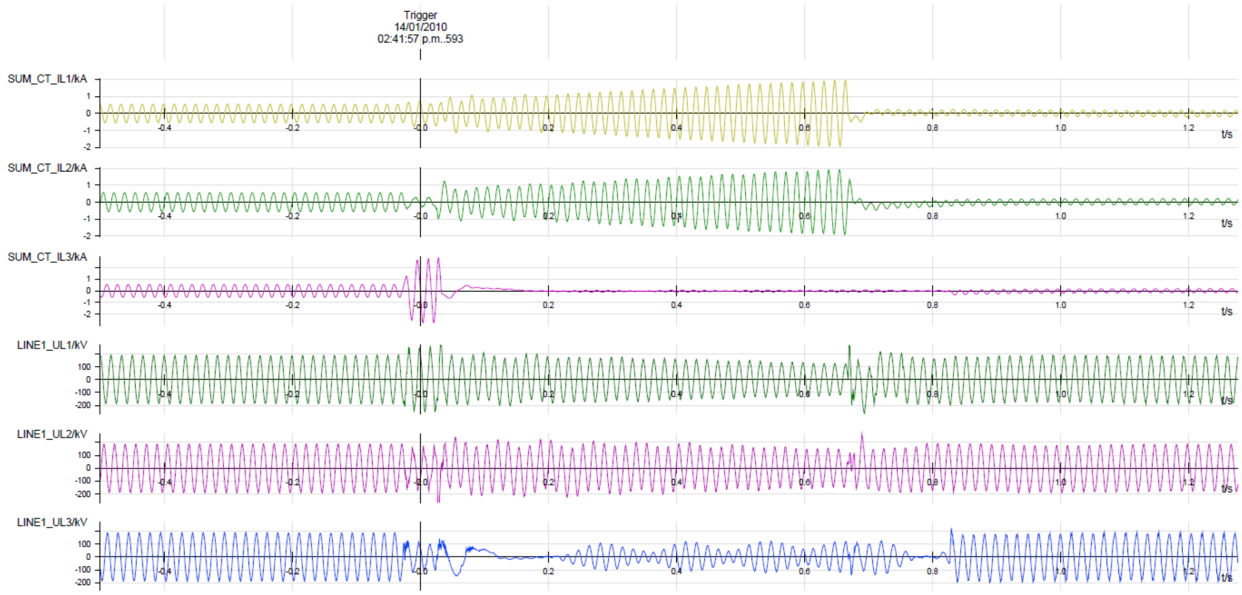

Figure 25: Power swing in L-2054 during the dead time of the reclosing (taken from [16])

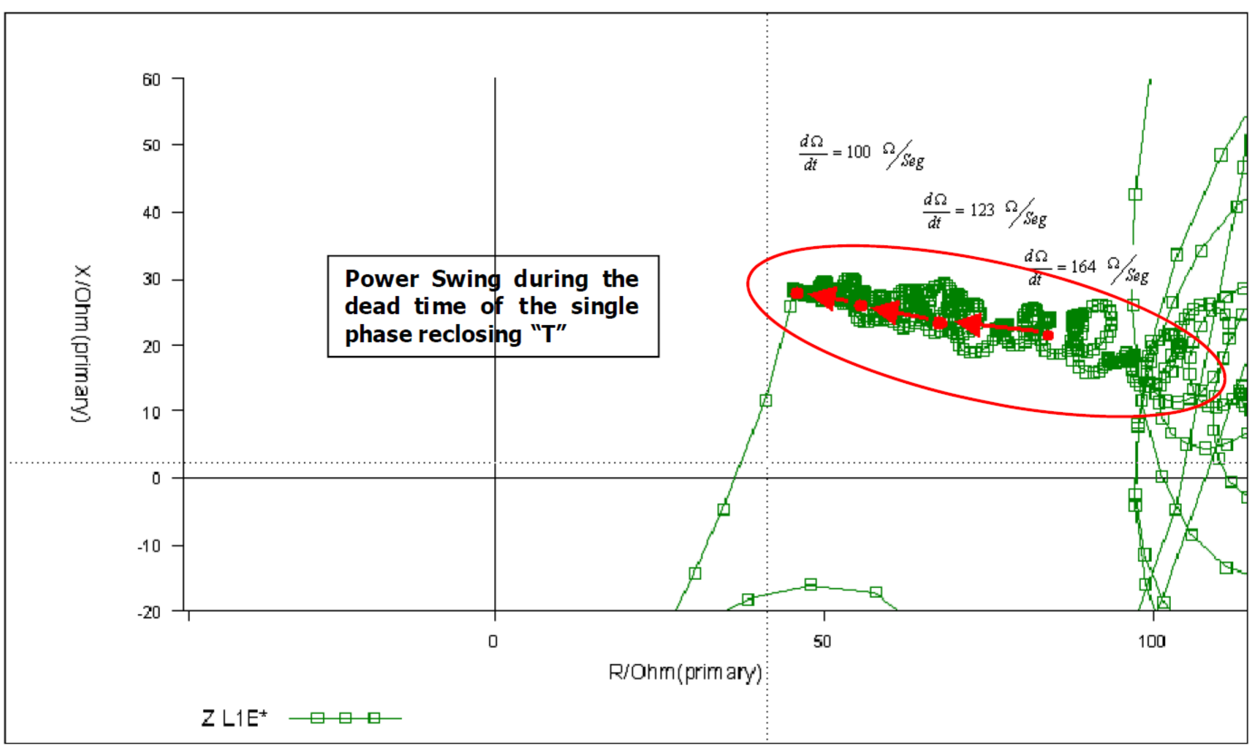

Figure 26: Impedance measured from the Cotaruse terminal during power swing (taken from [16])

The impedance seen in Figure 26 demonstrates a rate-of-change from 164 to 100 Ω/s. the impedance eventually enters the distance characteristic, resulting in tripping of the line at Cotaruse substation and sending a direct transfer trip to Socabaya substation, after L-2054 tripped, the South area collapsed.

Dynamic simulations for relay settings

A series of simulations are performed to evaluate the system response to faults applied near the SICN and SISUR interface. Three-phase faults are the most severe faults and will be used to evaluate the network responses. For each test, the fault is applied for 100ms before clearing the fault and tripping the line. Through these simulations, the scenarios, and lines where power swings (stable or unstable) occur are identified and the decision to implement OSB or OST can be made.

- Mantaro – Cotaruse lines (L-2051/L-2052)

Two faults are tested to evaluate these lines, the faults are applied on L-2052 and the measurements are taken for L-2051. The first is near Mantaro on L-2052, after clearing, this resulted in a stable power swing. The second fault is applied on the line side of the series capacitor of L-2052, this fault resulted in an unstable power swing and OOS conditions.

From this analysis, it was decided that for Mantaro-Cotaruse lines, that OSB is required but OST will not be implemented. Based on the presented studies, if the line is tripped under OOS condition, the lines Cotaruse-Socabaya are going to be energized from Socabaya, injecting around 140 MVAR, causing overvoltage in south area.

- Cotaruse - Socabaya lines (L-2053/L-2054)

Similarly, two faults are studied for the two lines L-2053 and L-2054. The fault is applied on L-2054 and the measurements are taken from L-2053. The first fault is applied near Cotaruse, this results in unstable power swings and OOS conditions. The second fault near Socabaya and results in stable power swings.

From this analysis, OOS protection must be implemented. Both OSB and OST should be applied to for stable and unstable power swings respectively.

- Other power lines in the Peruvian network

Additional scenarios were examined as part of the overall protection coordination examination. It is shown that some OOS conditions are not detected by the relays under analysis (in the SICN and SISUR interface) because the electrical center of the oscillations for these scenarios is in another location.

Through this coordination study the following conclusions were presented.

i. Power swings are typically three-phase phenomena but may appear during single-phase tripping and reclosing.
ii. The use of software to simulate the dynamic behaviour of the power system, and the relay characteristics simplifies setting the power swing tripping and blocking functions.
iii. The rate of change of impedance during a power swing can be identified through simulations. Knowing the rate-of-change of impedance allows for setting the timing for trip and block functions more easily.
iv. OST should not be applied to all line, the location for system separation should be carefully chosen.

Refer to [16] for more information concerning this study.

2.5.3 - New Method for Identifying Critical Cutsets

The paper [17] proposes a new method for identifying the critical cutsets in power systems, this new method is called the rolling double level hierarchical method. The critical cutset is set of elements (lines/transformers) that that when open can split the system into two sets of generators/buses. Information on the critical cutset is useful when implementing OOS protection in the system and so a fast and accurate method of determining this cutset is desirable.

The identification of the critical cutset can be solved as a clustering problem identifying critical and remaining bus groups. Cluster analysis is a technique for partitioning a set of objects into groups such that each group is homogeneous with respect to certain attributes based on a certain criterion. The clustering algorithms may group data points according to some parametric model of by grouping data points to some distance measure.

The method proposed in [17] uses rolling double level hierarchical clustering based on bus and generator variable fault trajectories. The first step is to perform hierarchical clustering based on generator and bus variable fault trajectories to gain generator and bus grouping results. These grouping results are then used for mutual verification to improve the reliability of the power system critical cutset detection results. The method also proposes a simple bus variable distance calculation method considering power system network topology, this reduces calculation time and guarantee internal connectivity of bus groups to improve the efficiency of the method.

The proposed method is tested using the New England 10-generator-39-bus system. The paper demonstrated that using the proposed method the critical cutsets for different network disturbances could be correctly identified.

Chapter 3 – Test Network Development

In this chapter, the test network model used for the simulation-based studies will be explained. Additionally, the network conditions and list of contingencies used in the study will also be discussed.

3.1. Description of the Test Network

To develop and test the OOS relay setting methodology, a test network is developed. The test network is based on an example case named SAVNW, available in the well-known power system simulation software PSSE example library [18]. The network diagram of the SAVNW case is presented in Figure 27. It has three voltage levels and three operating areas linked through tie-lines. The network is comprised of several generators of different types, loads and shunt capacitors. The SAVNW network is not a very large network, but it does contain many of the characteristics of a complex network and suitable for demonstrating the proposed methodology without getting preoccupied by the high dimensionality. As it is a PSSE example case, the network data and the dynamic model data are available in the format used in PSSE software. The network and the dynamic data are presented in the Appendix A – PSSE Network Quantities and Dynamic Model Parameters.

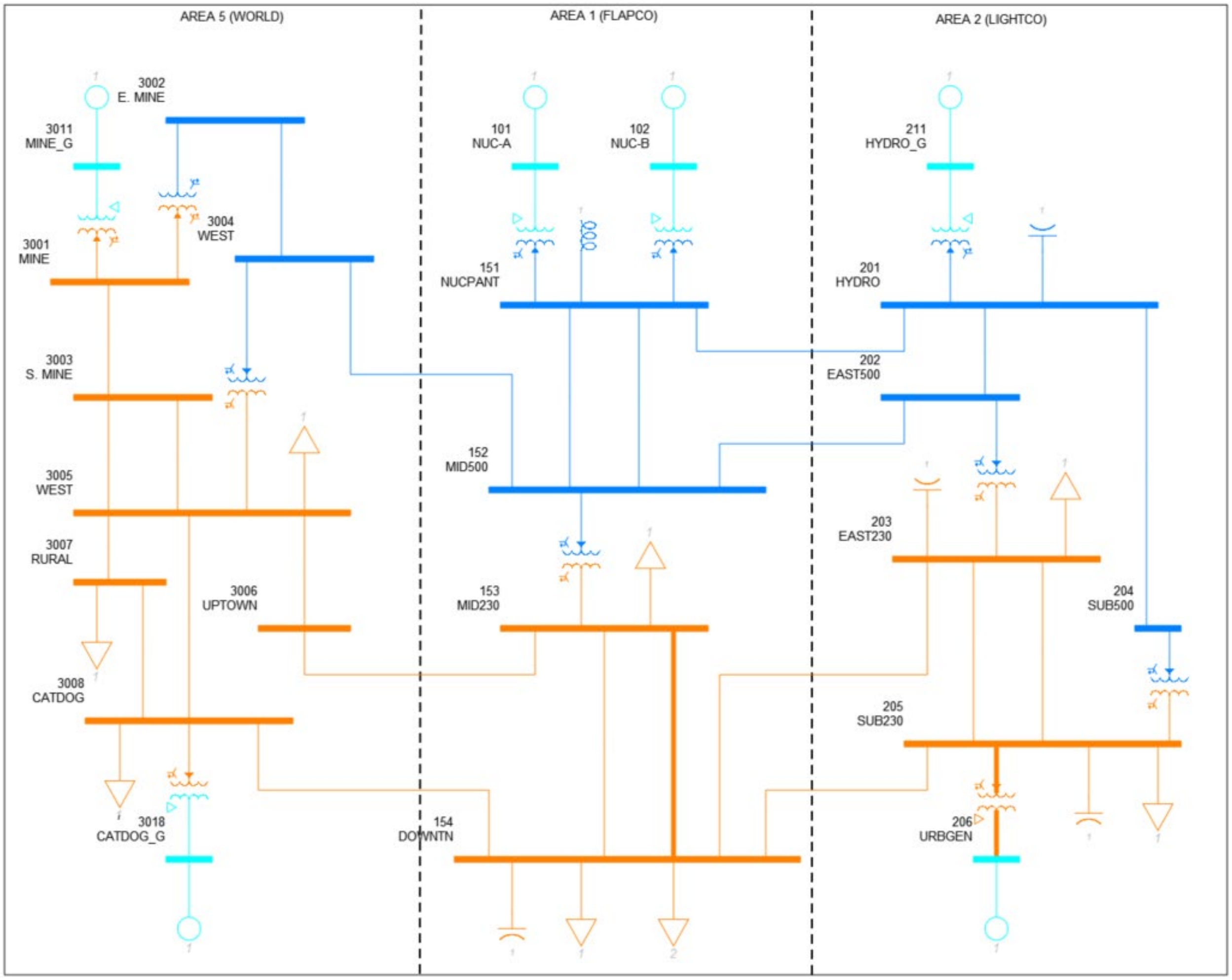

Figure 27: SAVNW study network.

3.1.1 – Test Network Modifications

For this study, the transmission line between buses 152 and 3004 which connects Area 1 and Area 5 will be used as the location for OOS protection.

The connection between areas 1 and 5 is weakened by disconnecting the lines from buses 154 to 3008 and from 153 to 3006, leaving only a single tie-line (152 to 3004). This is done to increase the likelihood of OOS conditions. Furthermore, this modification facilitates forming the two islanded systems (Area 5 and Areas1&2) during OOS conditions using a single relay.

A minor modification that doesn't affect electrical characteristics of the network is done to facilitate conveniently incorporating the OOS relay models to the dynamic simulations. The interfaces at buses 152 and 3004 are modified by including two dummy buses 90152 and 93004 and new zero-impedance lines connecting them (ZIP line between 152-90152 and 3004-93004). The new zero-impedance lines are used as the locations for the OOS relays, which are placed at either side of the tie-line. The modified SAVNW network is presented in Figure 28

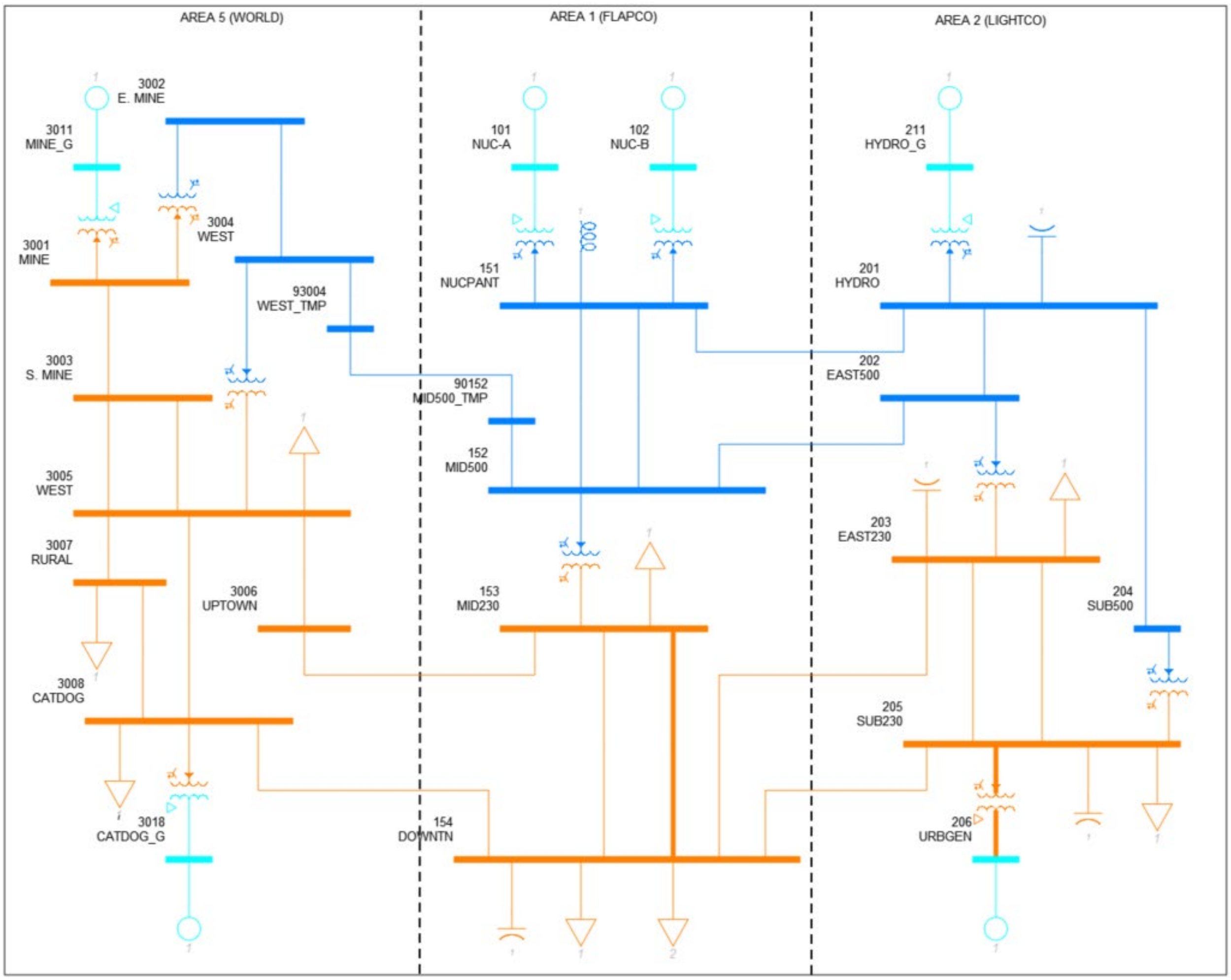

Figure 28: Modified SAVNW network

3.1.2 – Description of Study Scenarios

Multiple transfer scenarios are developed considering different generator dispatches and load levels. These transfer scenarios cause different levels and directions of power transfer across the interfaces between Areas 1 and 5, which will result in OOS when a disturbance occurs. Seven power flow cases are developed and are described in Table 5.

Table 5: Power Transfer Scenarios

Transfer Case	Description
SAVNW_n300	300 MW transfer from Area 5 to Area 1
SAVNW_n200	200 MW transfer from Area 5 to Area 1
SAVNW_n100	100 MW transfer from Area 5 to Area 1
SAVNW_0	0 MW transfer between Area 5 and Area 1
SAVNW_205	205 MW transfer from Area 1 to Area 5 (default SAVNW power flow)
SAVNW_300	300 MW transfer from Area 1 to Area 5
SAVNW_350	350 MW transfer from Area 1 to Area 5

Different transfer scenarios are created by modifying the generation dispatch in Area 2 and Area 5, when generation is increased in one area it is compensated by decreasing generation in the other. The generation dispatch for different transfer scenarios are presented in Table 6.

Table 6: Transfer Scenario Conditions

Bus Number	Bus Name	Area	PMax (MW)	SAVNW Transfer Case						
				n300	n200	n100	0	205	300	350
				PGen (MW)	PGen (MW)	PGen (MW)	PGen (MW)	PGen (MW)	PGen (MW)	PGen (MW)
101	NUC-A	1	810	750	750	750	750	750	750	750
102	NUC-B	1	810	750	750	750	750	750	750	750
206	URBGEN	2	900/1800	800	800	800	800	860	955	1000
211	HYDRO_G	2	616.25	145	248	350	451	600	600	600
3011	MINE_G	5	900	717.4	610.9	507.0	405.6	197.8	102.5	57.8
3018	CATDOG_G	5	117	100	100	100	100	100	100	100

When creating transfer scenarios, the rating of the machine at bus 206 (Pmax value) is increased (doubled) so that a greater power transfer from Area 1&2 to Area 5 can be achieved. When considering the power transfer from Area 1 to Area 5, the SAVNW_350 case represents a limiting transfer scenario, the transfer cannot be increased without further increasing generator limits. When considering the power transfer from Area 5 to Area 1, the SAVNW_300n case is not a limiting steady-state power transfer situation, but it is the case most susceptible to OOS conditions, thus closest to the dynamic stability limit.

3.1.3 – Contingencies

A comprehensive set of single element outage (N-1) contingencies are considered to create a disturbance that may initiate power swings and OOS conditions. Each contingency will have the following format:

- Run simulation for 6 seconds.
- Apply 3-phase fault at one end of the branch element.
- Run Simulation for 0.1 seconds.
- Clear fault and trip the network element.
- Run the simulation until 20 seconds.

For completeness, two versions of each contingency are created. The different versions of the contingency apply the fault at a different end of the tripped element. The full list of contingencies can be found in Appendix B – List of Disturbances Conditions Studied.

3.2. Models of Important System Components

3.2.1 – Out-of-Step Relay Models

The SLNOS[13] model is a straight-line blinder out-of-step relay model available in PSSE. A general description of the SLNOS model is provided in Section 2.3. This model can be configured for either tripping or blocking operations and can be setup either as a single blinder scheme or a double blinder scheme. For the studies, the SLNOS Relay will be configured to use as a double blinder scheme to detect OOS conditions and trip the study interface. The double blinder scheme of the SLNOS relay is presented in Figure 29.

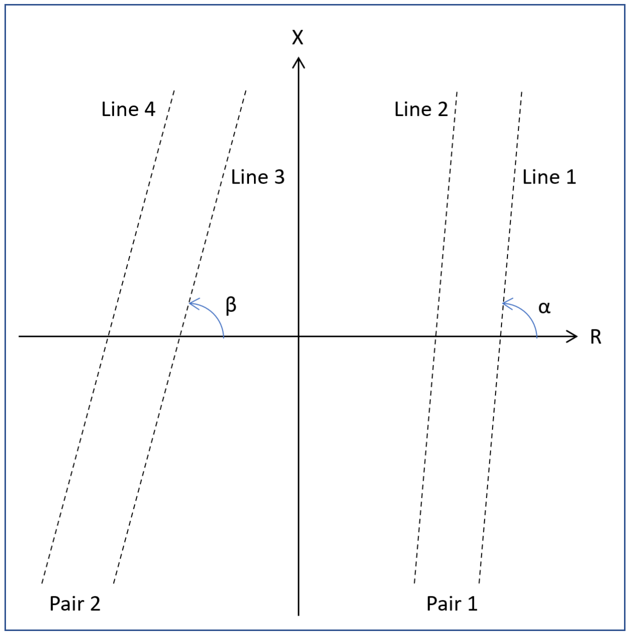

Figure 29: SLNOS Double Blinder Scheme

Initially this relay will be configured using a set of dummy parameters to identify OOS conditions and to determine the impedance swing speed. These parameters will then be updated to the relay parameters determined through the proposed methodology. This is discussed further in Chapter 4.

3.2.2 – Load Models

Multiple load models are used during the simulations, to examine the impact that a more detailed load model would have on the network stability and OOS identification by the relay.

Typically, if no specific load models are provided, the loads will be treated as static loads by the PSSE software. When a load is converted for dynamic simulations, it can be set as constant current, constant admittance, constant power load or some combination of these. For the dynamic simulations performed during this study, the loads are set as constant current loads.

A dynamic load model will also be used to test the system. A CMLD load model available in PSSE software, which is a composite load, can be used to model more complex loads. This load model facilitates including up to four different motors, an electrical load and a static load and can be used to model undervoltage load shedding conditions. It can also include a model a distribution feeder equivalent. The CMLD model is discussed in greater details in 2.4. A simple description of the load distribution used for the CMLD model is presented in Table 7. However, the simulation model does not include under frequency load shedding.

Table 7: CMLD load distribution

Load component	Percentage
3-phase Motor A	12
3-phase Motor B	14
3-phase Motor C	10
1-phase AC Motor D	3
Electrical Load	27
Static Load	34

The full list of CMLD parameters[19] can be found in Appendix A – PSSE Network Quantities and Dynamic Model Parameters.

3.3. EMT Model of the Test Network

3.3.1 – EMT vs. Phasor Domain simulations

The proposed methodology is intended for use with a phasor domain simulation tool such as PSSE. Phasor domain simulations use steady state equations to model the network but model machine mechanical dynamics and various control dynamics. The advantage of using phasor domain simulations is the speed of the dynamic simulations. Due to the volume of dynamic simulations required to identify OOS conditions and determine OOS relay settings, phasor domain simulations (such as those performed using PSSE) become the most practical approach when applying the proposed method in complex systems.

EMT simulations provide a more realistic representation of the power system. EMT simulation solve differential equations and model all network elements. EMT models consider all three phase of the network and will consider effects such as mutual coupling, nonlinearities such as machine saturation and simulates time domain waveforms. EMT simulations are also useful for modeling networks with high penetration of inverter-based resources[20]. Due to the increase in modeling complexities, EMT simulations have a greater computational burden and result in longer simulation times for larger networks.

Although the proposed methodology is intended for PSSE simulation, if appropriate computational resources to mange the engineering time are available, the methodology to determine OOS relay settings could be applied using EMT simulations.

3.3.2 – EMT Model Development for Validation of OOS Relay Parameters

An equivalent model of the modified SAVNW test system is developed using the well-known simulation software PSCAD/EMTDC[21]. This network equivalent is developed to validate the relay settings identified through PSSE simulation.

The network import tool PRSIM can be used to convert the network information. Using PRSIM[22], the network dynamic and sequence data of the SAVNW case can be imported and converted to an equivalent PSCAD model. PRSIM is able to import many of the PSSE dynamic models and convert to an equivalent PSCAD model, there are however certain PSCAD models that have not yet been added to the equivalent library. After importing the PSSE network and creating the PSCAD model, the PSCAD model is reviewed manually to determine that all network models have been correctly imported.

Three machines in the PSSE model of SAVNW network use an IEEET1 exciter model, this model is not currently supported in the PRSIM library. This model is replaced using a model with a similar transfer function. Figure 30 presents the transfer function block diagram for the IEEET1 model from the PSSE documentation [14].

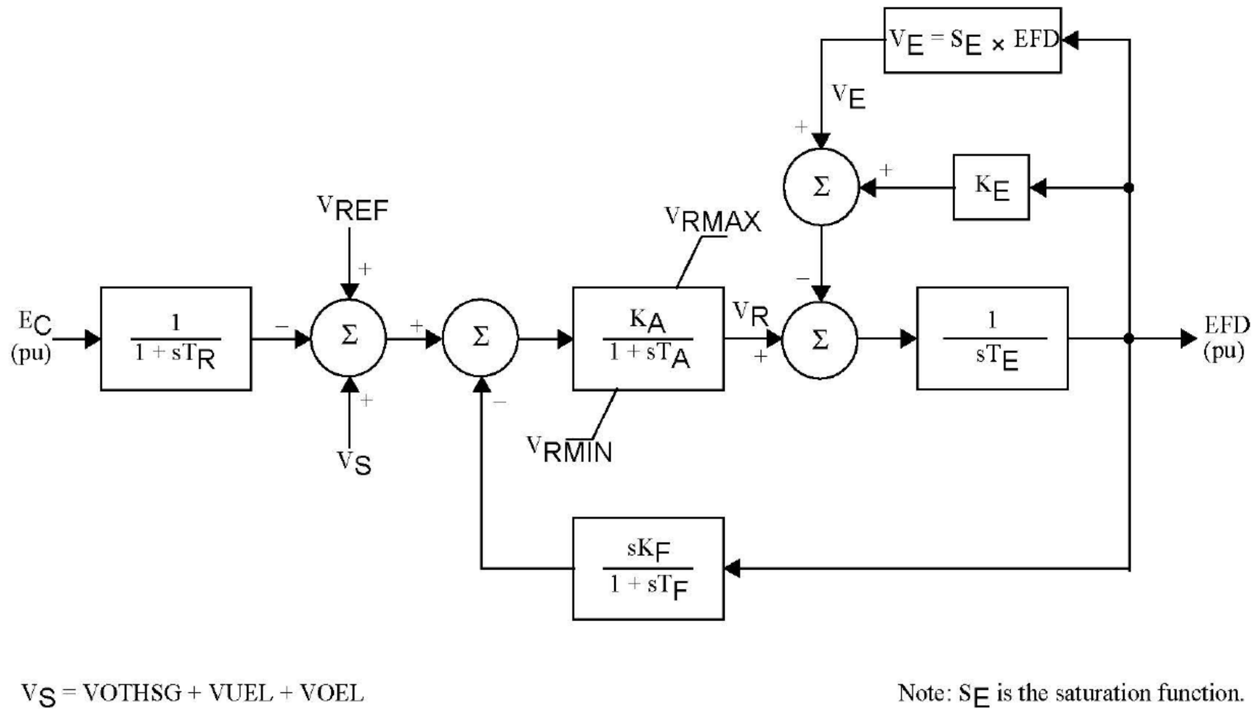

Figure 30: IEEET1 model transfer function diagram (PSSE) [14]

When examining the available models in PSCAD, it is found that the AC5A model has a similar transfer function diagram and could be used as an equivalent model if the parameters are set correctly. The block diagram of the AC5A exciter model from PSCAD is shown in Figure 31.

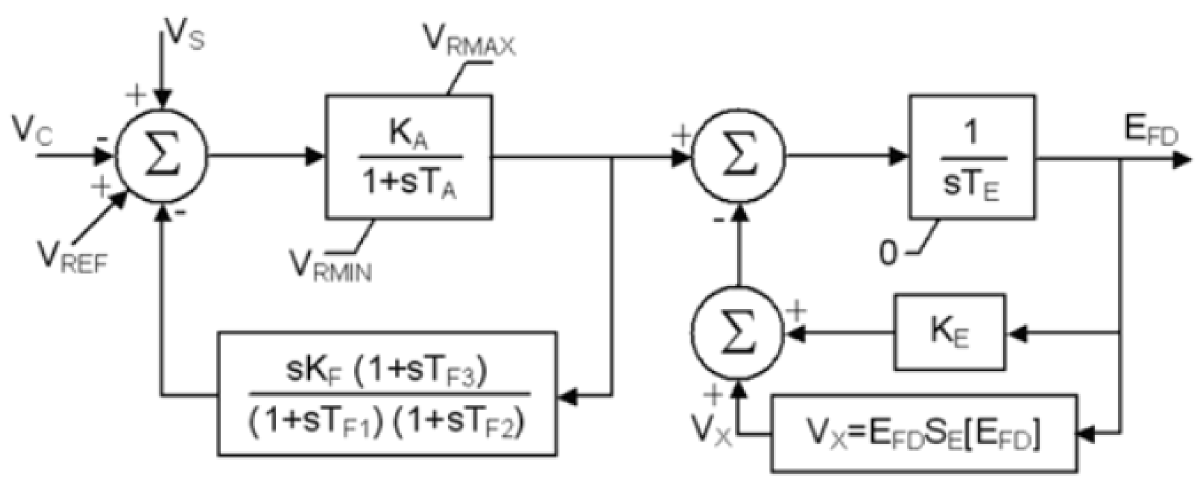

Figure 31: AC5A model transfer function (PSCAD)[21]

There are two main differences between the transfer functions of the IEEET1 and AC5A models. The first is the IEEET1 model has an initial block with a time constant TR, the second is the feedback loop, which has additional terms (TF2 and TF3) and is connected at a different location. We cannot make the two exciter models identical but the parameters of the AC5A model can be selected such that the two models are similar. The PSSE and PSCAD model parameters for these two models are presented in Table 8.

Table 8: IEEET1 and equivalent AC5A model parameters

IEEETA Parameters				AC5A Parameters			
Param.	Machine			Param.	Machine		
	101	102	206		101	102	206
TR	0	0	0	-	-	-	-
KA	400	400	40	KA	20	20	20
TA	0.04	0.04	0.06	TA	0.04	0.04	0.06
VRMAX	7.3	7.3	2.1	VRMAX	7.3	7.3	2.1
VRMIN	-7.3	-7.3	-2.1	VRMIN	-7.3	-7.3	-2.1
KE	1	1	0	KE	1	1	0
TE	0.8	0.8	0.5	TE	0.8	0.8	0.5
KF	0.03	0.03	0.08	KF	0.03	0.03	0.08
TF	1	1	0.8	TF1	1	1	0.8
-	-	-	-	TF2	0	0	0
-	-	-	-	TF3	0	0	0
E1	2.47	2.47	2.47	E1	2.47	2.47	2.47
SE(E1)	0.035	0.035	0.035	SE(E1)	0.035	0.035	0.035
E2	4.5	4.5	3.5	E2	4.5	4.5	3.5
SE(E2)	0.47	0.47	0.6	SE(E2)	0.47	0.47	0.6

Each of the IEEET1 models have a TR value of zero, so this model difference will not impact. The additional parameters in the feedback loop (TF2 and TF3) for the AC5A model are set to zero to match the IEEET1 model. The position of the feedback loop cannot be modified so this will be a persistent difference between the two models. The gain value KA is also lowered after preliminary simulation tests show that the original values for the IEEET1 from PSSE are too large for the PSCAD simulation and resulted in unstable simulations.

With these modifications to the study network, PSCAD model provides an EMT representation of the PSSE SAVNW network in PSCAD. There is no CMLD model currently available in PSCAD, only a single load type will be examined in the PSCAD studies. The PSSE static load case will be compared with the PSCAD case when performing the methodology validation.

3.3.3 – PSSE and PSCAD Test Network Comparison

A simple simulation is performed to determine whether the PSCAD and PSSE outputs are similar or whether the results are so different that these could not be considered an approximate equivalent network.

Two outage conditions were selected to examine the results in both PSCAD and PSSE. These will be examined for the power flow case SAVNW_n300 (as described in 3.1). The following two contingencies are selected:

- 211_201_1: Three-phase fault applied on the line connecting buses 211 and 201 (on 211 side), fault cleared after 0.1 seconds by removing faulted line.
- 3001_3003_1: Three-phase fault applied on the line connecting buses 3001 and 3003 (on 3001 side), fault cleared after 0.1 seconds by removing faulted line.

The outage condition 211_201_1 results in stable network conditions in both the PSSE and PSCAD network cases. Plots comparing PSSE and PSCAD values for the voltage and power transfer from Area 1 to Area 5 at bus 152 are shown in Figure 32 and Figure 33 respectively.

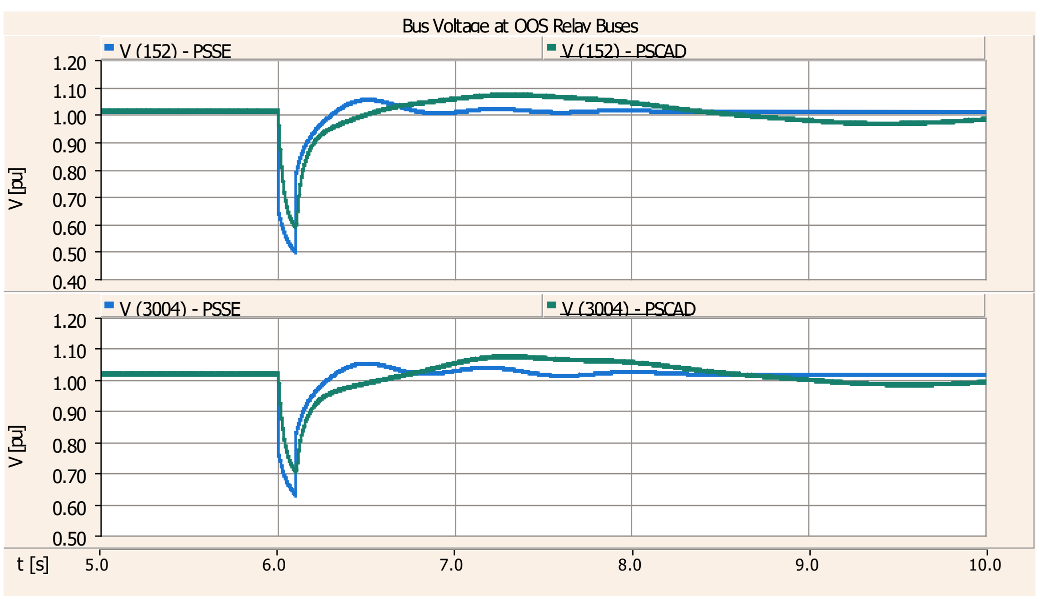

Figure 32: PSSE vs PSCAD: Interface Power Transfer Voltage – Disturbance SAVNW_211_201_1

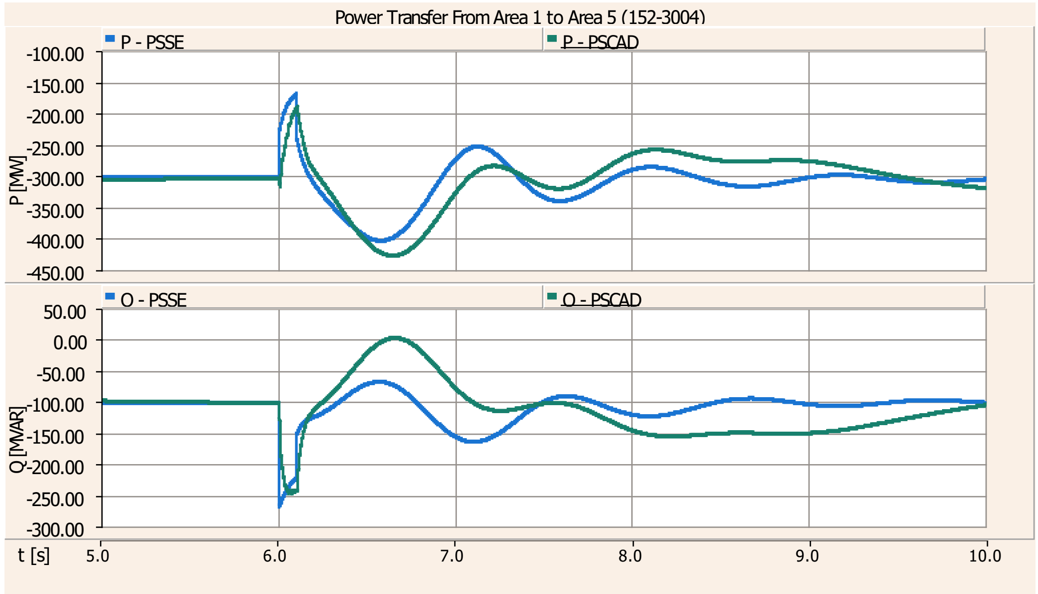

Figure 33: PSSE vs PSCAD: Relay Power Transfer (bus 152) – Disturbance SAVNW_211_201_1

The power flow prior to the disturbance matches very well between PSSE and PSCAD. Post disturbance the power flow does not match exactly but the response immediately after the disturbance and a few seconds later appear to follow a similar trend.

The disturbance 3001_3003_1 results in OOS conditions. The plot comparisons of the voltage and interface power transfer are presented in Figure 34 and Figure 35.

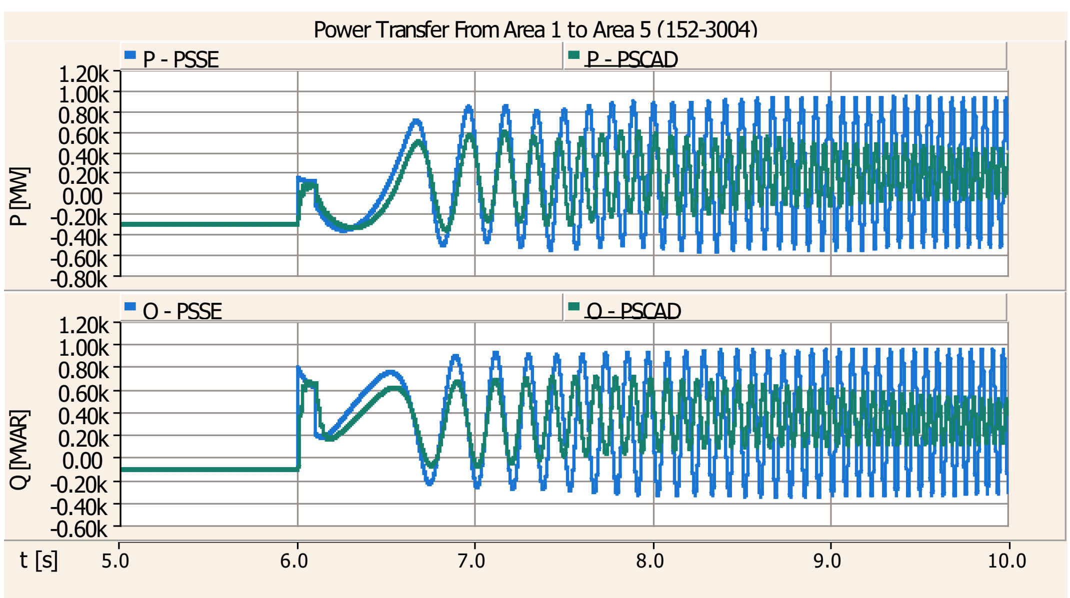

Figure 34: PSSE vs PSCAD: Interface Power Transfer Voltage – Disturbance SAVNW_3001_3003_1

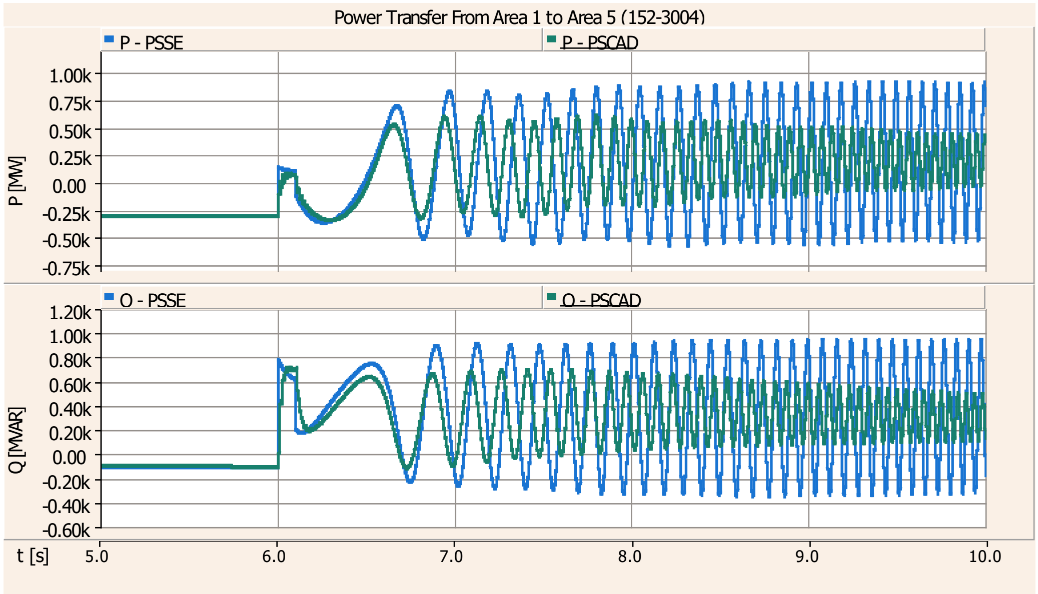

Figure 35: PSSE vs PSCAD: Relay Impedance (bus 152) Interface Power Transfer – Disturbance SAVNW_3001_3003_1

Both the power flow plots demonstrate the pre-disturbance value are match nicely. After the disturbance the PSSE and PSCAD response are similar for the first few oscillations. Even though as the simulations continue, the magnitudes and frequency of oscillations between PSCAD and PSSE begin to vary, initial period after the disturbance should be sufficient for determining OOS.

Based on these preliminary tests, the PSCAD model appears to be sufficient match for the PSSE SAVNW cases for the purposes of determining OOS conditions and testing OOS relay parameters.

The objective of developing EMT model is to validate the relay settings identified using PSSE simulations by demonstrating the identified parameters are valid when applied in a more detailed simulation model.

3.4. Chapter Summary

In this chapter, the test network to be used for testing the proposed method for determining OOS relay parameters is presented. The network is implemented in PSSE software for power flow and dynamic simulations. The test network is not very large but contains many of the characteristics of a complex system to demonstrate the challenges in setting of OOS relays. The conditions under which the test network will be studied are also presented, these conditions included power transfers in both directions on the studied line and an exhaustive set of N-1 conditions. The specifics of detailed load and relay models are presented to give a better understanding of the system. The inclusion of composite load models will further increase the complexity of the test network.

To validate relay parameters determined through PSSE simulations while following the proposed method, an EMT version of the test network is developed using PSCAD simulations software. The PSCAD simulations will only be used to validate the parameters identified through PSSE simulations. This comparison will be performed to investigate whether the settings found through phasor domain simulations are valid under more realistic representations of the power system and the protection relays.

Chapter 4 – General Approach to Identify the Out-of-Step Relay Settings

This chapter presents a general approach to identify the necessary information required for configuring the out-of-step relay settings. This approach involves system studies performed in a dynamic simulation program such as PSSE. The explanations given in this chapter include the types of system studies required and the system variables that should be recorded. These recorded network variables will be used to determine the settings for the targeted out-of-step relay.

4.1. Required System Studies

To obtain all necessary information required to identify the OOS relay settings, both power flow studies and dynamic simulation studies are required. Power flow studies are needed to establish the initial steady state operation under different network configurations and operating conditions to be considered. These operating scenarios should include all the expected operating conditions of the network as well as extreme conditions (within reason) and for a comprehensive set of outage conditions. The utility that operates the power network generally has a reasonable understanding of the credible pre-disturbance operating scenarios that need to be considered. Once the operating scenarios for the study have been established, the power flow studies can be performed to determine the initial loading point for the protected line under the considered pre-disturbance operating scenarios.

The power flow studies provide information on the steady state conditions of the test network, the dynamic simulations will demonstrate the network response to an event over time, it is in the dynamic simulations where the OOS behaviour of the network can be identified. During the dynamic simulations, the network simulation is run until a steady state condition has been met, this may take a few seconds (in simulation time) and is dependent on the network configuration and what models are used. After the system has reached a stable condition, an event is applied. The event is typically a fault followed by one or more element trips after clearing the fault. A description of the events applied in this study is presented in 3.1.

For these dynamic studies, a comprehensive set of events should be considered for each of the studied network conditions to identify the conditions which result in OOS. If there are remedial action schemes or other special protection schemes for the network, they should be considered during the study as these schemes may already address certain conditions which may results in OOS. When considering what network quantities that should be measured during the dynamic simulations, the quantities (voltage, current, active and reactive powers, impedances) at any interface where the OOS protection is intended to be implemented should be measured and recorded.

4.2. Developing Initial Settings for an Out-of-Step Relay

The following section outlines in detail the steps required to determine the initial settings for OOS relays.

4.2.1 – Impedance Speed Calculations

As discussed in 2.2, out of step relays measure the rate of impedance change at the studied interface to identify whether there is a power swing or an out-of-step condition, after a disturbance such as a fault. This is done by setting impedance blinders and checking the time taken by impedance to travel from the outer blinder to inner blinder, this is referred to as interzone travel time. When setting the OOS relay blinders, it is necessary to allow a sufficient distance between the inner and outer blinders so that the relay can reliably detect the difference between OOS events and faults.

For the OOS relay, typically a time of around 3 cycles [8][23] (0.048 seconds for 60 Hz system/0.06 sec for 50 Hz system) is selected for the interzone travel time setting. If the impedance travels the distance between the inner and outer blinder before the timer expires the event is determined to be a fault and the OOS relay should not activate. For the relay to detect all OOS events the distance between the outer and inner blinder should be large enough so that the fastest impedance swing does not cross from outer to inner a duration less than 3 cycles.

Determining the fastest speed of the impedance swing is not a straightforward task and the swing speed will depend on several factors including network conditions and events resulting in OOS. The first step in determining the fastest speed is to identify scenarios that result in OOS.

Once the OOS conditions have been identified, the R-X plots at the relay interface are closely examined so that measurements may be taken to calculate the speed of the impedance swing.

In this thesis, several different intervals are examined to determine the rate of change of impedance. During the dynamic simulations, the variations of the impedance (R and X values) with the time are recorded. The times when the impedance swing trajectory passes through blinders setup at several specific points will be used to calculate the speed as part of the investigation. The measurements are taken at several blinder locations to evaluate the difference in speed observed for different intervals (on the R-X plane). These locations are selected based on the impedance characteristics of the protected line. The following blinder locations are selected for impedance measurements:

- Vertical blinders at $R \approx \pm 1.333|Z_L|$, where Z_L is the impedance of the protected line
- Blinders with a tilt angle equal to the protected line impedance angle, set at $R \approx \pm 1.333|Z_L|$
- Vertical blinders at $R \approx \pm |Z_L|$
- Blinders with a tilt angle equal to the protected line impedance angle, set at $R \approx \pm |Z_L|$
- Vertical blinder set at $R = 0$

The selected locations where the time measurements are taken are presented in Figure 36. The example shown in Figure 36 assumes an impedance swing from left to right.

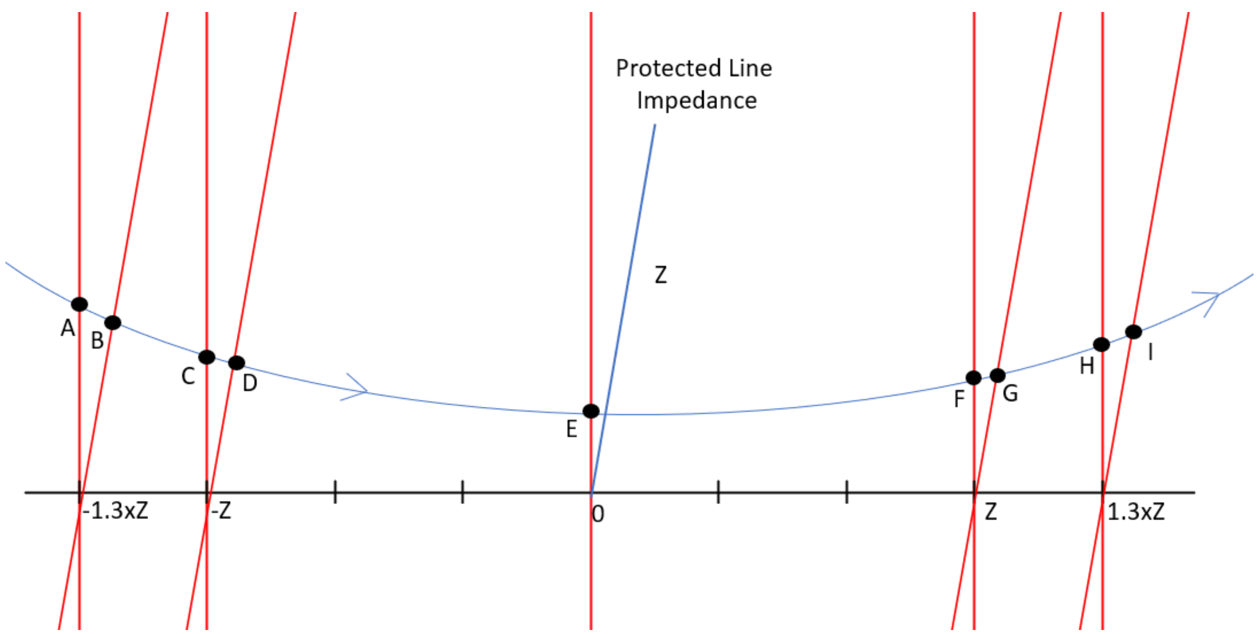

Figure 36: Example Impedance swing measurement points

Using the recorded time-impedance variations, several time intervals are determined based on the measurement points presented in Figure 36. These time intervals are presented in Table 9.

Table 9: Impedance intervals for speed calculations

Interval	Description
1	Outer vertical to outer vertical line (points A – H)
2	Outer angled line to outer angled line (points B – I)
3	Inner vertical line to inner vertical line (points C – F)
4	Inner angled line to inner angle line (points D – G)
5	Outer vertical line to zero (points A – E)
6	Outer angled line to zero (points B – E)
7	Outer vertical line to inner vertical line (points A – F)
8	Outer angled line to inner angled line (points B – G)

Using the selected intervals and time/impedance measurements the speed can be calculated using the simple equation:

$$Swing\ Speed = \frac{R_{point2} - R_{point1}}{t_{point2} - t_{point1}} \tag{4.1}$$

The calculation given in (4.1) has several approximations. When calculating the speed, it is assumed that the speed of the impedance swing is constant between the selected blinders. Also, to simplify the calculations when determining swing speed, only the resistive portion of the impedance swing is considered. This will result in the calculated swing speeds being slightly slower than the actual speed as the actual distance traveled will be longer than the distance used in the calculations.

After the speed has been calculated for all intervals and OOS conditions, the speeds can be compared to determine which conditions results in the fastest impedance swing. The speed calculations demonstrate that depending on the selected interval, the calculated speeds are different, indicating that the speed of the impedance swing is changing during the swing. It can also be noted that depending on the network conditions and contingency different intervals present the fastest speed.

Depending on the network conditions and event, the impedance swing will be either from right to left or vice versa. The fastest speed in both directions should be determined so that it is possible to apply different blinder spacing to two sides of the relay characteristics.

4.2.2 – Identifying Relay Blinder Impedance Limits

Once the fastest impedance swing speed for the protected interconnection has been determined, the preliminary relay settings can be determined. Some of the relay parameters are set based on the characteristics of the protected line, while others will be set according to the impedance swing speed calculation.

If the SLNOS1 out-of-step relay model (presented in 2.3) from PSSE is considered as a general OOS relay model, and the relay is set to use double blinder arrangement as depicted in Figure 37, the following information is required:

- Angle of first and second pair of impedance units (α and β)
- Resistive reach of each of the four blinders (points of intersection with resistance with resistance axis for outer blinders 1 and 4 and inner blinders 2 and 3)
- Interzone travel time (typically expressed in number of nominal frequency cycles, but can be expressed in seconds)

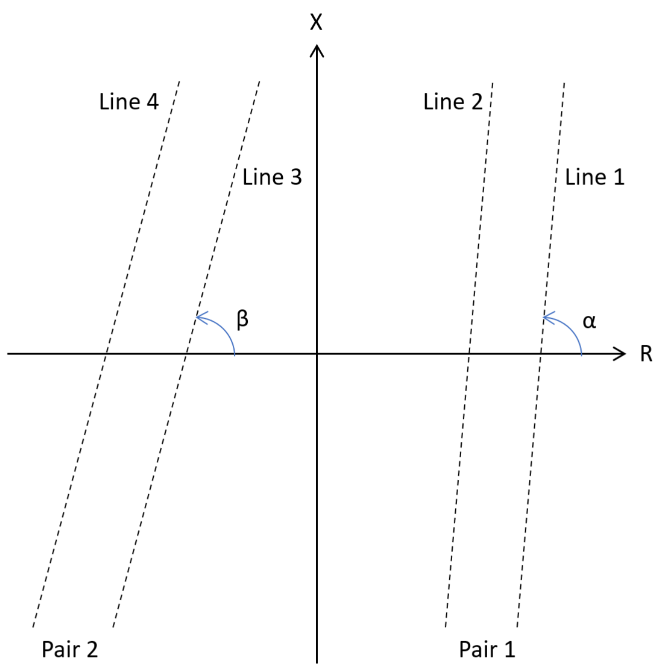

Figure 37: SLNOS1 double blinder relay characteristic

The angle of the impedance pair is typically set equal to the impedance angle of the protected line and can be calculated based on the R and X values of the line impedances. When determining the distance between inner and outer blinders, it is possible to set the distance first and determine the interzone travel time based on the maximum swing speed or set the travel time first and determine the distance between the blinders. The typical approach is to first set the interzone travel time, which is the time it takes for the impedance to cross from line 1 to line 2 or from line 4 to line 3. The travel time can be selected as any value; however, it is recommended that a value around 3 cycles be used which is well within the range provided in out-of-step relays of most manufacturers.

The intercept points for the inner and outer lines must be selected carefully and should consider several constraints based on the network characteristics and the impedance swing speed. These considerations include:

- Inner blinders should not encroach into the distance protection Zone 2. This is necessary to block the inadvertent operation of distance Zones 1 and 2 during power swings.
- Outer blinders should be at a sufficient distance from the maximum load point, i.e., the outer blinder should not encroach into a load region.
- The distance between the inner and outer line should be determined based on the maximum swing speed and the selected interzone travel time.

There is a question as to whether the inner blinder or outer blinder setting should be set first. In this study, it is recommended that the inner blinder be set first. If the inner blinder is set closer to the protected line impedance, when an OOS condition is detected, it is less likely that this is a false positive. If the blinders are set further away, the chance of detecting false OOS conditions is higher. The difference between an OOS condition and a false impedance swing are presented in Figure 38. Thus, if the inner blinder is set according to the distance protection, it can be set closer to the protected line impedance.

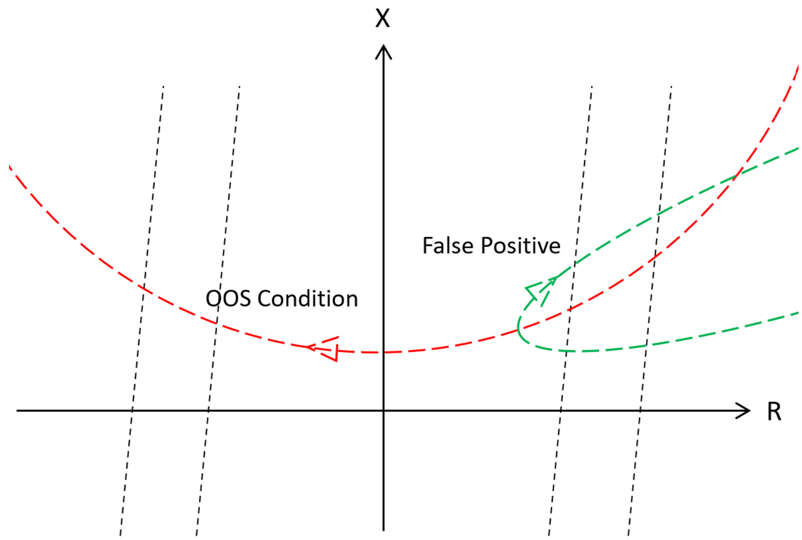

Figure 38: OOS impedance swing, actual and false positive

Determining Initial position of inner blinder (line 2 and 3 intercept points) based on distance relay protection zones.

The objective of distance protection [10][24]is to detect faults on the protected line or the adjacent line (remote line) and open the relevant breakers to clear the fault as soon as possible to minimize damage and ensure system stability. Like OOS protection, distance relays also make trip decisions by measuring the apparent network impedances. It is possible that under certain conditions (such as a stable power swing), the distance protection may incorrectly pick-up, resulting in a false positive that would result in unwanted network disconnections.

OOS protection can be used to detect power swings and block distance protection for stable power swings and trip the OOS relays when an unstable power swing is detected (stable and unstable power swings are discussed in 2.2). For this reason, it is important that the distance zone protection and OOS protection are properly coordinated, and the OOS protection should be set such that the distance protection zones relevant to the protected line is inside the inner blinders. Distance protection zones are determined based on the protected line characteristics and nearby network elements. The typical distance protection zones are presented in Table 10.

Table 10: Typical Distance Relay Settings

Zone	Reach	Time delay
Zone 1	80% – 85% of the protected transmission line impedance	Instantaneous
Zone 2	100% of the protected transmission line and up to 50% of the next shortest line emanating from the remote bus	0.25 sec – 0.4 sec
Zone 3	100% of the protected line plus 100% of the second longest line plus 25% of the shortest remote line	0.6 sec – 1.0 sec

A typical distance protection characteristic based on Mho circles is presented in Figure 39.

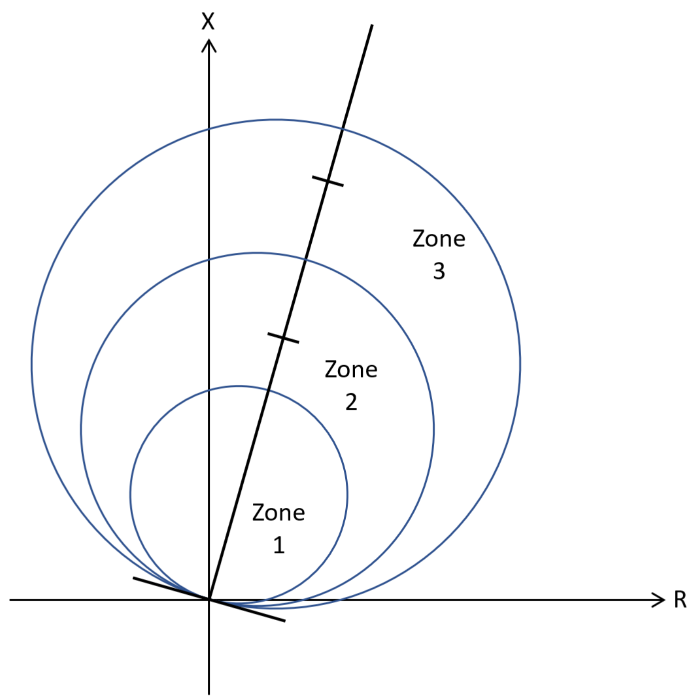

Figure 39: Typical distance protection characteristic

When setting the OOS relay inner blinder, it is important that the Zone 2 distance protection be inside the left and right (negative and positive) inner blinders. The timing for Zone 3 protection is typically set such that there should still be sufficient time for the OOS protection to operate if required and so there may be some overlap with OOS and Zone 3 protection. Acceptable relay characteristics considering distance protection are presented in Figure 40.

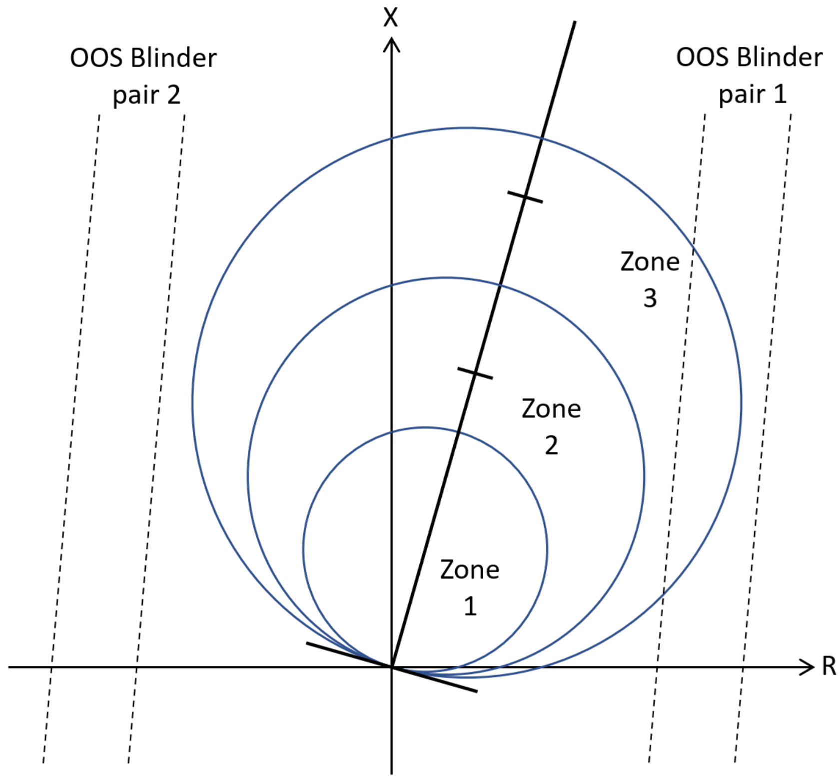

Figure 40: Acceptable distance and OOS relay parameters

If there are no distance protection settings provided, distance protection zones can be assumed based on the line characteristics of the network and typical distance protection settings (as presented in Table 10. The Zone 2 distance protection reach typically covers 100% of the protected line and 50% of the next shortest line emanating from the remote bus. If the actual distance relay settings are not known, the line impedance values can be used to estimate the distance protection zone and set the inner blinders (line intercepts) accordingly.

Once the distance protection Zone 2 reach has been established the inner blinder positions can be selected. To allow for a margin between the distance and OOS protection, it is recommended that the inner blinder position be set equal to the diameter of the Zone 2 protection in the positive and negative resistive impedance plane. Using the diameter of Zone 2 protection instead of the radiance will provide additional spacing which could facilitate earlier detection. This emphasizes the balance that must be struck when selecting the blinder locations. If the blinders are set too far from the line characteristic, there is a greater chance for false positives. If the blinders are set too close, then there may not be enough time to react before the power swing causes damage.

Determining initial loading point to determine acceptable outer blinder positions.

The initial loading point for the protected line will vary depending on the network conditions. It is important that the OOS protection be at a sufficient distance from the loading point so that the impedance does not enter the OOS protection zone for small disturbances. Also, when the network conditions change, the loading point should not enter the OOS protection zone. To determine the maximum outer blinder position, power flow studies should be performed to determine the initial loading point of the protected line under the different expected operating conditions. Through these tests it is possible to identify the loading point nearest to the origin, which will represent the limiting impedance for the OOS outer blinder.

Calculating outer blinder spacing

The spacing between the inner and outer blinder can be calculated based on the fastest measured swing speeds. The equation for computing the blinder spacing is shown in eq. 4.2.

$$Blinder\ Spacing = Speed \times Travel\ Time \times Safety\ Factor \tag{4.2}$$

The travel time is the interzone travel time and it is typically set to 3 or 4 cycles. An additional safety factor is added during the blinder spacing calculation to account for any variance in the measurements to avoid false dismissals. A safety factor of between 1.05 to 1.1 is suggested.

Independent blinder pair settings

The two blinder pairs of the OOS protection can be set independently. When considering relay characteristics as described above, it is possible to determine separate values for the left and right blinder pairs. The following points outline system characteristics which could result in different setting for each of the blinder pairs.

The inner blinder is set relative to the distance protection characteristic. This does not allow for much variation between left and right-side OOS blinders.

Depending on the characteristics and the operating configurations of the system, the initial load point may be in either the positive or negative resistive impedance planes. If there are load points located on both sides of the impedance plane (considering difference scenarios with power transfers in either direction through the protect line), then it is possible to select two different limits for the outer blinder.

When determining the speed of unstable power swings, the direction of the swing can be taken into consideration. The fastest speed from right-to-left and from left-to-right can be determined and used to calculate two different blinder spacings. The swing from right-to-left can be used to determine the positive side blinder pair, while the left-to-right swing can be used to determine the negative side blinder pair.

Final relay characteristic

After considering all the above parameters the OOS relay, the typical OOS characteristic should be like the characteristics presented in Figure 41.

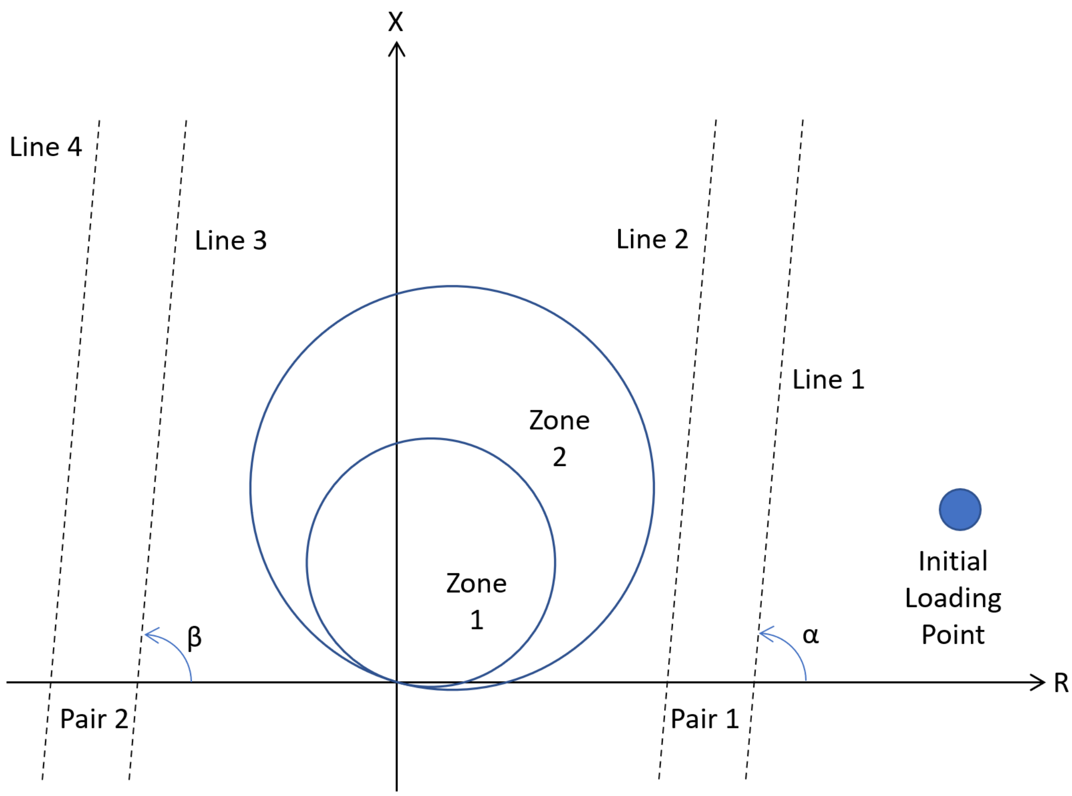

Figure 41: Determined typical OOS characteristic.

4.2.3 – Relay Parameter Validation

After the preliminary relay parameters are selected, they must be validated through dynamic simulations. Due to the nature of OOS conditions, even with these setting there may be conditions with false positives or false dismissals. The calculated relay parameters should be applied to the relay in the test network (SLNOS relay is used in the PSSE test network) and the dynamic simulations should be repeated.

Based on these new dynamic simulations, it is possible to identify the number of scenarios with either false positives (OOS relay activated under stable conditions) or false dismissals (OOS relay did not react for OOS condition). At this stage the relay parameters can be tuned by modifying the safety factor adjusting the relay positions within the limits. The new parameters can be tested and adjusted again, in an iterative process to determine parameters that minimize the number of false positives and false dismissals, although it is possible that there is no combination of parameters that will address all the problems. The iterative process to determine the final relay settings are presented in Figure 42.

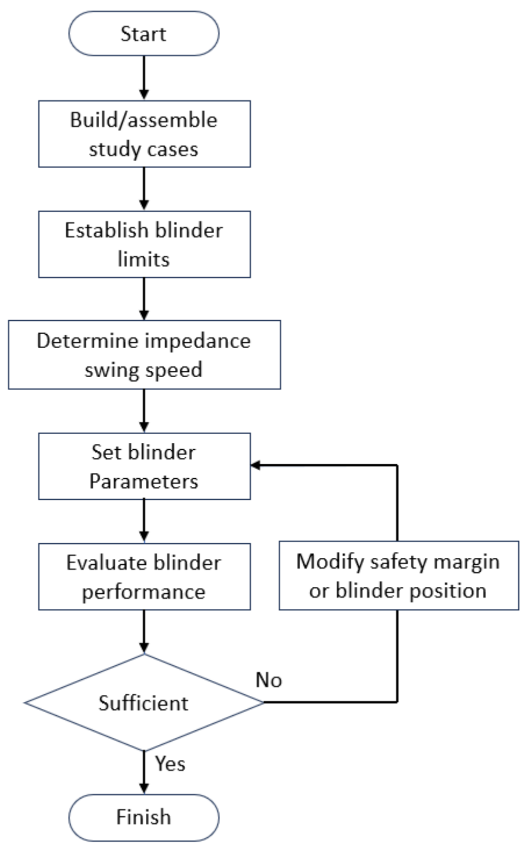

Figure 42: OOS parameter setting flowchart.

4.3. Chapter Summary

In this chapter, the studies, measurements, and calculations necessary to identify appropriate out-of-step relay parameters are presented. The power flow and dynamic studies necessary for identifying OOS conditions are discussed. The various steps required to identify the relay setting limits are discussed in detail, and a method for determining appropriate OOS relay parameters is proposed. The methodology presented in this chapter will be used to identify appropriate OOS relay parameters for the selected tie line in the test network introduced in Chapter 3.

Chapter 5 – Demonstration of Methodology and Validation

In this chapter, the relay settings are determined for the example study cases through the general approach presented in Chapter 4.

5.1. Determining Relay Parameters Through PSSE Studies

In this section the studies performed in PSSE using the modified versions of the PSSE example SAVNW network (presented in 3.1) are discussed, presenting a step-by-step discussion of how the required information for determining OOS blinder settings are determined.

5.1.1 – System Simulations and Identification of OOS network conditions

A set of dynamic simulations are performed using different network conditions and events to identify conditions (as described in 3.1) that result in stable power swings and OOS conditions.

The primary focus of these simulations is to identify OOS conditions, this is done by monitoring the apparent impedance (both R and X values) as seen by the relays (connected at both bus 152 and 3004). Additional channels are monitored to observe the power flow through the network and bus voltages.

The R and X values measured in each dynamic simulation are plotted in an X-Y plot, the plot is examined to observe whether any impedance swings are present for the specified network conditions. Two dynamic simulations, one resulting in stable power swing and the other resulting in an OOS situation (unstable power swing) are presented in Figure 43.

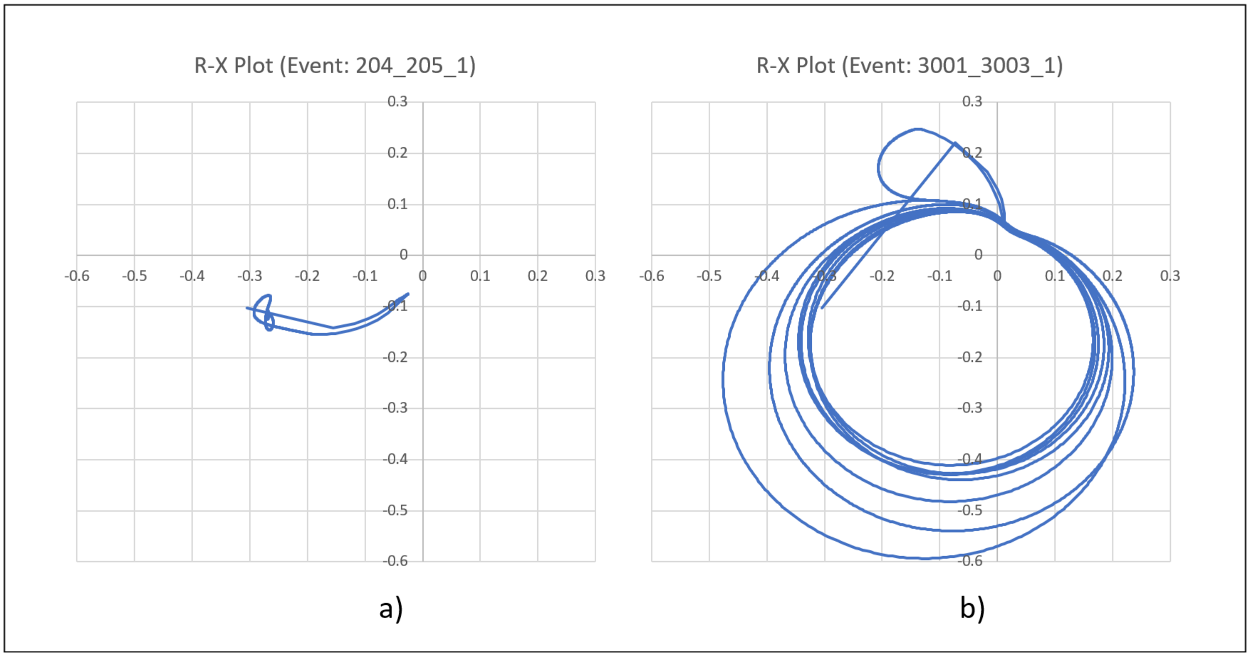

Figure 43: R-X Impedance Plots Obtained from PSSE Simulations, (a) Stable Power Swing, (b) OOS Conditions

Plots representing the R-X values measured from the relay at bus 152 for the scenario SAVNW_n300 (300 MW transfer from Area 5 to Area 1). The following two contingencies are examined in the above example.

- 204_201_1: Three-phase fault applied on the line connecting buses 201 and 204 (on 204 side), fault cleared after 0.1 seconds by removing the faulted line.
- 3001_3003_1: Three-phase fault applied on the line connecting buses 3001 and 3003 (on 3001 side), fault cleared after 0.1 seconds by removing the faulted line.

The first contingency (204_201_1) results in a stable post-event condition after a few oscillations. The second contingency (3001_3003_1) results in an OOS condition after the event. It is easily seen that for the stable power swing, the impedance does vary during the simulation, but it does not cross line characteristic impedance. Conversely when the network is going through an OOS condition, the R-X plot show that the impedance is going in circles, demonstrating an unstable power swing.

The output of each of the dynamic simulations is examined and all OOS conditions are identified. These dynamic simulations show that certain initial power flow conditions do not result in any OOS conditions. The power flow scenarios considered are tabulated in Table 11, with indication of the possibility of resulting in OOS conditions after a contingency.

Table 11: Network Cases without OOS Conditions

Network Case	Notes
SAVNW_n300	OOS conditions detected
SAVNW_n200	No OOS conditions
SAVNW_n100	No OOS conditions
SAVNW_0	No OOS conditions
SAVNW_205	No OOS conditions
SAVNW_300	OOS conditions detected
SAVNW_350	OOS conditions detected

There are three power flow scenario that result in OOS conditions after a fault. For these power flow scenarios, the type of load model used and the disturbances that cause OOS conditions are identified in Table 12. The disturbance is denoted by the branch on which a three-phase fault is applied and which side of the line the fault occurs. For example, disturbance 3001_3003_1 indicates a fault applied on the line between 3001 and 3003, ID 1 (3001 side), after 0.1 seconds the fault is cleared by tripping the faulted line.

Table 12: Description of Contingencies Resulting in OOS Conditions

No.	Network Case	Disturbance	Load Model
1	SAVNW_n300	3001_3003_1	Static
2	SAVNW_n300	3003_3001_1	Static
3	SAVNW_300	205_206_1	Static
4	SAVNW_300	206_205_1	Static
5	SAVNW_350	201_211_1	Static
6	SAVNW_350	205_206_1	Static
7	SAVNW_350	206_205_1	Static
8	SAVNW_n300	3001_3002_1	CMLD
9	SAVNW_n300	3002_3001_1	CMLD
10	SAVNW_n300	3001_3003_1	CMLD
11	SAVNW_n300	3003_3001_1	CMLD
12	SAVNW_n300	3002_3004_1	CMLD
13	SAVNW_n300	3004_3002_1	CMLD
14	SAVNW_n300	3003_3005_1	CMLD
15	SAVNW_n300	3005_3003_1	CMLD
16	SAVNW_n300	3004_3005_1	CMLD
17	SAVNW_n300	3005_3004_1	CMLD
18	SAVNW_300	211_201_1	CMLD
19	SAVNW_300	201_211_1	CMLD
20	SAVNW_350	211_201_1	CMLD
21	SAVNW_350	211_201_1	CMLD

5.1.2 – Impedance Speed Calculations

To determine the impedance swing, the rate of change of impedance between two boundaries must be identified, but first the boundary itself must be identified. The impedance plots for the case SAVNW_n300, considering disturbance 3001_3003_1 will be examined. The impedance for the period from 6.2 s to 6.7 seconds is plotted for impedance measured at bus 152 side and bus 3004. The possible boundaries presented in 4.2 Table 9 are also included. The R-X plots are presented in Figure 44.

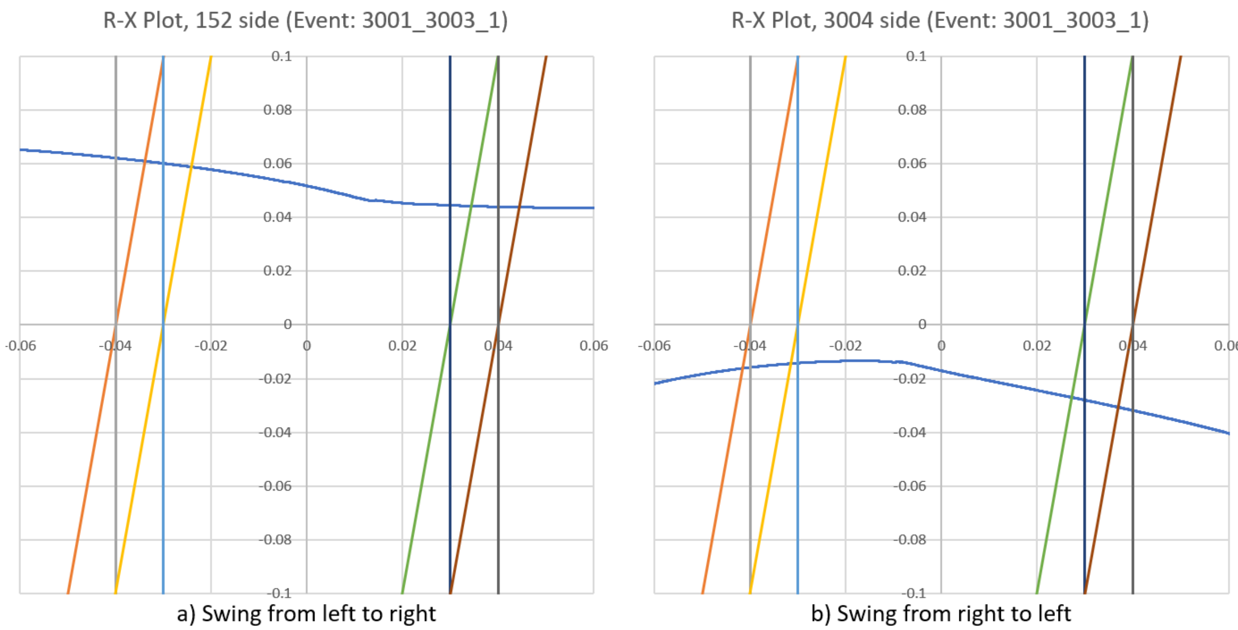

Figure 44: R-X plot for SAVNW_n300, Event: 3001_3003_1 (a) 152 relay measurements, b) 3004 relay measurements)

Based on the measured impedance, the speed is calculated for different boundaries (as proposed in 4.2). These measurements demonstrate that depending on the interval the calculated impedance speed is different, but nut by much. The calculated speeds for different intervals are presented in Table 13.

Table 13: Calculated Impedance Speed for Different Intervals

Interval	Description	152 Side Relay Meas.			3004 Side Relay Meas.		
		Δt	ΔR	Speed	Δt	ΔR	Speed
1	Outer vertical to outer vertical line	0.2500	0.0797	0.3187	0.2880	-0.0807	0.2803
2	Outer angled line to outer angled line	0.2390	0.0779	0.3261	0.2771	-0.0785	0.2833
3	Inner vertical line to inner vertical line	0.2010	0.0602	0.2997	0.2290	-0.0602	0.2627
4	Inner angled line to inner angle line	0.1900	0.0584	0.3073	0.2210	-0.0589	0.2667
5	Outer vertical line to zero	0.1329	0.0398	0.2998	0.1669	-0.0404	0.2419
6	Outer angled line to zero	0.1149	0.0339	0.2950	0.1540	-0.0369	0.2398
7	Outer vertical line to inner vertical line	0.2310	0.0700	0.3030	0.2690	-0.0705	0.2621
8	Outer angled line to inner angled line	0.2220	0.0683	0.3078	0.2591	-0.0685	0.2645

Based on different speed calculated in the above example, the interval between the outer blinder to the inner blinder is a good selection as the initial blinder position for preliminary speed measurements. The calculated speed for this interval between the outer and inner blinder is close to the median speed value. This interval is also similar to the interval typically used by OOS relays for measurements. The initial blinder will use the angled blinders instead of vertical blinders, to match blinders typically used by OOS relays.

The initial set of blinders are determined based on the characteristics of the protected line. The impedance of the line is 0.0315 pu with an angle of 84.29°. The R intercept of the inner and outer blinder are selected based on the line impedance as per the guidelines of section 4.2 (approximately $|Z_L|$ and $1.333|Z_L|$). Thus, the R intercept of the inner and outer blinder are initially set to ±0.03 pu and ±0.04 pu, with the angle equal to the line impedance angle. These are shown in Figure 45.

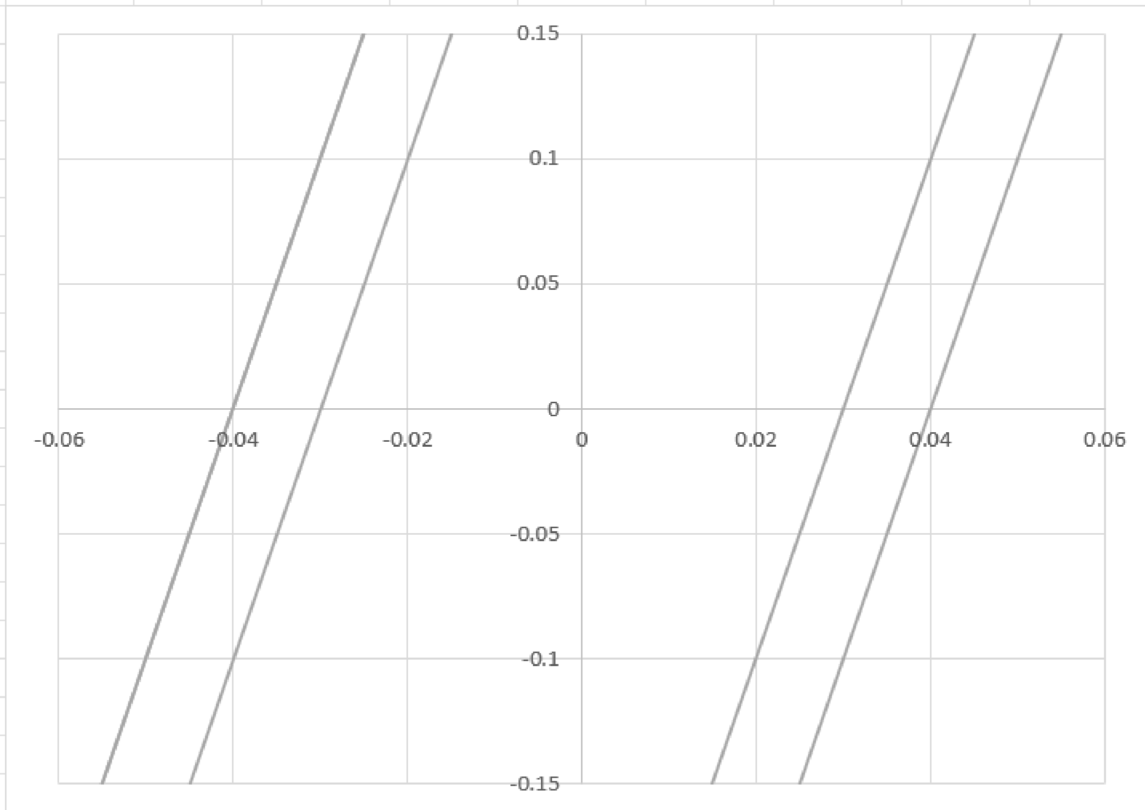

Figure 45: Initial Blinder setting for Speed Calculations

For each of the identified OSS cases given in Table 12, the speed of the impedance swing can be calculated based on the above blinder characteristics.

For each of the cases resulting in OOS conditions, the impedance trajectory is examined with respect to the characteristic presented in Figure 45 to determine the time and R coordinate of the points where the impedance trajectory intercepts with the blinders. To make the process of checking each of the OOS conditions efficient, a Matlab script is developed to calculate the swing speed. The Matlab script will scan a specified .out file (the output file created when running dynamic simulations in PSSE) and identify the time and impedance values when the measured impedance crosses one of the blinders. The script will then calculate the rate of change of impedance and identify the direction of the power swing based on the order of the blinder crossing.

After analyzing all OOS conditions, the identified blinder crossing points from both sides of the protected line for the static load scenarios are tabulated in Table 14 and Table 15. The identified blinder crossing points for the CMLD load scenarios are provided in Table 16 and Table 17.

Table 14: Time and R when OOS Impedance Trajectory Cross Blinders, (Static Load Scenario, 152 Side)

Scenario (Static Load)	Swing Direction	Side	Outer		Inner	
			Time (s)	R (pu)	Time (s)	R (pu)
SAVNW_n300, 3001_3003_1	Left->Right	152	6.4081	-0.0306	6.4304	-0.0210
SAVNW_n300, 3003_3001_1	Left->Right	152	6.4434	-0.0305	6.4676	-0.0210
SAVNW_350, 201_211_1	Right->Left	152	7.6470	0.0379	7.7003	0.0287
SAVNW_350, 205_206_1	Right->Left	152	6.3330	0.0388	6.4246	0.0301
SAVNW_350, 206_205_1	Right->Left	152	6.3733	0.0388	6.4691	0.0301
SAVNW_300, 205_206_1	Right->Left	152	6.3920	0.0388	6.5153	0.0301
SAVNW_300, 206_205_1	Right->Left	152	6.4423	0.0388	6.5799	0.0301

Table 15: Time and R when OOS Impedance Trajectory Cross Blinders, (Static Load Scenario, 3004 Side)

Scenario (Static Load)	Swing Direction	Side	Outer		Inner	
			Time (s)	R (pu)	Time (s)	R (pu)
SAVNW_n300, 3001_3003_1	Right->Left	3004	6.3736	0.0343	6.4058	0.0247
SAVNW_n300, 3003_3001_1	Right->Left	3004	6.4051	0.0342	6.4406	0.0247
SAVNW_350, 201_211_1	Left->Right	3004	7.6739	-0.0353	7.7191	-0.0259
SAVNW_350, 205_206_1	Left->Right	3004	6.3649	-0.0365	6.4373	-0.0274
SAVNW_350, 206_205_1	Left->Right	3004	6.4064	-0.0365	6.4825	-0.0274
SAVNW_300, 205_206_1	Left->Right	3004	6.4335	-0.0365	6.5340	-0.0274
SAVNW_300, 206_205_1	Left->Right	3004	6.4871	-0.0365	6.6012	-0.0274

Table 16: Time and R when OOS Impedance Trajectory Cross Blinders, (CMLD Load Scenario, 152 Side)

Scenario (CMLD Load)	Swing Direction	Side	Outer		Inner	
			Time (s)	R (pu)	Time (s)	R (pu)
SAVNW_350, 201_211_1	Right->Left	152	7.9967	0.0407	8.0693	0.0316
SAVNW_350, 211_201_1	Right->Left	152	8.116	0.0405	8.1766	0.0314
SAVNW_300, 211_201_1	Right->Left	152	8.1589	0.0407	8.2400	0.0317
SAVNW_n300, 3001_3002_1	Left->Right	152	6.4010	-0.0344	6.4392	-0.0246
SAVNW_n300, 3001_3003_1	Left->Right	152	6.3502	-0.0339	6.3816	-0.0241
SAVNW_n300, 3002_3001_1	Left->Right	152	6.4762	-0.0345	6.5203	-0.0246
SAVNW_n300, 3002_3004_1	Left->Right	152	6.4736	-0.0345	6.5177	-0.0246
SAVNW_n300, 3003_3001_1	Right->Left	152	6.3661	-0.0339	6.3987	-0.0241
SAVNW_n300, 3003_3005_1	Left->Right	152	6.4641	-0.0352	6.5291	-0.0253
SAVNW_n300, 3004_3002_1	Right->Left	152	6.5098	-0.0341	6.5550	-0.0242
SAVNW_n300, 3004_3005_1	Left->Right	152	6.7064	-0.0320	6.7477	-0.0221
SAVNW_n300, 3005_3003_1	Left->Right	152	6.5524	-0.0350	6.6366	-0.0251
SAVNW_n300, 3005_3004_1	Left->Right	152	6.5240	-0.0330	6.5569	-0.0230

Table 17: Time and R when OOS Impedance Trajectory Cross Blinders, (CMLD Load Scenario, 3004 Side)

Scenario (CMLD Load)	Swing Direction	Side	Outer		Inner	
			Time (s)	R (pu)	Time (s)	R (pu)
SAVNW_350, 201_211_1	Left->Right	3004	8.0015	-0.0381	8.065	-0.0288
SAVNW_350, 211_201_1	Left->Right	3004	8.1216	-0.0379	8.1748	-0.0286
SAVNW_300, 211_201_1	Left->Right	3004	8.1635	-0.0381	8.2341	-0.0289
SAVNW_n300, 3001_3002_1	Right->Left	3004	6.3720	0.0375	6.4176	0.0277
SAVNW_n300, 3001_3003_1	Right->Left	3004	6.3231	0.0369	6.3615	0.0273
SAVNW_n300, 3002_3001_1	Right->Left	3004	6.4430	0.0375	6.4955	0.0277
SAVNW_n300, 3002_3004_1	Right->Left	3004	6.4405	0.0375	6.4930	0.0278
SAVNW_n300, 3003_3001_1	Right->Left	3004	6.3381	0.0370	6.3779	0.0273
SAVNW_n300, 3003_3005_1	Right->Left	3004	6.4252	0.0381	6.4996	0.0284
SAVNW_n300, 3004_3002_1	Right->Left	3004	6.4702	0.0372	6.5274	0.0274
SAVNW_n300, 3004_3005_1	Right->Left	3004	6.6449	0.0355	6.7103	0.0258
SAVNW_n300, 3005_3003_1	Right->Left	3004	6.4950	0.0380	6.5965	0.0282
SAVNW_n300, 3005_3004_1	Right->Left	3004	6.4876	0.0364	6.5318	0.0265

Based on the selected interval, the speeds for the different measurements are calculated and compared to determine the fastest impedance swing from left to right and vice versa. The speed estimation for the static loads are presented in Table 18 and Table 19 while the speeds estimated for CMLD load cases are presented in Table 20and Table 21.

Table 18: Calculated speeds based on Impedance Measurements (Static Load Scenario, 152 Side)

Scenario (Static Load)	Swing Direction	Δt (s)	ΔR (pu)	Speed (pu/s)
SAVNW_n300, 3001_3003_1	Left->Right	0.0222	0.0096	0.4317
SAVNW_n300, 3003_3001_1	Left->Right	0.0242	0.0096	0.3955
SAVNW_350, 201_211_1	Right->Left	0.0533	-0.0092	0.1728
SAVNW_350, 205_206_1	Right->Left	0.0915	-0.0087	0.0949
SAVNW_350, 206_205_1	Right->Left	0.0958	-0.0087	0.0909
SAVNW_300, 205_206_1	Right->Left	0.1233	-0.0087	0.0705
SAVNW_300, 206_205_1	Right->Left	0.1376	-0.0087	0.0632

Table 19: Calculated Speeds Based on Impedance Measurements (Static Load Scenario. 3004 Side)

Scenario (Static Load)	Swing Direction	Δt (s)	ΔR (pu)	Speed (pu/s)
SAVNW_n300, 3001_3003_1	Right->Left	0.0322	-0.0095	0.2957
SAVNW_n300, 3003_3001_1	Right->Left	0.0354	-0.0095	0.2684
SAVNW_350, 201_211_1	Left->Right	0.0452	0.0094	0.2071
SAVNW_350, 205_206_1	Left->Right	0.0724	0.0091	0.1257
SAVNW_350, 206_205_1	Left->Right	0.0761	0.0091	0.1197
SAVNW_300, 205_206_1	Left->Right	0.1005	0.0091	0.0905
SAVNW_300, 206_205_1	Left->Right	0.1141	0.0091	0.0797

Table 20: Calculated speeds based on Impedance Measurements (CMLD Load Scenario, 152 Side)

Scenario (CMLD Load)	Swing Direction	Δt (s)	ΔR (pu)	Speed (pu/s)
SAVNW_350, 201_211_1_1	Right->Left	0.0726	-0.0090	0.1246
SAVNW_350, 211_201_1_1	Right->Left	0.0606	-0.0091	0.1501
SAVNW_300, 211_201_1_1	Right->Left	0.0811	-0.0090	0.1109
SAVNW_n300, 3001_3002_1_1	Left->Right	0.0382	0.0099	0.2588
SAVNW_n300, 3001_3003_1_1	Left->Right	0.0314	0.0098	0.3111
SAVNW_n300, 3002_3001_1_1	Left->Right	0.0000	0.0099	0.2246
SAVNW_n300, 3002_3004_1_1	Left->Right	0.0441	0.0099	0.2244
SAVNW_n300, 3003_3001_1_1	Right->Left	0.0326	0.0098	0.3000
SAVNW_n300, 3003_3005_1_1	Left->Right	0.0650	0.0099	0.1525
SAVNW_n300, 3004_3002_1_1	Right->Left	0.0453	0.0099	0.2179
SAVNW_n300, 3004_3005_1_1	Left->Right	0.0413	0.0099	0.2397
SAVNW_n300, 3005_3003_1_1	Left->Right	0.0842	0.0099	0.1177
SAVNW_n300, 3005_3004_1_1	Left->Right	0.0329	0.0100	0.3035

Table 21: Calculated Speeds Based on Impedance Measurements (CMLD Load Scenario. 3004 Side)

Scenario (CMLD Load)	Swing Direction	Δt (s)	ΔR (pu)	Speed (pu/s)
SAVNW_350, 201_211_1	Left->Right	0.0635	0.0093	0.1467
SAVNW_350, 211_201_1	Left->Right	0.0533	0.0094	0.1755
SAVNW_300, 211_201_1	Left->Right	0.0706	0.0093	0.1311
SAVNW_n300, 3001_3002_1	Right->Left	0.0457	-0.0097	0.2135
SAVNW_n300, 3001_3003_1	Right->Left	0.0384	-0.0097	0.2518
SAVNW_n300, 3002_3001_1	Right->Left	0.0526	-0.0098	0.1858
SAVNW_n300, 3002_3004_1	Right->Left	0.0526	-0.0098	0.1858
SAVNW_n300, 3003_3001_1	Right->Left	0.0398	-0.0096	0.2426
SAVNW_n300, 3003_3005_1	Right->Left	0.0744	-0.0098	0.1313
SAVNW_n300, 3004_3002_1	Right->Left	0.0572	-0.0097	0.1704
SAVNW_n300, 3004_3005_1	Right->Left	0.0655	-0.0098	0.1492
SAVNW_n300, 3005_3003_1	Right->Left	0.1014	-0.0098	0.0966
SAVNW_n300, 3005_3004_1	Right->Left	0.0442	-0.0099	0.2243

From the results presented in Table 18, Table 19, Table 20, and Table 21 the fastest impedance swing speed can be determined for swings in both direction and for both sides of the protected lines. The identified fastest speeds are listed in Table 22.

Table 22: Fastest Impedance Swing Speeds

Location	Static Load Model		CMLD Load Model	
	Direction	Speed (pu/s)	Direction	Speed (pu/s)
152	Left->Right	0.4317	Left->Right	0.3111
152	Right->Left	0.1728	Right->Left	0.1501
3004	Right->Left	0.2957	Right->Left	0.2518
3004	Left->Right	0.2071	Left->Right	0.1755

5.1.3 – Impedance Blinder Setting Selections

As described in Chapter 4, there are limiting factors that will influence the acceptable blinder locations for OOS protection relay. Selection of blinder location considering these limitations are discussed in Chapter 4, and its step-by-step application is presented here.

<u>Step 1 – Identify Initial load points.</u>

To identify the limits for the outer blinder, the initial load point closest to the origin must be determined. This is done by analyzing the load point of all expected operating conditions. The initial loading point for each of the study scenarios are presented in Table 23. These points are common to both types of load models.

Table 23: Initial Loading Points for Each Study Scenario

	152 Side		3004 Side	
	R (pu)	**X (pu)**	**R (pu)**	**X (pu)**
SAVNW_n300	-0.3047	-0.1035	0.2890	-0.1219
SAVNW_n200	-0.3566	-0.2377	0.3931	-0.2244
SAVNW_n100	-0.2985	-0.4702	0.5204	-0.5295
SAVNW_0	-0.3115	-0.0825	0.2700	-0.1273
SAVNW_205	0.2758	-0.2476	-0.4714	-0.1414
SAVNW_300	0.2481	-0.1509	-0.3419	-0.0558
SAVNW_350	0.2326	-0.1210	-0.3003	-0.0372

From Table 23, the loading point located nearest to the origin on both sides of the impedance plane can be identified when looking at both sides of the protected lines. The limiting impedance points based on these are summarized in Table 24. The values presented in Table 24 are used to determine the acceptable position for the outer blinder.

Table 24: Limiting Impedance Points

Impedance Plane	152 Side			3004 Side		
	R (pu)	**X (pu)**	**|Z| (pu)**	**R (pu)**	**X (pu)**	**|Z| (pu)**
Positive Plane	0.2326	-0.1210	0.2621	0.2700	-0.1273	0.2985
Negative Plane	-0.3047	-0.1035	0.3218	-0.3003	-0.0372	0.3026

<u>Step 2 – Determine the distance protection zone boundaries.</u>

The limiting factor for the inner blinder is the distance protection scheme. In the test system, there is no specified distance protection scheme. Thus, a Mho distance protection scheme with typical settings is assumed to determine the limit for the inner blinder. To find the distance protection settings, the impedance characteristics of the lines connected to buses 152 and 3004, given in Table 25, are used.

Table 25: Line Impedance of Protected and adjacent Lines

From	To	ID	kV	R (pu)	X (pu)	Comment
152	3004	1	500	0.003	0.03	Protected Line
3002	3004	1	500	0.006	0.054	Shortest next line at bus 3004
151	152	1	500	0.0026	0.046	
151	152	2	500	0.0026	0.046	
152	202	1	500	0.0008	0.01	Shortest next line at bus 152

As described in the methodology presented in Chapter 4, the Zone 2 protection characteristic limits the inner blinder position. The Zone 2 protection can be estimated based on the impedance of the protected line and 50% of the impedance of the shortest connected line. From this, the Zone 2 impedance can be calculated with the following equation (assuming that the impact of infeed is negligible):

$$Z_{zone2(3004)} = \left(R_1 + \frac{R_2}{2}\right) + j\left(X_1 + \frac{X_2}{2}\right) = \left(0.003 + \frac{0.0008}{2}\right) + j\left(0.03 + \frac{0.01}{2}\right) = 0.0034 + j0.035$$

$$Z_{zone2} = 0.0034 + j0.035 = 0.035165\angle 84.45°$$

$$Z_{zone2(152)} = \left(R_1 + \frac{R_2}{2}\right) + j\left(X_1 + \frac{X_2}{2}\right) = \left(0.003 + \frac{0.006}{2}\right) + j\left(0.03 + \frac{0.054}{2}\right) = 0.006 + j0.057$$

$$Z_{zone2} = 0.006 + j0.057 = 0.057315\angle 83.99°$$

The Zone 2 protection Mho circle has a diameter equal to the Zone 2 impedance magnitude and is centered at the mid point of the Zone 2 impedance.

The Zone 2 impedance magnitude at the respective relay is used to determine the initial location of the inner blinders. As discussed in Chapter 4, the position of the inner blinder is set equal to the impedance magnitude for Zone 2 (imposed solely in the R-plane) leaving approximately 50% margin from Zone 2 boundary. Based on this criterion, the inner impedance blinder is positioned at ±0.036 on the R-plane axis for the relay at bus 3004. The blinders will have the same angle as the protected line. The setting for the relay at bus 152 is determined in the same manner.

To simplify the simulations, the same inner blinder setting will be used for both the relays at the 152 and 3004 sides. The value of 0.036 will be selected, this value corresponds to the bus 3004 side relay, it will be sufficient for the bus 152 side relay as it is still outside Zone 2 which occupies roughly the resistive region between R = -0.0287 and R = 0.0287.

<u>Step 3 – Calculate blinder spacing.</u>

The spacing between the inner and outer blinder can be calculated based on the impedance swing speed, the equation to calculate the blinder spacing is presented in eq. 4.2. When calculating the blinder spacing, a safety factor of 5% and a travel time of 3 cycles based on a 60 Hz frequency is considered.

$$Blinder\ Spacing = Speed \times 1.05 \times time\ of\ 3\ Cycles\ (s)$$

It may be desirable to select different blinder spacings for the left and right side of the relay characteristics, since the speeds for the swing from right to left and left to right are different. The maximum speed for the swings from right to left are used to calculate the right side spacing while the maximum speed for the swing from left to right is used to calculate the left side spacing. Alternatively, the fastest swing speed in either direction can be used to consider a single spacing applied at both sides. The calculated blinder spacings are presented in Table 26 and Table 27 for static and CMLD load models respectively.

Table 26: Blinder Spacing (Static Load Scenarios)

Bus	Side	Speed	Spacing
152	Right	0.1728	0.0091
152	Left	0.4317	0.0227
3004	Right	0.2957	0.0155
3004	Left	0.2071	0.0109

Table 27: Blinder Spacing (CMLD Load Scenarios)

Bus	Side	Speed	Spacing
152	Right	0.1501	0.0079
152	Left	0.3111	0.0163
3004	Right	0.2518	0.0132
3004	Left	0.1755	0.0092

Step 4 – Determine blinder positions and verify it is in acceptable region.

Based on the estimation of the distance protection, the inner blinder should be greater than 0.3517 pu (when considering the blinders in the positive resistive impedance plane). A value of 0.036 is selected for the initial inner blinder position. The outer blinder position is determined by adding the calculated blinder spacing to the selected inner blinder position. The calculated outer blinder position is calculated and are presented in Table 28 and Table 29 for the cases with static and CMLD load models respectively.

Table 28: Inner and Outer Impedance Blinder Positions (Static Load)

Blinder Impedances [pu]	Blinder	
	Inner	Outer
152 Side, Positive Impedance	0.0360	0.0451
152 Side, Negative Impedance	-0.0360	-0.0587
3004 Side, Positive Impedance	0.0360	0.0515
3004 Side, Negative Impedance	-0.0360	-0.0469

Table 29: Inner and Outer Impedance Blinder Positions (CMLD Load)

Blinder Impedances [pu]	Blinder	
	Inner	Outer
152 Side, Positive Impedance	0.0360	0.0439
152 Side, Negative Impedance	-0.0360	-0.0523
3004 Side, Positive Impedance	0.0360	0.0492
3004 Side, Negative Impedance	-0.0360	-0.0452

It is necessary to check whether the initial load points are too close to locations of the outer blinder. When the outer blinders are extended in the reactive impedance plane, there is a large distance between the blinder pairs and the initial loading points, this will ensure that there are no false positives due to small overloading conditions in the network.

The distance protection zones, load impedance characteristics, and the blinders for the relays at bus 152 and bus 3004 are plotted in Figure 46 and Figure 47 respectively.

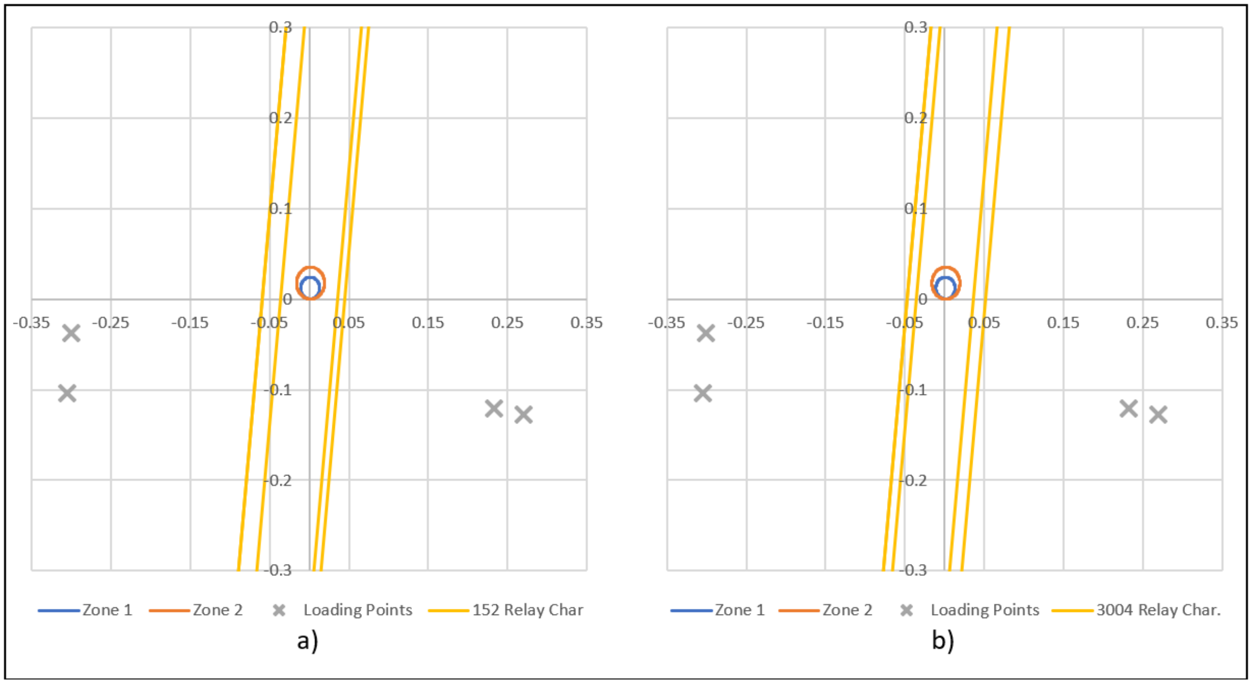

Figure 46: Blinders, Distance Protection Zones and Load Impedance Characteristics (a) 152 side (b) 3004 side (Static load)

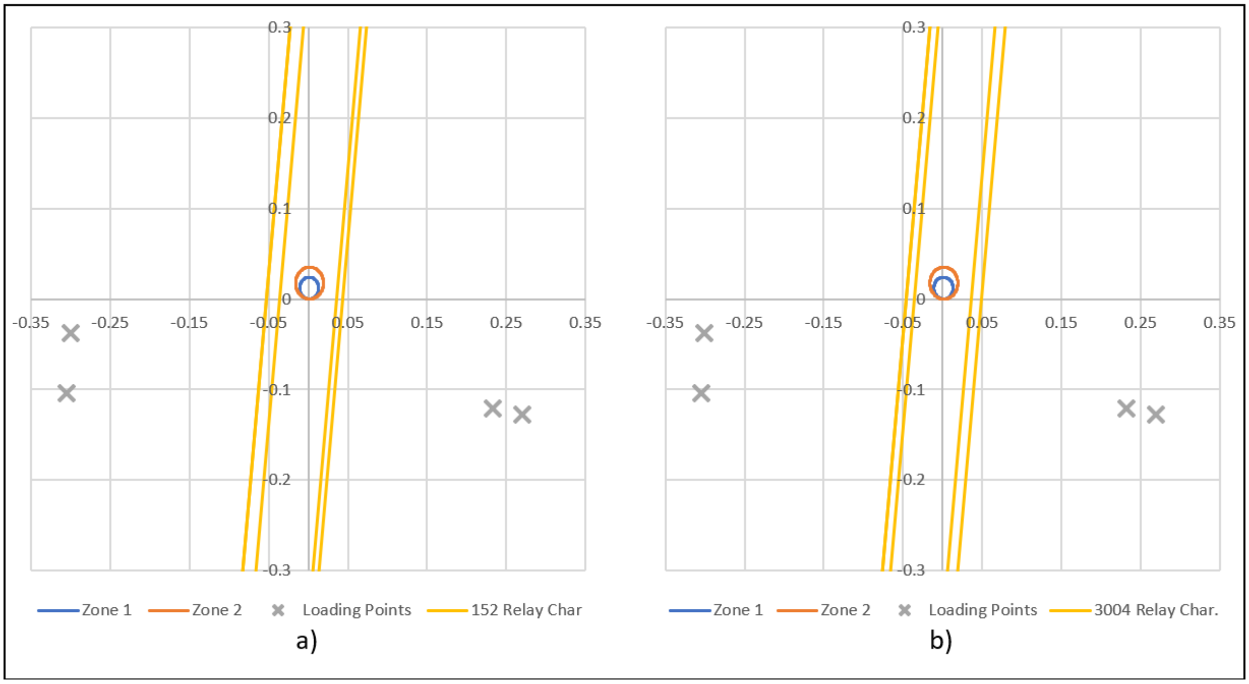

Figure 47: Blinders, Distance Protection Zones and Load Impedance Characteristics (a) 152 side (b) 3004 side (CMLD load)

Step 5 – Validate relay blinder positions.

The impedance characteristics determined using the proposed method is tested by performing an exhaustive set of dynamic simulations to determine the dependability and security; that is to check whether the relay will always activate for OOS conditions that it should detect and do not activate otherwise.

All load flow scenarios and contingencies are simulated again. The relays should not activate for the conditions that previously did not results in OOS situations. For the cases that resulted in OOS in the initial simulations, it is expected that the relay should detect the OOS condition and trip the protected line. Table 30 and Table 31 tabulate the results for the cases that demonstrated OOS conditions in the initial study. These table denote whether the relays activate (trip) or not (No Trip) when using the calculated blinder settings (referred to as Relay Parameter Set 1).

Table 30: OOS Relay Operation with Relay Parameter Set 1 (Static Model)

No.	Network Case	Disturbance	Load Model	Relay
1	SAVNW_n300	3001_3003_1	Static	No Trip
2	SAVNW_n300	3003_3001_1	Static	Trip
3	SAVNW_300	205_206_1	Static	Trip
4	SAVNW_300	206_205_1	Static	Trip
5	SAVNW_350	201_211_1	Static	No Trip
6	SAVNW_350	205_206_1	Static	Trip
7	SAVNW_350	206_205_1	Static	Trip

Table 31: OOS Relay Operation with Relay Parameter Set 1 (CMLD Model)

No.	Network Case	Disturbance	Load Model	Relay
1	SAVNW_n300	3001_3002_1	CMLD	Trip
2	SAVNW_n300	3002_3001_1	CMLD	Trip
3	SAVNW_n300	3001_3003_1	CMLD	No Trip
4	SAVNW_n300	3003_3001_1	CMLD	Trip
5	SAVNW_n300	3002_3004_1	CMLD	Trip
6	SAVNW_n300	3004_3002_1	CMLD	Trip
7	SAVNW_n300	3003_3005_1	CMLD	Trip
8	SAVNW_n300	3005_3003_1	CMLD	Trip
9	SAVNW_n300	3004_3005_1	CMLD	Trip
10	SAVNW_n300	3005_3004_1	CMLD	Trip
11	SAVNW_300	211_201_1	CMLD	Trip
13	SAVNW_350	211_201_1	CMLD	Trip
14	SAVNW_350	211_201_1	CMLD	No Trip

From the results presented above, using an OOS relay with parameter set 1, most of the OOS events are detected, and the line is tripped accordingly. However, there are certain OOS conditions that were not detected. There is no guarantee that a relay will be able to work for all out of step conditions, but the parameters for this test case may be adjusted to detect all OOS conditions in the study network.

The likely cause for the relay parameters to be insufficient for all cases is the inconsistent speed of the impedance characteristics. The speed used to calculate the blinder spacings were determined using a specific location in the R-X plane. A small safety factor is added to the blinder spacing calculations to account for the speed variance, but it seems not sufficient to accommodate all variations. As an adjustment to the blinder settings, there are two obvious options, the first is to increase the safety factor, the second is to adjust the position of the blinder pair. Both methods will be tested.

Originally a safety factor of 5% was used to calculate the blinder spacing, this will be increased to 10%, this will allow slightly larger distance between the blinders. The new parameter set considering the increased safety factor will be referred to Relay Parameter Set 2. The inner blinder was originally set to around ±0.036 pu, this is assumed based on the approximate diameter of the distance protection Zone 2. The inner blinder can be moved closer to the origin if it does not enter Zone 2 which is approximately between ±0.018 pu. Thus, another set of OOS relay settings is calculated using an inner blinder position of ±0.03 pu, and it is referred to as Relay Parameters Set 3. The updated relay parameters for both static load and CMLD load scenarios are presented in Table 32 and Table 33 respectively. Another set of settings is computed considering both modifications simultaneously (Parameter Set 4).

Table 32: Modified OOS Relay Parameter Sets (Static Load)

Blinder Impedance (in [pu])	**Set 2**		**Set 3**		**Set 4**	
	Inner	**Outer**	**Inner**	**Outer**	**Inner**	**Outer**
152 Side, Positive side	0.0360	0.0455	0.0300	0.0391	0.0300	0.0395
152 Side, Negative side	-0.0360	-0.0597	-0.0300	-0.0527	-0.0300	-0.0537
3004 Side, Positive side	0.0360	0.0523	0.0300	0.0455	0.0300	0.0463
3004 Side, Negative side	-0.0360	-0.0474	-0.0300	-0.0409	-0.0300	-0.0414

Table 33: Modified OOS Relay Parameter Sets (CMLD Load)

Blinder Impedance (in [pu])	Set 2		Set 3		Set 4	
	Inner	Outer	Inner	Outer	Inner	Outer
152 Side, Positive side	0.0360	0.0443	0.0300	0.0379	0.0300	0.0383
152 Side, Negative side	-0.0360	-0.0531	-0.0300	-0.0463	-0.0300	-0.0471
3004 Side, Positive side	0.0360	0.0498	0.0300	0.0432	0.0300	0.0438
3004 Side, Negative side	-0.0360	-0.0457	-0.0300	-0.0392	-0.0300	-0.0397

The relay performance with the modified settings is tested using dynamic simulations in PSSE. The results are tabulated in Table 34 and Table 35 for the static and CMLD load models respectively. The modifications to the safety factor and modifying the inner blinder position both assist in improving the accuracy of the relay. When both modifications are applied the relay can identify all OOS conditions.

Table 34: OOS Relay Trip Checks (Static Model)

No.	Network Case	Disturbance	Load Model	Relay Tripping			
				Set 1	Set 2	Set 3	Set 4
1	SAVNW_n300	3001_3003_1	Static	No Trip	Trip	No Trip	Trip
2	SAVNW_n300	3003_3001_1	Static	Trip	Trip	Trip	Trip
3	SAVNW_300	205_206_1	Static	Trip	Trip	Trip	Trip
4	SAVNW_300	206_205_1	Static	Trip	Trip	Trip	Trip
5	SAVNW_350	201_211_1	Static	No Trip	No Trip	Trip	Trip
6	SAVNW_350	205_206_1	Static	Trip	Trip	Trip	Trip
7	SAVNW_350	206_205_1	Static	Trip	Trip	Trip	Trip

Table 35: OOS Relay Trip Checks (CMLD Model)

No.	Network Case	Disturbance	Load Model	Relay Tripping			
				Set 1	Set 2	Set 3	Set 4
1	SAVNW_n300	3001_3002_1	CMLD	Trip	Trip	Trip	Trip
2	SAVNW_n300	3002_3001_1	CMLD	Trip	Trip	Trip	Trip
3	SAVNW_n300	3001_3003_1	CMLD	No Trip	Trip	Trip	Trip
4	SAVNW_n300	3003_3001_1	CMLD	Trip	Trip	Trip	Trip
5	SAVNW_n300	3002_3004_1	CMLD	Trip	Trip	Trip	Trip
6	SAVNW_n300	3004_3002_1	CMLD	Trip	Trip	Trip	Trip
7	SAVNW_n300	3003_3005_1	CMLD	Trip	Trip	Trip	Trip
8	SAVNW_n300	3005_3003_1	CMLD	Trip	Trip	Trip	Trip
9	SAVNW_n300	3004_3005_1	CMLD	Trip	Trip	Trip	Trip
10	SAVNW_n300	3005_3004_1	CMLD	Trip	Trip	Trip	Trip
11	SAVNW_300	211_201_1	CMLD	Trip	Trip	Trip	Trip
13	SAVNW_350	211_201_1	CMLD	Trip	Trip	Trip	Trip
14	SAVNW_350	211_201_1	CMLD	No Trip	No Trip	No Trip	Trip

The relay performance also needs to be tested for security, that is to ensure that OOS relay will not trip for stable power swings. The contingencies that do not result in OOS conditions are simulated with the settings of the relay and it is observed that there are no concerns with the security of the relay settings.

As an additional test, the relay settings identified from the simulations with static load model are applied to the OOS relay and repeated simulation with CMLD load model. Table 36 tabulates the performance of the OOS relay for all OOS conditions that were observed with CMLD model when using the parameters identified based on the static load model (presented in Table 28). As seen from Table 36, all the OOS conditions are correctly identified by the OOS relay.

Table 36: OOS Relay Operation in CMLD load scenarios with setting identified using static load model (Parameter Set 1)

No.	Network Case	Disturbance	Load Model	Relay
1	SAVNW_n300	3001_3002_1	CMLD	Trip
2	SAVNW_n300	3002_3001_1	CMLD	Trip
3	SAVNW_n300	3001_3003_1	CMLD	Trip
4	SAVNW_n300	3003_3001_1	CMLD	Trip
5	SAVNW_n300	3002_3004_1	CMLD	Trip
6	SAVNW_n300	3004_3002_1	CMLD	Trip
7	SAVNW_n300	3003_3005_1	CMLD	Trip
8	SAVNW_n300	3005_3003_1	CMLD	Trip
9	SAVNW_n300	3004_3005_1	CMLD	Trip
10	SAVNW_n300	3005_3004_1	CMLD	Trip
11	SAVNW_300	211_201_1	CMLD	Trip
13	SAVNW_350	211_201_1	CMLD	Trip
14	SAVNW_350	211_201_1	CMLD	Trip

When examined the fastest calculated impedance speed for both the static load and CMLD load scenarios (Table 26 and Table 27), the speed values in the static load model scenarios are faster than in the CMLD scenario, this could be a result of the motor load characteristics of the CMLD load model. Since the impedance rate of change is higher in the static load models, the calculated blinder spacings are larger than those computed for the CMLD scenarios. The increased blinder spacing allow for a larger window for the relay to detect OOS conditions, this in effect is like increasing the safety margin when adjusting the blinder. This analysis demonstrated that the relay setting identified using static load models are applicable even if the load model is changed to a

CMLD load model. However, the system must be further tested to see whether there are false positives.

5.2. Validating Relay Settings using EMT Simulation Software PSCAD

A version of the study case is implemented on Electromagnetic Transient (EMT) simulation tool PSCAD. In EMT simulations, the network is modeled with much more details considering all three phases. The relay model in the simulation program is implemented with all details including signal processing. The purpose of the test is to check whether the relay settings identified using phasor domain dynamic simulation studies performed in PSSE are valid when applied in a more realistic simulation model before applying in the field. The dynamic and power flow studies required to determine relay parameters can be performed in a shorter time in PSSE, specifically for large power systems. If the parameters identified from PSSE studies are proved to work well in the system and relays simulated in PSCAD, more confidence can be gained in the proposed setting methodology that relies on PSSE simulations.

The relay settings are entered into the detailed OOS relay model in PSCAD. The protection relay used in PSCAD requires settings to be entered in ohm-secondary. These values are computed considering typical voltage and current transformer ratios and their rated secondary values. The relay rated values are compiled in Table 37.

Table 37: Power System and Instrument Transformer Parameters

Parameter	Rating
MVA	100
Voltage (Primary)	500 kV
Current (Primary)	0.11547 kA
Impedance (Primary)	2500 ohm
Voltage (Secondary)	69 V
Current (Secondary)	5 A
Impedance (Secondary)	17.925 ohm
VT Ratio	4184
CT Ratio	30

In the PSCAD simulation case, loads are modeled as static loads, as such the blinder settings calculated with static load model in PSSE are used for the PSCAD relay model. The parameters are calculated considering Relay Parameter Set 4 are presented in Table 38 and Table 39 for the relays at bus 152 and bus 3004 respectively.

Table 38: PSCAD OOS Relay Blinder Settings (152 Side)

Blinder position	Impedance	
	Pu	Ohms-secondary
Inner zone positive reach	0.0300	0.5378
Inner zone negative reach	-0.0300	-0.5378
Outer zone positive reach	0.0395	0.7081
Outer zone negative reach	-0.0537	-0.9634

Table 39: PSCAD OOS Relay Blinder Settings (3004 Side)

Blinder position	Impedance	
	pu	Ohms-secondary
Inner zone positive reach	0.0300	0.5378
Inner zone negative reach	-0.0300	0.5378
Outer zone positive reach	0.0463	0.8293
Outer zone negative reach	-0.0414	-0.7420

In addition to the blinder settings, there are additional information required to describe the protected line and some timer settings. These additional parameters are presented in Table 40.

Table 40: Additional PSCAD OOS Relay Parameters

Parameter	Value
Line data: Impedance magnitude	75.374 [ohm]
Line data: Impedance angle	84.289 [deg]
Trip during out-of-step	Trip of way in
Power swing timer setting for tripping (T_trip)	0.05 [s]

After the relay parameters are entered, the network is examined under the OOS conditions determined in PSSE studies to verify that the relays will operate as intended. Due to the modeling differences between PSSE and PSCAD, it is not expected that the network response is identical, but based on preliminary tests, the models have a sufficiently close match.

The simulations are performed under three different initial power flow settings with multiple outage conditions. As a demonstration of the simulation results, the following section provides a comparison between the PSSE and PSCAD simulations for case n300, event 3001_3003_1.

PSCAD and PSSE Comparison

To examine the correct operation of the relay in the PSCAD model, the trajectory of the impedance seen by the relay will be examined along with several internal signals from the relay model which detect when the impedance swing passes through the blinders. The description of these signals is presented in Table 41.

Table 41: Internal OOS signal description, PSCAD Relay

Signal Name	Description
PK_1	Picks up when impedance swing enters the outer blinder, ends when impedance swing exits opposite outer blinder
PK_2	Picks up when impedance swing enters the inner blinder, ends when impedance swing exits opposite inner blinder
PK_4	Picks up T_trip sec after this impedance swing enters the outer blinder. Will only pick up if PK_2 is active.
TI_1	Timer - starts when PK1 picks up and ends when PK2 picks up. Tracks time for the impedance swing to cross from the outer to inner blinder
TI_3	Timer - starts when PK4 picks up and ends when PK1 ends.
T1	Out of Step Tripping signal, high when relay tripping is required.

The scenario SAVNW_n300 is examined, the event 3001_3003_1 is applied. When examining the impedance seen by the relay, a power swing can be seen after applying the fault. Figure 48 depicts the R-X plot for the period from 6 to 7 seconds, the impedance swing is traveling form the negative resistive plane to the positive resistive plane (from left to right).

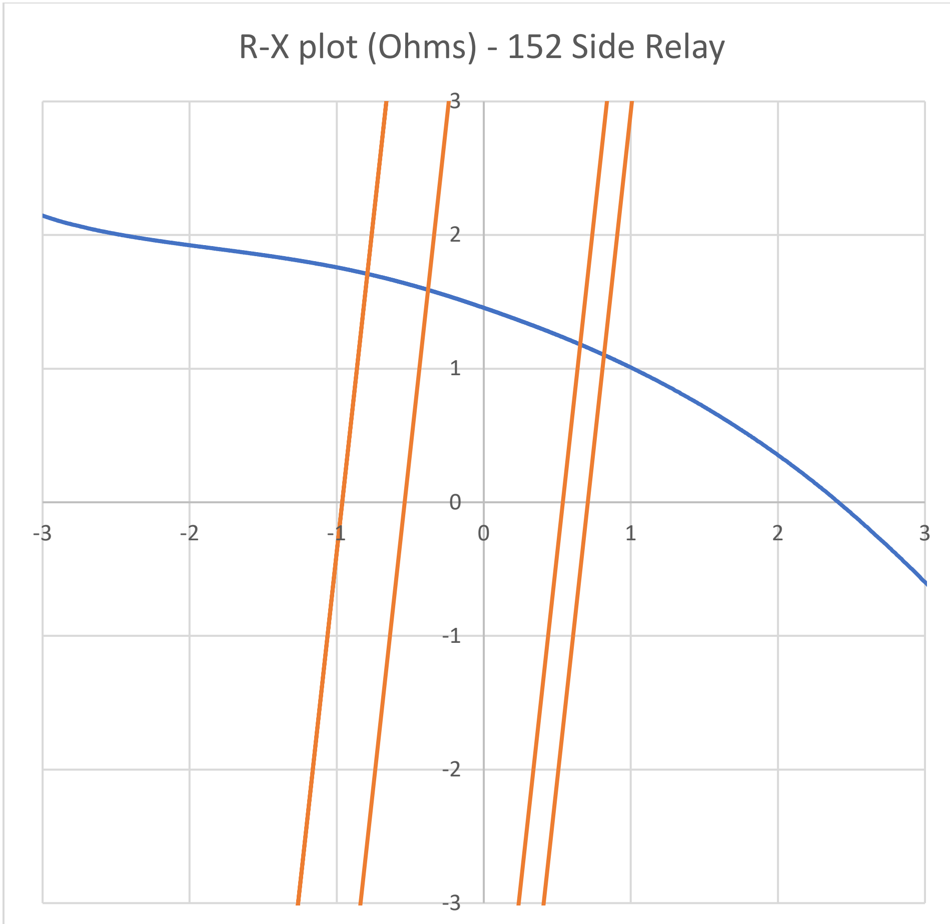

Figure 48: R-X measurement at 152 side relay

Figure 49 depicts several of the internal signals produced by the PSCAD relay model. These signals are plotted for the interval from 6.3 s to 6.7 s and demonstrate that the relay has successfully detected the OOS condition and issued the tripping signal.

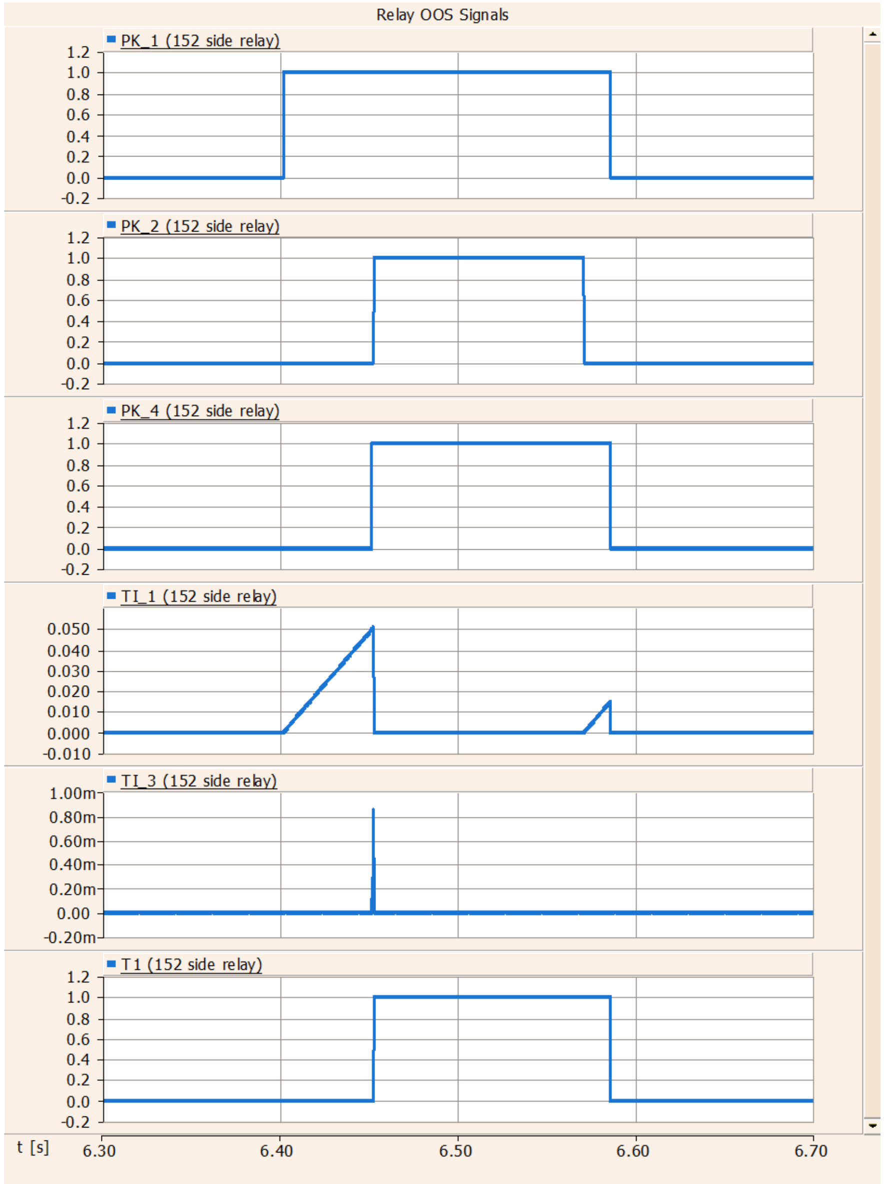

Figure 49: PSCAD Relay Signals

Examining the out-of-step tripping signal T1 demonstrates that the relay is successfully detecting OOS conditions and issuing the relay tripping signal with the relay settings identified in the PSSE studies. The impedance swing can be examined along-side the relay signals to confirm that the signals are being issued correctly.

When examining the signals PK_1 and PK_2, these signals pick-up at approximately 6.4 seconds and 6.454 seconds respectively. The timer signal TI_1 begins when the PK_1 picks up, the timer T1_3 begins 0.05 seconds (T_Trip) after TI_1 begins. These signals are presented in Figure 50.

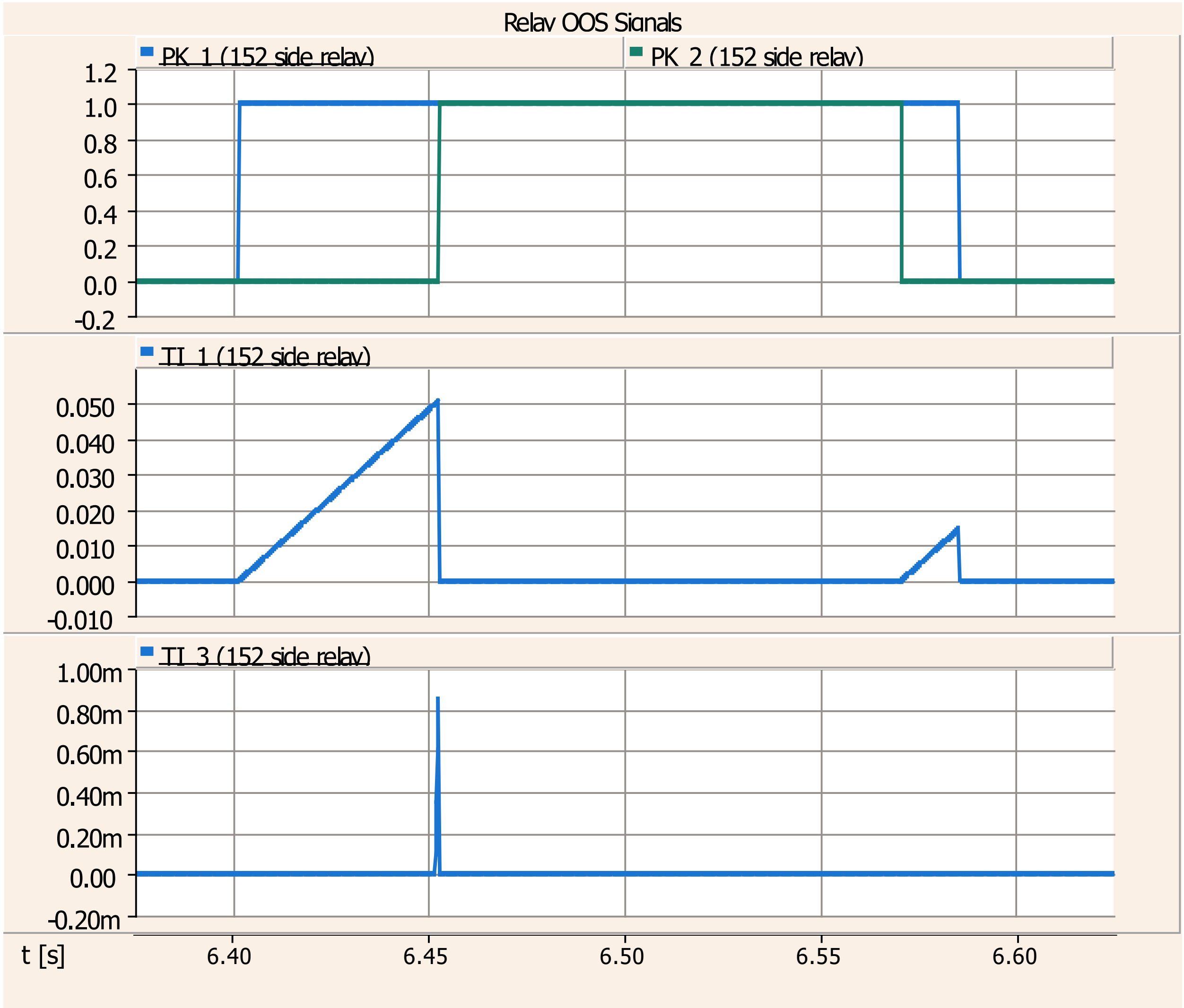

Figure 50: Relay Signals PK_1, PK_2, TI_1, TI_3 (152 side)

If the R-X plot is examined for the period between 6.4 seconds and 6.454 seconds, it is apparent that the PK_1 signal picks up when the impedance swing crosses the outer blinder (negative side) and PK_2 signal picks up when the impedance swing crosses the inner blinder (negative side). Timer TI_1 counts the time for the impedance swing to cross from the outer to inner blinder. The R-X plot for the interval 6.4-6.454 seconds is presented in Figure 51

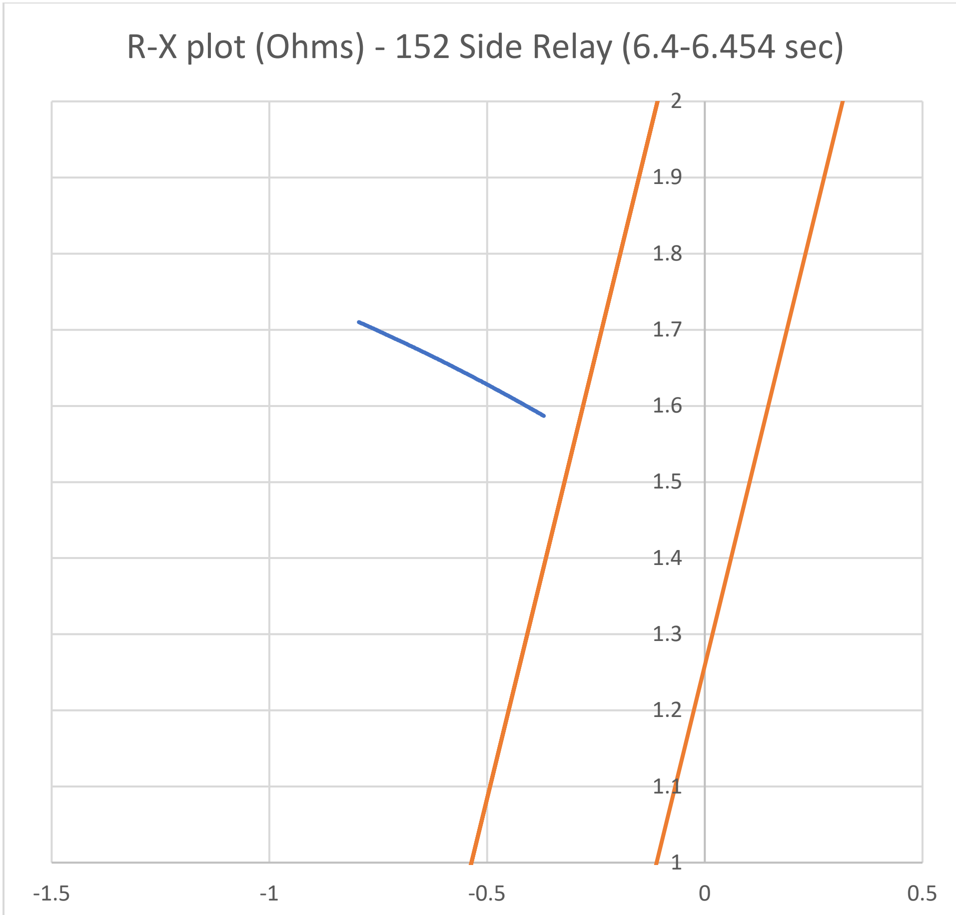

Figure 51: R-X measurement at 152 side relay (6.4-6.454 sec)

The timer signal TI_3 begins T_Trip seconds after the timer signal TI_1, if the impedance swing exits the interval between the outer and inner blinders than the trip signal will be issued if the relay is set to trip on the way in. Close examination of these signals, it can be observed that the since the time TI_3 is active, the trip signal is issued at the same instance that PK_2 picks up (passing inner blinder). The signals PK_2, TI_3 and tripping signal T_1 are plotted in Figure 52.

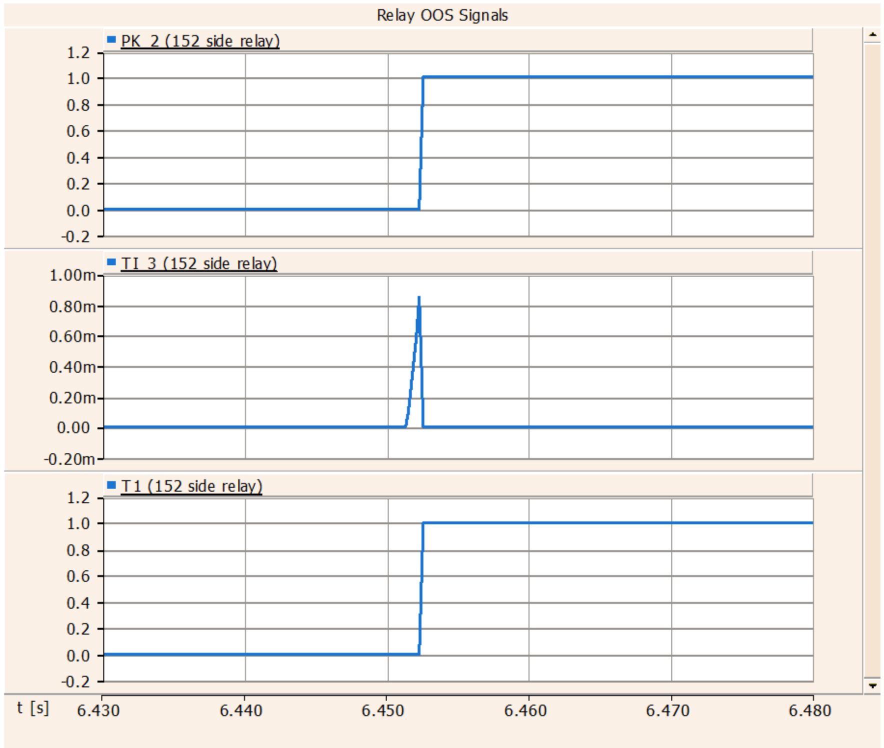

Figure 52: PSCAD Relay Signals (152 side)

5.3. Chapter Summary

In this chapter, the methodology proposed in Chapter 4 is used to determine the out-of-step relay settings for a test network. The initial relay parameters calculated are tested and refined through an iterative process until they are considered satisfactory for the network. It is not guaranteed that there is a set of relay parameters that address all the OOS conditions encountered in a system, it is up to the user to decide what are the most important events that the relay should cover. Using the test network, it is possible to obtain a set of relay parameters that are sufficient for all OOS conditions in the test network.

The relay parameters determined through the PSSE study are further examined by applying the relay settings to an equivalent network in a separate simulation software, in this case PSCAD. The PSCAD simulations demonstrate that the relay parameters determined in the PSSE following the proposed methodology are robust enough to use in the field.

Chapter 6 – Conclusion

6.1. Summary of Thesis

Although the apparent positive sequence impedance based out-of-step protection is standard, determining appropriate blinder locations and time settings is not straightforward when applying to a complex transmission system. In this thesis, background of the line OOS protection and setting process is reviewed and a systematic procedure to determine the setting for an OOS relay using dynamic simulations is proposed. Each step of the proposed methodology is discussed and demonstrated through a case study using a test network.

The proposed methodology involves the following steps: Identification of the set of power flow conditions and list of contingencies that need to be considered; Determination of impedance swing speeds using phasor domain dynamic simulations with a temporary set of blinders; establishment of limits for the blinder settings considering steady state loading and distance protection settings; initial placement of blinders considering the limits and maximum swing speed; and Refinement of the initial relay setting through an iterative process of testing and adjustment until the optimal settings for the OOS relay are found.

The proposed method is applied to a -test network demonstrating the steps and appropriate settings for two OOS relays located at opposite ends of a tie-line are determined. The simplified test network is developed in PSSE, and the necessary simulations are performed using this simulation software. After identifying the OOS relay settings through the PSSE simulations, an EMT simulation model of the same network implemented in PSCAD simulation software is also used to further validate the setting process.

6.2. Conclusion and Contributions

This thesis proposed a systematic procedure to determine the setting of a transmission line OOS protection relay using dynamic simulations. The proposed method is applicable to large complex power systems as the procedure is based on dynamic simulations and many of the steps can be automated through scripting. It is validated using a test network which is not very large but adequately represents the challenges of setting OOS relays in a complex power system. The proposed procedure is applied to determine the settings of two OOS relays on either side of a tie line in the test network. The studies presented in this thesis demonstrate that the proposed methodology can successfully identify the OOS relay settings.

The studies to determine and refine the relay settings are performed using the phasor domain simulation tool PSSE. When these settings are applied to a relay and network represented using detailed models in an electromagnetic transient simulation software PSCAD/EMTDC, settings are found to be satisfactory. PSCAD/EMTDC simulations are a more realistic representation of the network and the protection relay. This analysis demonstrates that the simulations performed in the phasor domain (PSSE) are adequate for determining credible OOS relay settings.

The case study considered two types of load representations, using static load model and complex load model available in PSSE. The results showed maximum swing speeds observed with static load model are somewhat faster compared to the corresponding swing speeds observed with complex load model. Therefore, the two simulation models resulted in slightly different settings indicating that the load model has some influence on the OOS relay settings. Since the faster swing speeds result in large blinder spacings, the relay parameters identified using the static load model worked well when tested in the simulations with CMLD load model. However, the opposite, that is the application of relay settings identified using CMLD load model for the static load scenarios could lead to non-detection of OOS conditions.

6.3. Recommendations for Future Work

There are some additional studies that could be performed to further refine the methodology and expand on the robustness.

Test the methodology on a large-scale network.

To simplify the calculations, the test network used was relatively small (~20 bus network). The methodology should be tested using a larger more complex network to ensure the methodology effectiveness. There are some considerations when using a larger network, unless there are known out-of-step conditions it can be difficult to determine these conditions. As the complexity of the network increase the number of events to check to determine the OOS conditions also increase, this will increase the number of simulations that must be studied to identify the required information for determining relay limits and initial blinder positions.

Test the methodology in a system with multiple relays to investigate how the methodology could be adapted for relay coordination.

The test network used during this study used an OOS relay at a single location. In a larger network there may be multiple location protected by relays and may require coordination between relays to trip the necessary lines to protect the network. The Coordination between relays may require consideration when determining the relay settings and should be investigated to determine how the methodology may be modified to reflect this.

Inspect the impact of trip-on-way-in (TOWI) and trip-on-way-out (TOWO)

The relay tested in PSSE uses trip-on-way-in logic, however, trip-on-the-out is also tripping logic which OOS relay models may use. As described in 2.2, there and benefits and detriments to TOWI and TOWO. For instance, using TOWO tripping logic there is a risk of tripping the relay too late to save the network. Using TOWI tripping logic, if the relay attempts to trip while the power angle approaches 180 degrees there is a chance that a restrike may occur. Both these issues could influence the position of the blinders and should be considered and studied.

References

[1] "Power Swing and Out-of-Step Considerations on Transmission Lines", Report by IEEE PES PSRC working Group D6, 2005. Available at https://www.pes-psrc.org/reports, accessed Aug 2023,

[2] "1996 System Disturbances – Review of Selected 1996 Electric System Disturbances in North America", North American Electric Reliability Council, August 2002,

[3] "Protection System Response to Power Swings", North American Electric Reliability Council, Aug 2013,

[4] Yuanqi Liu and Yutian Liu, "Aspects on Power System Islanding for Preventing Widespread Blackout," 2006 IEEE International Conference on Networking, Sensing and Control, Ft. Lauderdale, FL, USA, 2006, pp. 1090-1095, doi: 10.1109/ICNSC.2006.1673304

[5] Demetrious A Tziouvaras, Daquin Hou "Out-of-step protection fundamentals and advancements," 57th Annual Conference for Protective Relay Engineers, 2004, College Station, TX, USA, 2004, pp. 282-307, doi: 10.1109/CPRE.2004.238495

[6] Hadi Saadat "Power System Analysis", © 1999 by McGraw-Hill

[7] Sumit Paudyal, Gokaraju, Mohinday S. Sachdev "Application of Equal Area Criterion Conditions in Time Domain for Out-of-Step Protection", IEEE Transactions on Power Delivery, Vol. 25, No. 2, April 2010, pp 600-609

[8] GER-3180 "Application of Out-of-Step Blocking and Tripping Relays", by John Berdy,

[9] Q. Verzosa Jr. "Realistic Testing of Power Swing Blocking and Out-of-Step Tripping Function", 66th Annual Conference for Protective Relay Engineers, College Station, TX, USA 2014. pp.430-449

[10] Prabha Kundur "Power System Stability and Control" © 1994 by McGraw-Hill

[11] "Srinu Babu Matta and Seethalekshmi K "Out-of-step detection in emerging power systems key issues and challenges", The Journal of CPRI, Vol 10. No. 3, September 2014 pp 427-440

[12] Normann Fischer, Gabriel Benmouval, Daquin Hou, Demetrios Tziouvaras, Jown Dyrne-Finley, Brian Smyth "Tutorial on Power Swing Blocking and Out-of-Step Tripping",

Presented at 39th Annual Western Protective Relay Conference, Spokane, Washington, October 16-18, 2012

[13] PSSE 33.9 Program Application Guide Volume II, May 2016

[14] PSSE 33.12.2 Model Library, April 2020

[15] Gabriel Benmouyal, Daqing Hou, Demetrios Tziouvaras "Zero-Setting Power-Swing Blocking Protection", 31st Annual Western Protective Relay Conference, Spokane, WA, October19-21, 2004

[16] Yofre Jacome, Charles F Henville "Setting Out-of-step Blocking or Tripping Using Dynamic Simulations", Presented to Western Protective Relay Conference 2011, Spokane, Washington, USA.

[17] "Ke Wang, "Power System Critical Cutset Identification based on Rolling Double Level Hierarchical Clustering", Applied Energy Symposium and Forum, Renewable Energy Integration with Mini/Microgrids, REM 2018, 29-30 September 2018. Rhodes, Greece,

[18] PSSE 33.10 Program Application Guide Volume I, April 2017

[19] P.Pourbeik, "Developing Dynamic Load Models for Australian Eastern Interconnected System", Report prepared for Australian Energy Market Operator, June 2019

[20] "Supporting paper: EMT Models in NERC MOD, TPL, and FAC Standards" NERC Inverter-Based Resource Performance Subcommittee (IRPS), 2022

[21] PSCAD Official Website https://pscad.com/software/pscad/overview,

[22] PRSIM Software Overview, available at https://www.pscad.com/software/prsim/ overview, accessed Aug 2023

[23] P. e. J. Mooney and N. Fischer, "Application Guidelines for Power Swing Detection on Transmission Systems," 2006 Power Systems Conference: Advanced Metering, Protection, Control, Communication, and Distributed Resources, Clemson, SC, USA, 2006, pp. 159-168, doi: 10.1109/PSAMP.2006.285385

[24] E.O. Schweitzer. III and Jeff Roberts, "Distance Relay Element Design" SEL Journal of Reliable Power, Volume 1, Number 1, July 2010

Appendix A – PSSE Network Quantities and Dynamic Model Parameters

The following tables provide the dynamic parameters used in the PSSE dynamic simulations.

Network Data

Table 42: Bus Data

Bus Number	Bus Name	Base kV	Area Num
101	NUC-A	21.6	1
102	NUC-B	21.6	1
151	NUCPANT	500	1
152	MID500	500	1
153	MID230	230	1
154	DOWNTN	230	1
201	HYDRO	500	2
202	EAST500	500	2
203	EAST230	230	2
204	SUB500	500	2
205	SUB230	230	2
206	URBGEN	18	2
211	HYDRO_G	20	2
3001	MINE	230	5
3002	E. MINE	500	5
3003	S. MINE	230	5
3004	WEST	500	5
3005	WEST	230	5
3006	UPTOWN	230	5
3007	RURAL	230	5
3008	CATDOG	230	5
3011	MINE_G	13.8	5
3018	CATDOG_G	13.8	5
90152	MID500_TMP	500	1
93004	WEST_TMP	500	1

Table 43: Bus Load Data

Bus Number	Id	Pload (MW)	Qload (Mvar)
153	1	200	100
154	1	600	450
154	2	400	350
203	1	300	150
205	1	1200	700
3005	1	100	50
3007	1	200	75
3008	1	200	75

Table 44: Fixed Shunt Data

Bus Number	Id	B-Shunt (Mvar)
151	1	-600
154	1	300
201	1	300
203	1	50
205	1	300

Table 45: Transformer Data

From Bus #	From Bus Name	To Bus #	To Bus Name	Id	Specified R (pu or watts)	Specified X (pu)
101	NUC-A	151	NUCPANT	1	0.0003	0.0136
102	NUC-B	151	NUCPANT	1	0.0003	0.0136
152	MID500	153	MID230	1	0	0.005
201	HYDRO	211	HYDRO_G	1	0.0007	0.02125
202	EAST500	203	EAST230	1	0.0004	0.01625
204	SUB500	205	SUB230	1	0.0003	0.015
205	SUB230	206	URBGEN	1	0.00026	0.01333
3001	MINE	3002	E. MINE	1	0.0003	0.015
3001	MINE	3011	MINE_G	1	0.0002	0.01
3004	WEST	3005	WEST	1	0.0004	0.01625
3008	CATDOG	3018	CATDOG_G	1	0.00021	0.085

Table 46: Transmission Line Data

From Bus #	From Bus Name	To Bus #	To Bus Name	Id	Line R (pu)	Line X (pu)	Charging B (pu)
151	NUCPANT	152	MID500	1	0.0026	0.046	3.5
151	NUCPANT	152	MID500	2	0.0026	0.046	3.5
151	NUCPANT	201	HYDRO	1	0.001	0.015	1.2
152	MID500	202	EAST500	1	0.0008	0.01	0.95
152	MID500	90152	MID500_TMP	1	0	0.0001	0
153	MID230	154	DOWNTN	1	0.005	0.045	0.1
153	MID230	154	DOWNTN	2	0.006	0.054	0.15
154	DOWNTN	203	EAST230	1	0.004	0.04	0.1
154	DOWNTN	205	SUB230	1	0.00033	0.00333	0.09
201	HYDRO	202	EAST500	1	0.002	0.025	2
201	HYDRO	204	SUB500	1	0.003	0.03	2.5
203	EAST230	205	SUB230	1	0.005	0.045	0.08
203	EAST230	205	SUB230	2	0.005	0.045	0.08
3001	MINE	3003	S. MINE	1	0	0.008	0
3002	E. MINE	3004	WEST	1	0.006	0.054	0.09
3003	S. MINE	3005	WEST	1	0.006	0.054	0.09
3003	S. MINE	3005	WEST	2	0.006	0.054	0.09
3004	WEST	93004	WEST_TMP	1	0	0.0001	0
3005	WEST	3006	UPTOWN	1	0.0035	0.03	0.07
3005	WEST	3007	RURAL	1	0.003	0.025	0.06
3005	WEST	3008	CATDOG	1	0.006	0.05	0.12
3007	RURAL	3008	CATDOG	1	0.003	0.025	0.06
90152	MID500_TMP	93004	WEST_TMP	1	0.003	0.03	2.5

Table 47: Generator Data

Bus Number	ID	Area	Pmax (MW)	Pmin (MW)	PGen (MW) - SAVNW Transfer Case						
					n300	**n200**	**n100**	**0**	**205**	**300**	**350**
101	1	1	*810*	*0*	750	750	750	750	750	750	750
102	1	1	810	0	750	750	750	750	750	750	750
206	1	2	900/1800	0	800	800	800	800	860	955	1000
211	1	2	616.25	0	145	248	350	451	600	600	600
3011	1	5	900	0	717.4	610.9	507	405.6	197.8	102.5	57.8
3018	1	5	117	0	100	100	100	100	100	100	100

Generator Data

Table 48: Generator Data (GENROU) - Bus 101, ID 1

Model Type: GENROU		
Con	Description	Value
J	T'do (> 0)	6.5
J+1	T''do (> 0)	0.06
J+2	T'qo (> 0)	0.2
J+3	T''qo (> 0)	0.05
J+4	H, Inertia	4
J+5	D, Speed Damping	0
J+6	Xd	1.8
J+7	Xq	1.75
J+8	X'd	0.6
J+9	X'q	0.8
J+10	X''d = X''q	0.3
J+11	Xl	0.15
J+12	S (1.0)	0.09
J+13	S (1.2)	0.38

Table 49: Generator Data (GENROU) - Bus 102, ID 1

Model Type: GENROU		
Con	Description	Value
J	T'do (> 0)	6.5
J+1	T''do (> 0)	0.06
J+2	T'qo (> 0)	0.2
J+3	T''qo (> 0)	0.05
J+4	H, Inertia	4
J+5	D, Speed Damping	0
J+6	Xd	1.8
J+7	Xq	1.75
J+8	X'd	0.6
J+9	X'q	0.8
J+10	X''d = X''q	0.3
J+11	Xl	0.15
J+12	S (1.0)	0.09
J+13	S (1.2)	0.38

Table 50: Generator Data (GENROU) - Bus 206, ID 1

Model Type: GENROU		
Con	**Description**	**Value**
J	T'do (> 0)	4.5
J+1	T''do (> 0)	0.07
J+2	T'qo (> 0)	0.15
J+3	T''qo (> 0)	0.05
J+4	H, Inertia	2.5
J+5	D, Speed Damping	0
J+6	Xd	1.4
J+7	Xq	1.35
J+8	X'd	0.5
J+9	X'q	0.7
J+10	X''d = X''q	0.25
J+11	Xl	0.1
J+12	S (1.0)	0.09
J+13	S (1.2)	0.38

Table 51: Generator Data (GENSAL) - Bus 211, ID 1

Model Type: GENSAL		
Con	**Description**	**Value**
J	T'do (> 0)	5
J+1	T"do (> 0)	0.05
J+2	T"qo (> 0)	0.2
J+3	Inertia H	5
J+4	Speed Damping D	0
J+5	Xd	1
J+6	Xq	0.75
J+7	X'd	0.4
J+8	X"d = X"q	0.26
J+9	X1	0.1
J+10	S (1.0)	0.11
J+11	S (1.2)	0.62

Table 52: Generator Data (GENROU) - Bus 3011, ID 1

Model Type: GENROU		
Con	**Description**	**Value**
J	T'do (> 0)	5
J+1	T''do (> 0)	0.06
J+2	T'qo (> 0)	0.2
J+3	T''qo (> 0)	0.06
J+4	H, Inertia	3
J+5	D, Speed Damping	0
J+6	Xd	1.6
J+7	Xq	1.55
J+8	X'd	0.7
J+9	X'q	0.85
J+10	X''d = X''q	0.35
J+11	Xl	0.2
J+12	S (1.0)	0.09
J+13	S (1.2)	0.38

Table 53: Generator Data (GENROU) - Bus 3018, ID 1

Model Type: GENROU		
Con	**Description**	**Value**
J	T'do (> 0)	5
J+1	T''do (> 0)	0.06
J+2	T'qo (> 0)	0.2
J+3	T''qo (> 0)	0.06
J+4	H, Inertia	3
J+5	D, Speed Damping	0
J+6	Xd	1.6
J+7	Xq	1.55
J+8	X'd	0.7
J+9	X'q	0.85
J+10	X''d = X''q	0.35
J+11	Xl	0.2
J+12	S (1.0)	0.09
J+13	S (1.2)	0.38

Exciter Data

Table 54: Exciter Data (IEEET1) - Bus 101, ID 1

Model Type: IEEET1		
Con	Description	Value
J	TR (sec)	0
J+1	KA	400
J+2	TA (sec)	0.04
J+3	VRMAX or zero	7.3
J+4	VRMIN	-7.3
J+5	KE or zero	1
J+6	TE (>0) (sec)	0.8
J+7	KF	0.03
J+8	TF (>0) (sec)	1
J+9	Switch=0	0
J+10	E1	2.47
J+11	SE(E1)	0.035
J+12	E2	4.5
J+13	SE(E2)	0.47

Table 55: Exciter Data (IEEET1) - Bus 102, ID 1

Model Type: IEEET1		
Con	Description	Value
J	TR (sec)	0
J+1	KA	400
J+2	TA (sec)	0.04
J+3	VRMAX or zero	7.3
J+4	VRMIN	-7.3
J+5	KE or zero	1
J+6	TE (>0) (sec)	0.8
J+7	KF	0.03
J+8	TF (>0) (sec)	1
J+9	Switch=0	0
J+10	E1	2.47
J+11	SE(E1)	0.035
J+12	E2	4.5
J+13	SE(E2)	0.47

Table 56: Exciter Data (IEEET1) - Bus 206, ID 1

Model Type: IEEET1		
Con	**Description**	**Value**
J	TR (sec)	0
J+1	KA	40
J+2	TA (sec)	0.06
J+3	VRMAX or zero	2.1
J+4	VRMIN	-2.1
J+5	KE or zero	0
J+6	TE (>0) (sec)	0.5
J+7	KF	0.08
J+8	TF (>0) (sec)	0.8
J+9	Switch=0	0
J+10	E1	2.47
J+11	SE(E1)	0.035
J+12	E2	3.5
J+13	SE(E2)	0.6

Table 57: Exciter Data (SCRX) - Bus 211, ID 1

Model Type: SCRX		
Con	**Description**	**Value**
J	TA/TB	0.1
J+1	TB (> 0)	10
J+2	K	200
J+3	TE	0.05
J+4	EMIN	-5
J+5	EMAX	5
J+6	CSWITCH (0=bus fed, 1=solid fed)	1
J+7	rc/rfd	10

Table 58: Exciter Data (SEXS) – Bus 3011, ID 1

Model Type: SEXS		
Con	**Description**	**Value**
J	TA/TB	0.1
J+1	TB (> 0)	10
J+2	K	100
J+3	TE	0.1
J+4	EMIN	0
J+5	EMAX	4

Table 59: Exciter Data (SEXS) – Bus 3018, ID 1

Model Type: SEXS		
Con	**Description**	**Value**
J	TA/TB	0.1
J+1	TB (> 0)	10
J+2	K	100
J+3	TE	0.1
J+4	EMIN	0
J+5	EMAX	4

Governor Data

Table 60: Governor Data (TGOV1) – Bus 101, ID 1

Model Type: TGOV1		
Con	**Description**	**Value**
J	R	0.05
J+1	T1 (>0) (sec)	0.05
J+2	V MAX	1.05
J+3	V MIN	0.3
J+4	T2 (sec)	1
J+5	T3 (>0) (sec)	1
J+6	Dt	0

Table 61: Governor Data (TGOV1) – Bus 102, ID 1

Model Type: TGOV1		
Con	**Description**	**Value**
J	R	0.05
J+1	T1 (>0) (sec)	0.05
J+2	V MAX	1.05
J+3	V MIN	0.3
J+4	T2 (sec)	1
J+5	T3 (>0) (sec)	1
J+6	Dt	0

Table 62: Governor Data (TGOV1) – Bus 206, ID 1

Model Type: TGOV1		
Con	**Description**	**Value**
J	R	0.05
J+1	T1 (>0) (sec)	0.05
J+2	V MAX	0.9
J+3	V MIN	0.3
J+4	T2 (sec)	3
J+5	T3 (>0) (sec)	9
J+6	Dt	0

Table 63: Governor Data (HYGOV) – Bus 211, ID 1

Model Type: HYGOV		
Con	**Description**	**Value**
J	R, Permanent Droop	0.05
J+1	r, Temporary Droop	0.3
J+2	Tr (> 0) Governor Time Constant	5
J+3	Tf (> 0) Filter Time Constant	0.05
J+4	Tg (> 0) Servo Time Constant	0.5
J+5	VELM, Gate Velocity Limit	0.2
J+6	GMAX, Maximum Gate Limit	1
J+7	GMIN, Minimum Gate Limit	0
J+8	TW (> 0) Water Time Constant	1.25
J+9	At, Turbine Gain	1.2
J+10	Dturb, Turbine Damping	0.5
J+11	qNL, No Load Flow	0.08

SLNOS Relay Data

Table 64: SLNOS Relay Data

Model Type: SLNOS2		
Con	**Description**	**Value**
J	Tzone, interzone travel time (cycles)	3
J+1	ALPHA, angle of first pair of impedance units(a)	84.29
J+2	INT1, intercept of first line	0.0395
J+3	INT2, intercept of second line	0.03
J+4	BETA, angle of second pair of impedance units(b)	84.29
J+5	INT3, intercept of third line	-0.03
J+6	INT4, intercept of fourth line	-0.0537
J+7	THRESH, threshold current (pu)	0
J+8	Tbself, self trip breaker time (cycles)	3
J+9	Tbtran, transfer trip breaker and delay time (cycles)	3
J+10	BL1typ, first blinder type (+/-1 or +/-2)	1

Model Type: SLNOS2		
Con	Description	Value
J+11	BL1int, first blinder intercept (pu)	0.3
J+12	BL1rot, first blinder rotation (degrees)	180
J+13	BL2typ, second blinder type (+/-1 or +/-2)	-1
J+14	BL2int, second blinder intercept (pu)	-0.3
J+15	BL2rot, second blinder rotation (degrees)	180

CMLDZNU2 Load Data

Table 65: CMLDZNU2 Load Data

Model Type: CMLDZNU2		
Con	Description	Value
J	Load base for xfr & feeder, MVA or calculated if <= 0	-0.8
J+1	Substation compensation B, pu on load base	0
J+2	Red – Feeder resistance, pu on load base	0.0001
J+3	Xfdr – Feeder reactance, pu on load base	0.0001
J+4	Fb – Not used, Fb = 0.0	0.75
J+5	Xxf – Transformer reactance, pu on load base	0.0001
J+6	Tfixhs – High side fixed transformer tap	1
J+7	Tfixls – Low side fixed transformer tap	1
J+8	LTC – LTC flag (1=active, 0=inactive)	1
J+9	Tmin – LTC min tap (on low side)	0.9
J+10	Tmax – LTC max tap (on low side)	1.1
J+11	Step – LTC Tstep (on low side)	0.0063
J+12	Vmin – Min value of V target range on xfr low side	1
J+13	Vmax – Max value of V target range on xfr low side	1.02
J+14	TD – LTC control time delay, s	30
J+15	TC – LTC tap adjustment time delay, s	5
J+16	Rcmp – xfr compensating R, pu on load base	0
J+17	Xcmp – xfr compensating X, pu on load base	0
J+18	FmA – Composite load motor A fraction	0.05
J+19	FmB – Composite load motor B fraction	0.05
J+20	FmC – Composite load motor C fraction	0.05
J+21	FmD – Composite load motor D fraction	0.03
J+22	Fel – Composite load electronic fraction	0.25
J+23	Pfel – Electronic load power factor	1
J+24	Vd1 – Voltage electronic loads start to drop	0.7
J+25	Vd2 – Voltage all electronic load has dropped	0.5
J+26	PFs – Static load lower factor	1
J+27	P1e – First exponent for static load P	1
J+28	P1c – First coefficient for static load P	1
J+29	P2e – Second exponent for static load P	2

Model Type: CMLDZNU2		
Con	Description	Value
J+30	P2c – Second coefficient for static load P	0
J+31	Pfrq – Frequency sensitivity for static P	0
J+32	Q1e – First exponent for static load Q	1
J+33	Q1c – First coefficient for static load Q	0
J+34	Q2e – Second exponent for static load Q	2
J+35	Q2c – Second coefficient for static load Q	1
J+36	Qfrq – Frequency sensitivity for static load Q	-1
J+37	Mtyp – Motor A phase, always 3	3
J+38	LF – Motor A real power to power base ratio	0.75
J+39	Ra – Motor A stator resistance, pu on motor base	0.04
J+40	X – Motor A synchronous reactance, pu	1.8
J+41	X' – Motor A transient reactance, pu	0.12
J+42	X" – Motor A sub-transient reactance, pu	0.104
J+43	To' – Motor A transient open circuit time constant, s	0.114
J+44	To" – Motor A sub-transient open circuit time constant, s	0.0025
J+45	H – Motor A inertia constant	0.1
J+46	etrq – Motor A exp for variation of torque with speed	0
J+47	Vtr1 – Motor A 1st undervoltage trip voltage, pu	0.65
J+48	Ttr1 – Motor A 1st undervoltage trip delay, s	0.1
J+49	Ftr1 – Motor A 1st undervoltage trip fraction	0.2
J+50	Vrc1 – Motor A 1st undervoltage reclose voltage, pu	0.1
J+51	Trc1 – Motor A 1st undervoltage reclose delay, s	9999
J+52	Vtr2 – Motor A 2nd undervoltage trip voltage, pu	0.5
J+53	Ttr2 – Motor A 2nd undervoltage trip delay, s	0.02
J+54	Ftr2 – Motor A 2nd undervoltage trip fraction	0.75
J+55	Vrc2 – Motor A 2nd undervoltage reclose voltage, pu	0.65
J+56	Trc2 – Motor A 2nd undervoltage reclose delay, s	0.1
J+57	Mtyp – Motor B phase, always 3	3
J+58	LF – Motor B real power to power base ratio	0.75
J+59	Ra – Motor B stator resistance, pu on motor base	0.03
J+60	X – Motor B synchronous reactance, pu	1.8
J+61	X' – Motor B transient reactance, pu	0.19
J+62	X" – Motor B sub-transient reactance, pu	0.14
J+63	To' – Motor B transient open circuit time constant, s	0.24
J+64	To" – Motor B sub-transient open circuit time constant, s	0.0031
J+65	H – Motor B inertia constant	0.5
J+66	etrq – Motor B torque speed exponent	2
J+67	Vtr1 – Motor B 1st undervoltage trip voltage, pu	0.55
J+68	Ttr1 – Motor B 1st undervoltage trip delay, s	0.02
J+69	Ftr1 – Motor B 1st undervoltage trip fraction	0
J+70	Vrc1 – Motor B 1st undervoltage reclose voltage, pu	0.65
J+71	Trc1 – Motor B 1st undervoltage reclose delay, s	0.05
J+72	Vtr2 – Motor B 2nd undervoltage trip voltage, pu	0.5
J+73	Ttr2 – Motor B 2nd undervoltage trip delay, s	0.025

Model Type: CMLDZNU2		
Con	**Description**	**Value**
J+74	Ftr2 – Motor B 2nd undervoltage trip fraction	0
J+75	Vrc2 – Motor B 2nd undervoltage reclose voltage, pu	0.6
J+76	Trc2 – Motor B 2nd undervoltage reclose delay, s	0.05
J+77	Mtyp – Motor C phase, always 3	3
J+78	LF – Motor C real power to power base ratio	0.75
J+79	Ra – Motor C stator resistance, pu on motor base	0.03
J+80	X – Motor C synchronous reactance, pu	1.8
J+81	X' – Motor C transient reactance, pu	0.19
J+82	X" – Motor C sub-transient reactance, pu	0.14
J+83	To' – Motor C transient open circuit time constant, s	0.24
J+84	To" – Motor C sub-transient open circuit time constant, s	0.0031
J+85	H – Motor C inertia constant	0.1
J+86	etrq – Motor C torque speed exponent	2
J+87	Vtr1 – Motor C 1st undervoltage trip voltage, pu	0.58
J+88	Ttr1 – Motor C 1st undervoltage trip delay, s	0.03
J+89	Ftr1 – Motor C 1st undervoltage trip fraction	0
J+90	Vrc1 – Motor C 1st undervoltage reclose voltage, pu	0.68
J+91	Trc1 – Motor C 1st undervoltage reclose delay, s	0.05
J+92	Vtr2 – Motor C 2nd undervoltage trip voltage, pu	0.53
J+93	Ttr2 – Motor C 2nd undervoltage trip delay, s	0.03
J+94	Ftr2 – Motor C 2nd undervoltage trip fraction	0
J+95	Vrc2 – Motor C 2nd undervoltage reclose voltage, pu	0.62
J+96	Trc2 – Motor C 2nd undervoltage reclose delay, s	0.1
J+97	Tstall – Motor D stall delay time, s	0.03
J+98	Trestart – Motor D restart from stall delay time, s	0.3
J+99	Tv – Motor D voltage time constant for contactors, s	0.03
J+100	Tf – Motor D frequency time constant for contactors, s	0.12
J+101	CompLF – Motor D real power to motor base ratio	1
J+102	CompPF – Motor D power factor at 1.0 pu voltage	0.98
J+103	Vstall – Motor D stall Voltage, pu	0.45
J+104	Rstall – Motor D stall resistance, pu of motor base	0.1
J+105	Xstall – Motor D stall reactance, pu of motor base	0.1
J+106	LFadj – Adjustment to stall voltage if COMPLF /= 1.0	0
J+107	Kp1 – Motor D real power coefficient when voltage > Vbrk	0
J+108	Np1 – Motor D real power exp when voltage > Vbrk	1
J+109	Kq1 – Motor D reactive power coefficient when voltage > Vbrk	6
J+110	Nq1 – Motor D reactive power exp when voltage>Vbrk	2
J+111	Kp2 – Motor D real power coefficient when voltage < Vbrk	12
J+112	Np2 – Motor D real power exp when voltage < Vbrk	3.2
J+113	Kq2 – Motor D reactive power coefficient when voltage < Vbrk	11
J+114	Nq2 – Motor D reactive power exp when voltage<Vbrk	2.5
J+115	Vbrk – Motor D "break-down" voltage,	0.86
J+116	Frst – Motor D fraction capable of restart after stall	0.2
J+117	Vrst – Motor D voltage for restart after stall, pu	0.95

Model Type: CMLDZNU2		
Con	**Description**	**Value**
J+118	CmpKpf – Motor D real power frequency dependency	1
J+119	CmpKqf – Motor D reactive power freq. dependency	-3.3
J+120	Vc1off – Motor D voltage contactors start opening, pu	0.5
J+121	Vc2off – Motor D voltage all contactors opened, pu	0.4
J+122	Vc1on – Motor D voltage contactors start closing, pu	0.6
J+123	Vc2on – Motor D voltage all contactors closed, pu	0.52
J+124	Tth – Motor D heating time constant, s	18
J+125	Th1t – Motor D temperature where tripping begins, pu	0.7
J+126	Th2t – Motor D temperature where completely tripped	1.9
J+127	Fuvr – Motor D fraction with undervoltage relays	0.1
J+128	UVtr1 – Motor D 1st undervoltage pick-up, pu	0.5
J+129	Ttr1 – Motor D 1st undervoltage trip delay, s	0.02
J+130	UVtr2 – Motor D 2nd undervoltage pick-up, pu	0.1
J+131	Ttr2 – Motor D 2nd under voltage trip delay, s	9999
J+132	frcel – Fraction electronic load that can reconnect	0.8

Appendix B – List of Disturbances Conditions Studied

The following lists the disturbances applied while performing PSSE dynamic simulations.

Table 66: Full list of contingencies for PSSE dynamic simulations

Contingency Name	Description
FLAT_RUN	No event applied
101_151_1	fault applied on the branch between bus 101 and bus 151, circuit ID 1. Fault duration of 0.1 s, applied at the 101 side of the line. The fault is cleared by tripping faulted branch
102_151_1	fault applied on the branch between bus 102 and bus 151, circuit ID 1. Fault duration of 0.1 s, applied at the 102 side of the line. The fault is cleared by tripping faulted branch
151_101_1	fault applied on the branch between bus 151 and bus 101, circuit ID 1. Fault duration of 0.1 s, applied at the 151 side of the line. The fault is cleared by tripping faulted branch
151_102_1	fault applied on the branch between bus 151 and bus 102, circuit ID 1. Fault duration of 0.1 s, applied at the 151 side of the line. The fault is cleared by tripping faulted branch
151_152_1	fault applied on the branch between bus 151 and bus 152, circuit ID 1. Fault duration of 0.1 s, applied at the 151 side of the line. The fault is cleared by tripping faulted branch
151_201_1	fault applied on the branch between bus 151 and bus 201, circuit ID 1. Fault duration of 0.1 s, applied at the 151 side of the line. The fault is cleared by tripping faulted branch
152_151_1	fault applied on the branch between bus 152 and bus 151, circuit ID 1. Fault duration of 0.1 s, applied at the 152 side of the line. The fault is cleared by tripping faulted branch
152_153_1	fault applied on the branch between bus 152 and bus 153, circuit ID 1. Fault duration of 0.1 s, applied at the 152 side of the line. The fault is cleared by tripping faulted branch
152_202_1	fault applied on the branch between bus 152 and bus 202, circuit ID 1. Fault duration of 0.1 s, applied at the 152 side of the line. The fault is cleared by tripping faulted branch
153_152_1	fault applied on the branch between bus 153 and bus 152, circuit ID 1. Fault duration of 0.1 s, applied at the 153 side of the line. The fault is cleared by tripping faulted branch
153_154_1	fault applied on the branch between bus 153 and bus 154, circuit ID 1. Fault duration of 0.1 s, applied at the 153 side of the line. The fault is cleared by tripping faulted branch
154_153_1	fault applied on the branch between bus 154 and bus 153, circuit ID 1. Fault duration of 0.1 s, applied at the 154 side of the line. The fault is cleared by tripping faulted branch

Contingency Name	Description
154_203_1	fault applied on the branch between bus 154 and bus 203, circuit ID 1. Fault duration of 0.1 s, applied at the 154 side of the line. The fault is cleared by tripping faulted branch
154_205_1	fault applied on the branch between bus 154 and bus 205, circuit ID 1. Fault duration of 0.1 s, applied at the 154 side of the line. The fault is cleared by tripping faulted branch
201_151_1	fault applied on the branch between bus 201 and bus 151, circuit ID 1. Fault duration of 0.1 s, applied at the 201 side of the line. The fault is cleared by tripping faulted branch
201_202_1	fault applied on the branch between bus 201 and bus 202, circuit ID 1. Fault duration of 0.1 s, applied at the 201 side of the line. The fault is cleared by tripping faulted branch
201_204_1	fault applied on the branch between bus 201 and bus 204, circuit ID 1. Fault duration of 0.1 s, applied at the 201 side of the line. The fault is cleared by tripping faulted branch
201_211_1	fault applied on the branch between bus 201 and bus 211, circuit ID 1. Fault duration of 0.1 s, applied at the 201 side of the line. The fault is cleared by tripping faulted branch
202_152_1	fault applied on the branch between bus 202 and bus 152, circuit ID 1. Fault duration of 0.1 s, applied at the 202 side of the line. The fault is cleared by tripping faulted branch
202_201_1	fault applied on the branch between bus 202 and bus 201, circuit ID 1. Fault duration of 0.1 s, applied at the 202 side of the line. The fault is cleared by tripping faulted branch
202_203_1	fault applied on the branch between bus 202 and bus 203, circuit ID 1. Fault duration of 0.1 s, applied at the 202 side of the line. The fault is cleared by tripping faulted branch
203_154_1	fault applied on the branch between bus 203 and bus 154, circuit ID 1. Fault duration of 0.1 s, applied at the 203 side of the line. The fault is cleared by tripping faulted branch
203_202_1	fault applied on the branch between bus 203 and bus 202, circuit ID 1. Fault duration of 0.1 s, applied at the 203 side of the line. The fault is cleared by tripping faulted branch
203_205_1	fault applied on the branch between bus 203 and bus 205, circuit ID 1. Fault duration of 0.1 s, applied at the 203 side of the line. The fault is cleared by tripping faulted branch
204_201_1	fault applied on the branch between bus 204 and bus 201, circuit ID 1. Fault duration of 0.1 s, applied at the 204 side of the line. The fault is cleared by tripping faulted branch
204_205_1	fault applied on the branch between bus 204 and bus 205, circuit ID 1. Fault duration of 0.1 s, applied at the 204 side of the line. The fault is cleared by tripping faulted branch
205_154_1	fault applied on the branch between bus 205 and bus 154, circuit ID 1. Fault duration of 0.1 s, applied at the 205 side of the line. The fault is cleared by tripping faulted branch

Contingency Name	Description
205_203_1	fault applied on the branch between bus 205 and bus 203, circuit ID 1. Fault duration of 0.1 s, applied at the 205 side of the line. The fault is cleared by tripping faulted branch
205_204_1	fault applied on the branch between bus 205 and bus 204, circuit ID 1. Fault duration of 0.1 s, applied at the 205 side of the line. The fault is cleared by tripping faulted branch
205_206_1	fault applied on the branch between bus 205 and bus 206, circuit ID 1. Fault duration of 0.1 s, applied at the 205 side of the line. The fault is cleared by tripping faulted branch
206_205_1	fault applied on the branch between bus 206 and bus 205, circuit ID 1. Fault duration of 0.1 s, applied at the 206 side of the line. The fault is cleared by tripping faulted branch
211_201_1	fault applied on the branch between bus 211 and bus 201, circuit ID 1. Fault duration of 0.1 s, applied at the 211 side of the line. The fault is cleared by tripping faulted branch
3001_3002_1	fault applied on the branch between bus 3001 and bus 3002, circuit ID 1. Fault duration of 0.1 s, applied at the 3001 side of the line. The fault is cleared by tripping faulted branch
3001_3003_1	fault applied on the branch between bus 3001 and bus 3003, circuit ID 1. Fault duration of 0.1 s, applied at the 3001 side of the line. The fault is cleared by tripping faulted branch
3001_3011_1	fault applied on the branch between bus 3001 and bus 3011, circuit ID 1. Fault duration of 0.1 s, applied at the 3001 side of the line. The fault is cleared by tripping faulted branch
3002_3001_1	fault applied on the branch between bus 3002 and bus 3001, circuit ID 1. Fault duration of 0.1 s, applied at the 3002 side of the line. The fault is cleared by tripping faulted branch
3002_3004_1	fault applied on the branch between bus 3002 and bus 3004, circuit ID 1. Fault duration of 0.1 s, applied at the 3002 side of the line. The fault is cleared by tripping faulted branch
3003_3001_1	fault applied on the branch between bus 3003 and bus 3001, circuit ID 1. Fault duration of 0.1 s, applied at the 3003 side of the line. The fault is cleared by tripping faulted branch
3003_3005_1	fault applied on the branch between bus 3003 and bus 3005, circuit ID 1. Fault duration of 0.1 s, applied at the 3003 side of the line. The fault is cleared by tripping faulted branch
3004_3002_1	fault applied on the branch between bus 3004 and bus 3002, circuit ID 1. Fault duration of 0.1 s, applied at the 3004 side of the line. The fault is cleared by tripping faulted branch
3004_3005_1	fault applied on the branch between bus 3004 and bus 3005, circuit ID 1. Fault duration of 0.1 s, applied at the 3004 side of the line. The fault is cleared by tripping faulted branch
3005_3003_1	fault applied on the branch between bus 3005 and bus 3003, circuit ID 1. Fault duration of 0.1 s, applied at the 3005 side of the line. The fault is cleared by tripping faulted branch

Contingency Name	Description
3005_3004_1	fault applied on the branch between bus 3005 and bus 3004, circuit ID 1. Fault duration of 0.1 s, applied at the 3005 side of the line. The fault is cleared by tripping faulted branch
3005_3006_1	fault applied on the branch between bus 3005 and bus 3006, circuit ID 1. Fault duration of 0.1 s, applied at the 3005 side of the line. The fault is cleared by tripping faulted branch
3005_3007_1	fault applied on the branch between bus 3005 and bus 3007, circuit ID 1. Fault duration of 0.1 s, applied at the 3005 side of the line. The fault is cleared by tripping faulted branch
3005_3008_1	fault applied on the branch between bus 3005 and bus 3008, circuit ID 1. Fault duration of 0.1 s, applied at the 3005 side of the line. The fault is cleared by tripping faulted branch
3006_3005_1	fault applied on the branch between bus 3006 and bus 3005, circuit ID 1. Fault duration of 0.1 s, applied at the 3006 side of the line. The fault is cleared by tripping faulted branch
3007_3005_1	fault applied on the branch between bus 3007 and bus 3005, circuit ID 1. Fault duration of 0.1 s, applied at the 3007 side of the line. The fault is cleared by tripping faulted branch
3007_3008_1	fault applied on the branch between bus 3007 and bus 3008, circuit ID 1. Fault duration of 0.1 s, applied at the 3007 side of the line. The fault is cleared by tripping faulted branch
3008_3005_1	fault applied on the branch between bus 3008 and bus 3005, circuit ID 1. Fault duration of 0.1 s, applied at the 3008 side of the line. The fault is cleared by tripping faulted branch
3008_3007_1	fault applied on the branch between bus 3008 and bus 3007, circuit ID 1. Fault duration of 0.1 s, applied at the 3008 side of the line. The fault is cleared by tripping faulted branch
3008_3018_1	fault applied on the branch between bus 3008 and bus 3018, circuit ID 1. Fault duration of 0.1 s, applied at the 3008 side of the line. The fault is cleared by tripping faulted branch
3011_3001_1	fault applied on the branch between bus 3011 and bus 3001, circuit ID 1. Fault duration of 0.1 s, applied at the 3011 side of the line. The fault is cleared by tripping faulted branch
3018_3008_1	fault applied on the branch between bus 3018 and bus 3008, circuit ID 1. Fault duration of 0.1 s, applied at the 3018 side of the line. The fault is cleared by tripping faulted branch
90152_93004_1	fault applied on the branch between bus 90152 and bus 93004, circuit ID 1. Fault duration of 0.1 s, applied at the 90152 side of the line. The fault is cleared by tripping faulted branch
93004_90152_1	fault applied on the branch between bus 93004 and bus 90152, circuit ID 1. Fault duration of 0.1 s, applied at the 93004 side of the line. The fault is cleared by tripping faulted branch

Appendix C – Validation of PSSE CMLD Model Operation

As described in Chapter 4, the study model is examined using two different load models, a static model (constant current) and a composite model (CMLD). A set of default parameters obtained from [19] is used for the CMLD model, the full set of CMLD parameters are presented in Appendix A – PSSE Network Quantities and Dynamic Model Parameters. Before examining the impact of the different model types on the network, some of the characteristics of the CMLD model are examined through some preliminary simulations and examinations.

Load Portion Examination

The CMLD model is composed of six separate elements, four motors (A, B, C and D), an electrical load portion and a static load portion. The portion of each different element is specified when configuring the model, each load with an associated model will split the total load (MW/MVAR) into different portions as specified. A simple test shows that if the CMLD model is with portions for Motor A-D and electrical load set to zero, the CMLD model will behave identically to the static model.

Load Shedding

Motor A, B and C have identical configurations but can be set individually. Each of the motors can be set with two-stage load shedding elements. The load shedding is based on the voltage at the load bus, if the voltage is below the threshold for a specified time, a portion of the load will be shed, additionally, there is also a set of parameters to reconnect the shed load based if the voltage recovers above a specified threshold for a given time.

A simple test is performed to verify the load shedding ability of the CMLD model. A very simple study model is developed, consisting of a generator bus, intermediate bus and load bus. A diagram of the simple test system is presented in Figure 53.

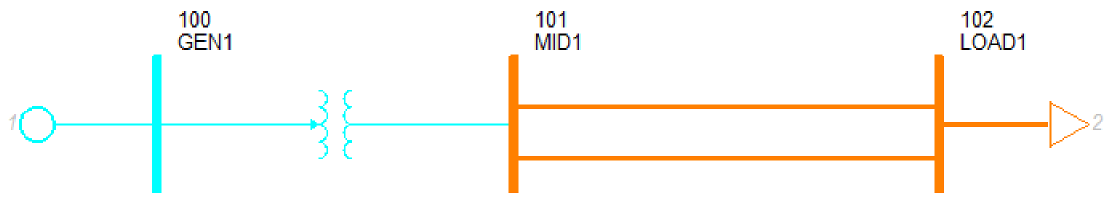

Figure 53: Simplified Load Shedding Test System

A CMLD model is configured such that the entire load is assigned to motor A. The motor A load shedding scheme is configured with two stage tripping. The CMLD load shedding settings are presented in Table 67.

Table 67: CMLD Motor A Load Shedding Settings (Test System)

	Undervoltage trip Voltage [pu]	Undervoltage trip delay [s]	Trip fraction
Stage 1	0.7	0.1	30
Stage 2	0.5	0.1	30

A dynamic simulation is performed where two faults are applied at the load bus. The first fault result in the load bus voltage decreasing to 0.55 pu, this is applied for 0.1 s. A few seconds later a more severe fault is applied where voltage drop just below 0.4 pu. The voltage and power at the load bus are plotted in Figure 54.

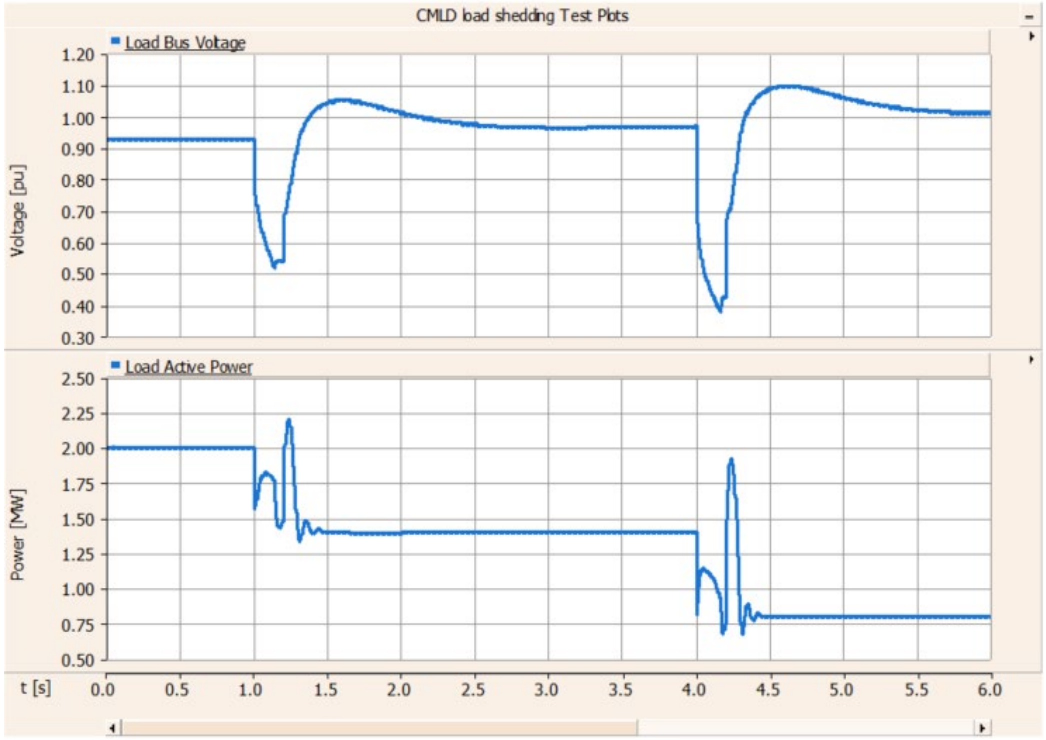

Figure 54: Simplified Load Shedding Test System Voltage and Power

The voltage and power in Figure 54 clearly demonstrate the CMLD model load tripping functions as intended. For the first fault the voltage drops below 0.7 pu, after the time delay the load power drops 30% of the initial load (from 2 MW to 1.4 MW). After the second fault is applied, the voltage drops below the 0.5 pu voltage threshold and after the time delay the load power drops an addition 30% of the initial load (1.4 MW to 0.8 MW).